INFORMATION TO USERS

This manuscript has been reproduced from the microfilm master. UMI films the text directly from the original or copy submitted. Thus, some thesis and dissertation copies are in typewriter face, while others may be from any type of computer printer.

The quality of this reproduction is dependent upon the quality of the copy submitted. Broken or indistinct print, colored or poor quality illustrations and photographs, print bleedthrough, substandard margins, and improper alignment can adversely affect reproduction.

In the unlikely event that the author did not send UMI a complete manuscript and there are missing pages, these will be noted. Also, if unauthorized copyright material had to be removed, a note will indicate the deletion.

Oversize materials (e.g., maps, drawings, charts) are reproduced by sectioning the original, beginning at the upper left-hand corner and continuing from left to right in equal sections with small overlaps.

Photographs included in the original manuscript have been reproduced xerographically in this copy. Higher quality 6" x 9" black and white photographic prints are available for any photographs or illustrations appearing in this copy for an additional charge. Contact UMI directly to order.

ProQuest Information and Learning
300 North Zeeb Road, Ann Arbor, MI 48106-1346 USA
800-521-0600



Downloaded from SHAREOK. Persistent Handle URL: https://hdl.handle.net/11244/475

UNIVERSITY OF OKLAHOMA

GRADUATE COLLEGE

MECHANISM OF CELLULAR INTOXICATION BY LARGE CLOSTRIDIAL TOXINS

A Dissertation

SUBMITTED TO THE GRADUATE FACULTY

in partial fulfillment of the requirements for the

degree of

Doctor of Philosophy

BY

Maen M. QADAN
Norman, Oklahoma
2002

UMI Number: 3053171

UMI®

UMI Microform 3053171

Copyright 2002 by ProQuest Information and Learning Company.
All rights reserved. This microform edition is protected against
unauthorized copying under Title 17, United States Code.

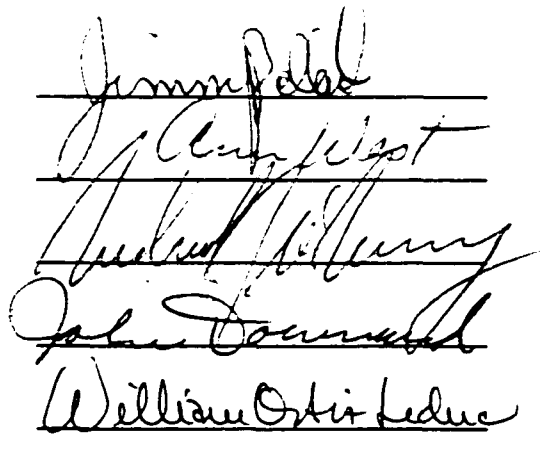
ProQuest Information and Learning Company
300 North Zeeb Road
P.O. Box 1346
Ann Arbor, MI 48106-1346

© Copyright 2002 by MAEN M. QADAN
All Rights Reserved

MECHANISM OF CELLULAR INTOXICATION BY
LARGE CLOSTRIDIAL TOXINS

A Dissertation APPROVED FOR THE
DEPARTMENT OF BOTANY AND MICROBIOLOGY

BY



ACKNOWLEDGMENTS

I can't believe that I finally got to the part were I can acknowledge people that made the last five years tolerable. None of this could have been possible without the support, sacrifice, and love of my parents. I know many people think they have great parents, but I am very sure that I have the best. My words can't describe how grateful I am for what they did, and how much effort they invested in me. Whatever I say will never be enough, but the great thing about them is that I don't need to thank them. My brothers Motaz, Motamed, and Motasem are my joy. I wanted to be there for them while they go through the awkward stages of growing up to help them out, or just to make fun of them. The thought of failing them was unbearable. I simply wanted to be my brother's hero because they mean the world to me.

I would like to thank my uncle Farouk and aunt Ishraf since they are responsible for peeking my interest in this field, and not to mention my acceptance at the University of Oklahoma. My uncle simply opened the door of science for me. I also would like to thank my warm-hearted uncle Shafiq, whose advice I value the most, my aunt Amal for her love and concern, and my cousins whom I always looked up to, Fawaz, Basil, and Samer. Uncle Ammar's help came at a very critical time of my life, and I want him to know that his support will never be forgotten. I have a big family, with lots of uncles and aunts who always made me feel as one of their own, and I can write another dissertation about how great it is to be around them.

Tom and Carolyn are the best in-laws one can get. Tom fixes everything from cars to airplanes, and if you have an emergency he will be there as soon as possible, he will fly there if he has to, literally. Carolyn is where you go to beg for money, or

complain and look for attention when times are tough, in other words a second mother. She bailed me out a couple of times and for that I will always be thankful. Johnathan my brother in-law is the person that keeps reminding me that one should have fun in life. Riding motorcycles at supersonic speed for an example. I will miss watching OU games with him, or movies that my wife doesn't find very tasteful. His advice always comes in handy and humbling.

I consider myself very lucky with the mentor that I had for the last five years. Now that I know that there is not much he can do to stop my graduation, I feel comfortable talking about him freely. Jimmy was very patient with me right from the beginning. He noticed the hardship that I went through, but he believed in me, and trusted my abilities. He took it as a personal challenge to create a young scientist from scratch that is ready to take on the whole world. His greatest deed is that he cares about everybody and everything. He loves science and he taught me how to like it, and by being a great family man and a great friend, he showed me how one can succeed in both professional and social life. Jimmy represents the honest, patriotic, hardworking men of this country, and if I ever become a citizen of this nation, I know what to measure up to. I will always brag about being his first graduate student, and how I stayed when others left, but ever since I met him I believed that good things will happen to me. He can make the molecular mechanism of action of whatever sound interesting, so imagine how a funny story sounds like coming from him. If he is in the mood to make fun of you, don't even try to fight back, just cut your losses and shut up. I will greatly miss bugging the hell out of him and raising his blood pressure.

Neil Coleman, although an undergraduate student then, showed me how to be a good graduate student. I can't remember meeting anybody that can work harder than him. I know he is going to be a great doctor somewhere in Kansas while building barns and raising ten kids. He can raise yours too if you want him to.

Amy is and always will be one of my best friends. If you want to see scientific techniques performed to perfection, watch Amy run experiments. Every time I look through her notebooks I feel like burying mine far far away. Amy thinks she is *ok* when it comes to science, I think she is really humble. I can gossip about anybody with her, without the slightest feeling of regret. It helps with blood pressure problems. I hope that things go as planned and our families will meet again in San Diego.

Another great guy that I had the chance to work with is Carr Vincent. He is simply the brightest and the funniest. That's all I need to say about him.

Mahdieh is originally from Iran. I could not relate to anybody more than her in our lab. She always had a big smile on her face, and she made sure that everybody is doing fine. I had a great time working as a teaching assistant with her, since I did not have to do a lot when she was around. You had to be really nasty if she complained about you.

I have two brothers in Norman, Mostafa and Wael. I actually listen to Mostafa's advice every once and a while. In my book that means a lot. I consider him to be the older brother I never had. Wael is someone you can depend on when everybody turns you down. I don't think the word NO exists in his dictionary. As a chef he is second only to my mother.

I had the chance to work with two great technicians last year. Joy takes care of everything I don't want to do. She is a blessing to our lab. Be nice to her and she will take care of you. Lisa fills the lab with love, care and candy. If everybody is tired of your wining and complaining she will still listen.

I also had the honor of working with a great post-doc recently. Isabelle is too nice to be in this business, but somehow she gets everybody in line without stepping on anybody's toes. I believe English should be spoken in her accent.

Last year a male graduate student joined the lab, and they are becoming scarce in this business. Dan was my savior this last year, because finally there was somebody to talk to about OU beating the hell out of Texas, or who got recruited to the football team, or why the hell does OSU exist? You know, guy talk. He always has a joke or two of the good kind only. Training him was one of the easiest tasks I've ever done. He absorbs directions easily, and he goes through scientific articles as if he is reading fairy tales. After meeting him, I think there might be a direct link between human beings and sponge.

This summer we tricked Elaine to join our lab. She can tell stories with visual and sound effects. She recently introduced theme music and surround system. She has a great sense of humor but the poor girl is very involved in politics. Sometimes I feel like I should be nice to her because she is going to be the first female president of the USA. She is very smart and well spoken, but if you see a sharp pencil in her hand, stay away, and stay alive.

I have special thanks for Lea Spyres for performing the bafilomycin assays in chapter I and II. She also provided me with great help and scientific advice. I am grateful to Jeremy Daniels for running the immunoblot in chapter III.

Matt Ramsey ran the 2-D gel analysis and the mass spectrometry in chapter III. He is a talented graduate student that will very soon come across a great discovery in the world of science. I admire his Louisiana spirit, and how proud he is to be from the south. If you ever feel like breaking some bones in your body, ask him to play rugby with you.

I also want to thank Dr. Barbara Safiejko-Mroczka for her help with running the video time-lapse experiments, and the immunostained pictures in chapter III.

My committee members Dr. William Ortiz, Dr. Michael McInerney, Dr. John Downard, and Dr. Ann West provided great advice throughout the last five years. I am very grateful for the help they provided, and will always be proud of having their names on my dissertation.

I kept the best for last. My sweetheart and the love of my life, Carrie, is the person who makes me want to be better always. Her smile is enough to wipe away the frustration of a long fruitless day, and her touch can heal the worst of pains. She always says "everything is going to be ok" and she always proves right. Her mere presence is enough to make me happy, and she is the only person I know of who thinks that being around me is a treat. She keeps me humbled with her great sense of direction, because I suck when it comes to finding my way around. I call her my little navigator, because I believe she is linked to a global positioning system. She is very patient and understanding. She never complained about the long days and the sleepless nights of

work, the short vacations, or even missing family gatherings. She is my best friend before she is my wife, and when she is away from me one can tell.

Table of Contents

Acknowledgments.....IV

Table of Contents.....X

Table of figures.....XII

Abstract.....XIV

Chapter I. pH Induced Conformational Changes in *Clostridium difficile* toxin B.

Abstract.....2

Introduction.....3

Materials and Methods.....5

Results.....8

Discussion.....18

References.....21

Chapter II. pH Enhanced Cytopathic Effects of *Clostridium sordellii* Lethal Toxin.

Abstract.....24

Introduction.....25

Materials and Methods.....27

Results.....32

Discussion.....47

References.....49

Chapter III. *Clostridium difficile* toxin B activates dual caspase-dependent and caspase-independent apoptosis in intoxicated cells.

Abstract.....53

Introduction.....54

Materials and Methods.....56

Results.....62

Discussion.....78

References.....82

Chapter IV. Multiple Death Pathways Are Triggered By *Clostridium sordellii* Lethal Toxin.

Abstract.....86

Introduction.....87

Materials and Methods.....89

Results.....93

Discussion.....104

References.....108

Summary 112

Table of Figures

Chapter I. pH Induced Conformational Changes in *Clostridium difficile* toxin B.

Figure 1.....9

Figure 2.....11

Figure 3.....13

Figure 4.....14

Figure 5.....16

Figure 6.....17

Chapter II. pH Enhanced Cytopathic Effects of *Clostridium sordellii* Lethal Toxin.

Figure 1.....33

Figure 2.....35

Figure 3.....40

Figure 4 (A).....41

Figure 4 (B).....44

Figure 5.....45

Figure 6.....46

Chapter III. *Clostridium difficile* toxin B activates dual caspase-dependent and caspase-independent apoptosis in intoxicated cells.

Figure 1.....63

Figure 2.....64

Figure 3.....66

Figure 4.....69

Figure 5.....71

Figure 6.....72

Figure 7.....74

Figure 8.....76

Chapter IV. Multiple Death Pathways Are Triggered By *Clostridium sordellii* Lethal Toxin.

Figure 1.....94

Figure 2.....95

Figure 3.....96

Figure 4.....98

Figure 5.....99

Figure 6.....102

Figure 7.....103

Abstract

Toxin B from *Clostridium difficile* is a monoglucosylating toxin that inactivates small GTPases Rho, Rac and Cdc42 during intoxication of mammalian cells. Like many intracellular toxins, TcdB can be roughly divided into enzymatic, translocation and receptor binding domains. Proceeding from the amino to carboxy terminus, the first ~550 amino acids contain the enzymatic region, which is followed by a putative translocation region and receptor-binding domain located within the remaining two-thirds of the toxin. In chapter I, we investigated the impact acidic pH has on cytosolic entry and structural changes within toxin B. Bafilomycin A1 was used to block endosomal acidification and subsequent toxin B translocation. Cytopathic effects could be completely blocked by addition of bafilomycin A1 up to 20 min following toxin treatment. Furthermore, providing a low extracellular pH could circumvent the effect of bafilomycin A1 and other lysosomotropic agents. Acid pH induced structural changes were followed by using the fluorescent probe TNS, inherent tryptophan fluorescence and relative susceptibility to a specific protease. As the toxin was exposed to lower pH there was an increase in TNS fluorescence suggesting the exposure of hydrophobic domains by toxin B. The change in hydrophobicity appears to be reversible since raising the pH back to neutrality abrogates TNS fluorescence. Furthermore, tryptophan fluorescence was quenched at the acidic pH indicating domains may be moving into more aqueous environments. Toxin B also demonstrated variable susceptibility to *Staphylococcus aureus* V8 protease at neutral and acidic pH, further suggesting pH induced structural changes in this protein.

Clostridium sordellii lethal toxin (TcsL) is a large clostridial toxin (LCT) that glucosylates Ras, Rac and Ral. In chapter II, using a suite of inhibitors, steps in cell entry by TcsL were dissected and entry appears to be dependent on endosomal acidification, but in contrast to TcdB, TcsL was substantially slower in its time-course of entry. TcsL cytopathic effects (CPE) were blocked by bafilomycin A1 and neutralized by antiserum up to 2 h following treatment of cells with the toxin. This slow time course of intoxication and relatively high cytopathic dose were alleviated by exposing TcsL to acid pH resulting in a time-couse similar to TcdB. The optimal pH range for activation was pH 4.0 to pH 5.0, which increased the rate of intoxication over 5 fold, lowered the minimal intoxicating dose by over 100 fold, and allowed complete substrate modification within 2 h as shown by differential glucosylation. Fluorescence analysis of TcsL, using 2-(p-toluidinyl) naphthalene-6-sulfonic acid as a probe, suggested that acid pH stimulated a hydrophobic transition in the protein, a likely prelude to membrane insertion. Finally, acid entry by TcsL caused TcdB-like morphological changes on CHO cells, suggesting acid activation may be impacting substrate recognition profiles for TcsL.

In chapter III, we show that TcdB has the potential to stimulate caspase-dependent and caspase-independent apoptosis. The apoptotic pathways became evident when caspase-3-processed-vimentin was detected in TcdB-treated HeLa cells. Caspase-3 activation was subsequently confirmed in TcdB-intoxicated HeLa cells. Interestingly, caspase inhibitor delayed TcdB-induced cell death, but did not alter the time-course of cytopathic effects. A similar effect was also observed in MCF-7 cells, which are deficient in caspase-3 activity. The time course to cell death was almost identical between cells treated with TcdB plus caspase inhibitor and cells intoxicated with the TcdB

enzymatic domain ($TcdB^{1-556}$). Unlike TcdB treated cells, intoxication with $TcdB^{1-556}$ or expression of $TcdB^{1-556}$ in a transfected cell line, did not stimulate caspase-3 activation yet cells exhibited cytopathic effects and cell death. Although $TcdB^{1-556}$ treated cells did not demonstrate caspase-3 activation these cells were apoptotic as determined by differential annexin-V/propidium iodide staining and nucleosomal DNA fragmentation. These data indicate TcdB triggers caspase-independent apoptosis as a result of substrate inactivation and caspase-dependent apoptosis due to a second, yet undefined, activity of TcdB. This is the first example of a bacterial virulence factor with the potential to stimulate multiple apoptotic pathways in host cells.

In chapter IV, we show that TcsL has the capacity to activate multiple death pathways in intoxicated cells. Initially, we generated a fusion protein encoding the TcsL enzymatic domain (residues 1-556) with a truncated version of anthrax toxin lethal factor (LFn). When delivered to the cytosol of the cell with anthrax protective antigen (PA), $LFnTcsL^{1-556}$ caused cytopathic effects at a rate faster than wild-type TcsL; however, cell death in fusion treated cells was delayed compared to TcsL. In light of this disparity in cytotoxicity between $LFnTcsL^{1-556}$ and TcsL, we analyzed a death pathway in treated cells by quantifying caspase-3 activation. In contrast to TcsL, PA plus $LFnTcsL^{1-556}$ did not stimulate any detectable caspase-3 activation under conditions that caused cell rounding and cell death. Furthermore, a broad-spectrum caspase inhibitor delayed cell death in HeLa cells intoxicated with TcsL, but the inhibitor did not afford the same protection to PA, $LFnTcsL^{1-556}$ treated cells. In addition, a caspase-3 deficient cell line (MCF-7), treated with TcsL, showed delayed cell death, but an almost identical time-course of cytopathic effects compared to HeLa cells. Interestingly, nucleosomal DNA

fragmentation and annexin-V positive staining was detected in cells treated with TcsL or PA, LFnTcsL$^{1-556}$ suggesting both are capable of triggering apoptosis. These data suggest that TcsL uses multiple functional domains to activate more than one death pathway in intoxicated cells.

Chapter I
pH Induced Conformational Changes in in *C. difficile* toxin B

Abstract

Toxin B from *Clostridium difficile* is a monoglucosylating toxin that targets substrates within the cytosol of mammalian cells. In this study we investigated the impact acidic pH has on cytosolic entry and structural changes within toxin B. Bafilomycin A1 was used to block endosomal acidification and subsequent toxin B translocation. Cytopathic effects could be completely blocked by addition of bafilomycin A1 up to 20 min following toxin treatment. Furthermore, providing a low extracellular pH could circumvent the effect of bafilomycin A1 and other lysosomotropic agents. Acid pH induced structural changes were followed by using the fluorescent probe TNS, inherent tryptophan fluorescence and relative susceptibility to a specific protease. As the toxin was exposed to lower pH there was an increase in TNS fluorescence suggesting the exposure of hydrophobic domains by toxin B. The change in hydrophobicity appears to be reversible, since raising the pH back to neutrality abrogatés TNS fluorescence. Furthermore, tryptophan fluorescence was quenched at the acidic pH indicating domains may be moving into more aqueous environments. Toxin B also demonstrated variable susceptibility to *Staphylococcus aureus* V8 protease at neutral and acidic pH, further suggesting pH induced structural changes in this protein.

Introduction

The large clostridial toxins are a unique class of virulence factors produced by at least three pathogenic clostridial species. *Clostridium difficile* produces toxins A and B, *Clostridium novyi* produces alpha-toxin and *Clostridium sordellii* produces lethal toxin and haemorrhagic toxin. These toxins are not only unique because of their exceptionally large size (ranging from 260 kD to 304 kD), but also demonstrate a novel enzymatic activity(1, 3, 4). Each of these toxins targets members of the Rho family of GTPases by acting as glycosyltransferases. Toxin A, toxin B, lethal toxin and haemorrhagic toxin all use UDP-glucose as a cosubstrate, whereas alpha-toxin uses UDP-GlcNAc to modify targets. Ultimately, each of these toxins disrupts the actin cytoskeleton of target cells.

The mechanism of action for *C. difficile* toxins A and B is of particular interest since this organism causes pseudomembranous colitis, a serious human disease usually occurring in hospitalized patients undergoing antibiotic therapy(2). *C. difficile* toxin A acts as an enterotoxin and is considered to be the major contributor to the intestinal damage caused by *C. difficile*. Toxin B is an effective cytotoxin that demonstrates less cell tropism than toxin A and is responsible for systemic intoxication(1).

While there has been significant progress in identifying the enzymatic action of these toxins, little is known about how these proteins translocate to the cytosol of target cells. By definition, intracellular bacterial toxins must cross the target cell membrane in order to enter the interior of the target cell. The most common mechanism for accomplishing this appears to be via a 3-step process, 1) receptor binding, 2) receptor triggered

endocytosis, and 3) membrane insertion and translocation following endosomal acidification. In this pathway, the cell is triggered to endocytose the toxin following its binding to a target cell receptor. Subsequent acidification, proteolysis and reduction may contribute to stimulating the toxin to insert into and cross the vesicle membrane. Several bacterial toxins appear to enter the cell using this process, although subsequent steps in translocation are varied. For example anthrax toxin uses a binary combination of proteins to provide membrane translocation while diphtheria toxin acts as a single polypeptide that is reduced, proteolyzed and translocated following endosomal acidification(5, 10). In the case of both of these toxins, acidification of the endosomal vesicle triggers structural changes and membrane insertion by the toxin.

Previous reports indicate that toxin B also requires an acidified endosome for toxic activity(7, 8). These earlier reports involved a protein reported to be 440 kD in size, much larger than toxin B. Herein, we briefly readdress this issue and clarify these experiments using a protein clearly shown to be toxin B. Additionally, we report the use of fluorescent approaches and proteolytic digest to provide the first insight into pH induced structural changes in toxin B. The results from this study suggest toxin B shows a significant increase in hydrophobicity and change in structure at acidic pH, all perhaps as a prelude to membrane insertion and translocation.

Materials and Methods

Cell culture. Chinese Hamster Ovary-K1(CHO) cells were used in these studies. This line was maintained in Ham's F-12 medium (Gibco BRL, Rockville, MD) supplemented with 10% fetal bovine serum. Cultures were grown at 37°C in the presence of 6% CO_2

Purification of toxin B. A modified protocol derived from two previously reported methods was used to isolate toxin B(11, 13). In this protocol *Clostridium difficile* strain VPI 10463 (ATCC, Manassas, VA) was grown in 10,000 to 12,000 MW cut off dialysis tubing suspended in 10 liters of brain heart infusion broth. The culture was grown at 37°C for 72 h, at which point the culture was centrifuged and the supernatant was collected. Toxin B was subsequently purified by consecutive steps of ammonium sulfate precipitation, anion exchange (Q-sepharose), gel filtration and high resolution anion exchange (mono-Q) chromatography. The final product was passed once over a benzamidine sepharose column (Amersham Pharmacia, Piscataway, NJ) to remove trace amounts of contaminating proteases. A cocktail of protease inhibitors, TLCK, TPCK and PMSF (Sigma Chemical, St. Louis, MO), was included during each step of the isolation protocol. Purification steps were followed by cytotoxicity on CHO cells, Western blot analysis using toxin B polyclonal antiserum (a generous gift from Dr. Rodney Tweten) and visualization by SDS-PAGE. Following the final step of purification, the protein concentration was determined using a Bradford assay (Bio-Rad Laboratories, Hercules, CA) and the sample was frozen at –80°C in 100 µl aliquots. Prior to assays, samples were thawed on ice and used immediately. Due to increased degradation, toxin B was not refrozen after thawing.

Bafilomycin A1 assays. CHO cells were plated at $5x10^4$ cells/well in a 96 well plate and incubated overnight. The following day, toxin B was added to cells at a final concentration of 0.5 μg/ml. At the indicated time-points, the cells were washed to remove unbound toxin, and bafilomycin A1 (Sigma Chemical, St. Louis, MO) was added to the cells at a final concentration of $5x10^{-7}$ M. Each sample was followed for 8 and 16 h and cytopathic effects were determined by visualization.

Acid pulse experiments. CHO cells were plated at $5x10^4$ cells/well in a 96 well plate and incubated overnight. The following day cells were incubated with either 100mM ammonium chloride or $5x10^{-7}$ M Bafilomycin A1 for 30 min. Toxin B was added to cells at concentrations ranging from 10 pmol to 1 fmol. Cells were incubated with toxin B for 1 h then washed to remove unbound toxin. A pH pulse was performed by lowering the pH to 4.0 with buffered medium for 10 min and then raising it again to pH 7.8 using neutralized medium. The cells were then followed for 8 h and cytopathic effect was determined by visualization.

TNS fluorescence analysis of Toxin B. 2-(p-toluidinyl) naphthalene-6-sulfonic acid, sodium salt [TNS] (Molecular Probes, Eugene, OR) solutions were prepared in the appropriate buffers for each of the pHs to be analyzed. The following buffers were used for each of the indicated pHs: pH 4.0, 4.5, 5.0, and 5.5, 100 mM NaCl, 100 mM ammonium acetate, 1mM EDTA; pH 6.0 and 6.5, 100 mM NaCl, 100 mM MES, 1 mM EDTA; pH 7.0 and 7.5 100 mM sodium chloride, 100 mM HEPES, 1mM EDTA. TNS

was added to each buffer to a final concentration of 150 μM. Twenty pmol of toxin B was added to each buffer in a final volume of 2 ml. These were allowed to incubate at 37°C for 20 min. Each sample was analyzed on a SLM 8100 photon counting fluoremeter (Spectronic Instruments, Rochester, NY) with an excitation of 366 nm and an emission scan of 380 nm to 500 nm using a slit width of 2.0. For the pH shift experiments 40 pmol of toxin B was dialyzed into 50 mM ammonium acetate, 1mM EDTA, 100 mM NaCl, pH 4.0 and 20 pmol of this sample was saved. The remaining 20 pmol of toxin B was incubated for 5 min at 37°C. The pH was then adjusted to pH 7.5 by the gradual addition of 1 N NaOH. The volume for both the pH 4.0 and pH 7.5 samples was adjusted to 1.5 ml and .5 ml of 20 mM TNS was added (this resulted in a final TNS concentration approximately 5 fold less than that used in the previous experiment). The samples were then analyzed as described above. Since the pH 7.5 sample was not within the buffering range of ammonium acetate, the pH of the sample was checked following the analysis to confirm that the neutral pH condition was maintained.

Tryptophan analysis. Tryptophan fluorescence was analyzed at pH 7.0 and pH 4.0. Twenty pmol of toxin B was incubated at pH 7.0 (100 mM HEPES) or pH 4.0 (100 mM ammonium acetate). Samples were analyzed using an excitation of 270 nm and an emission scan of 300 nm to 400 nm. Slit widths were set at 4.0.

V8 protease analysis. . Toxin B was dialyzed overnight against 1 L of 50 mM ammonium acetate pH 4.0 or 50 mM ammonium bicarbonate pH 7.8. Dialysis was carried out at 4°C in a microdialyzer using 12,000 to 14,000 MW cut-off membranes. V8

protease (Boehringer Mannheim, Indianapolis, IN) was made as a stock at 1 mg/ml in either 50 mM ammonium acetate buffer pH 4.0 or 50 mM ammonium acetate buffer pH 7.8. Toxin B (50 pmol) at both pHs was incubated with increasing dilutions of V8 protease (100 ng to 100 pg) at 37°C for 90 min. The reactions were stopped by the addition of SDS-PAGE tracking dye and analyzed immediately by SDS-PAGE.

Results

Bafilomycin A1 inhibition of toxin B cytopathic effects. Bafilomycin A1 is a potent inhibitor of the endosomal vacuolar ATPase pump and blocks the acidification of early and late endosomes as well as lysosomes (12). In these studies we used bafilomycin A1 to confirm the role of endosomal acidification on toxin B entry. Furthermore, we were able to gain insight into the time-course of toxin B translocation. As shown in figure 1, treatment of CHO cells with bafilomycin A1 prevents cytopathic effects by toxin B. A complete protective effect can be achieved by adding bafilomycin A1 up to 20 min following toxin B treatment. Approximately 20% of the killing can also be prevented by addition of bafilomycin A1 up to 50 min following treatment. Only after almost 60 min does addition of the inhibitor have no effect on toxin activity. Samples observed at 18 h start to show cytopathic effects at the earlier time-points, suggesting about a 20 minute window of time for entry. These results suggested that toxin B may remain within the vacuolar compartment for a significant period of time following entry.

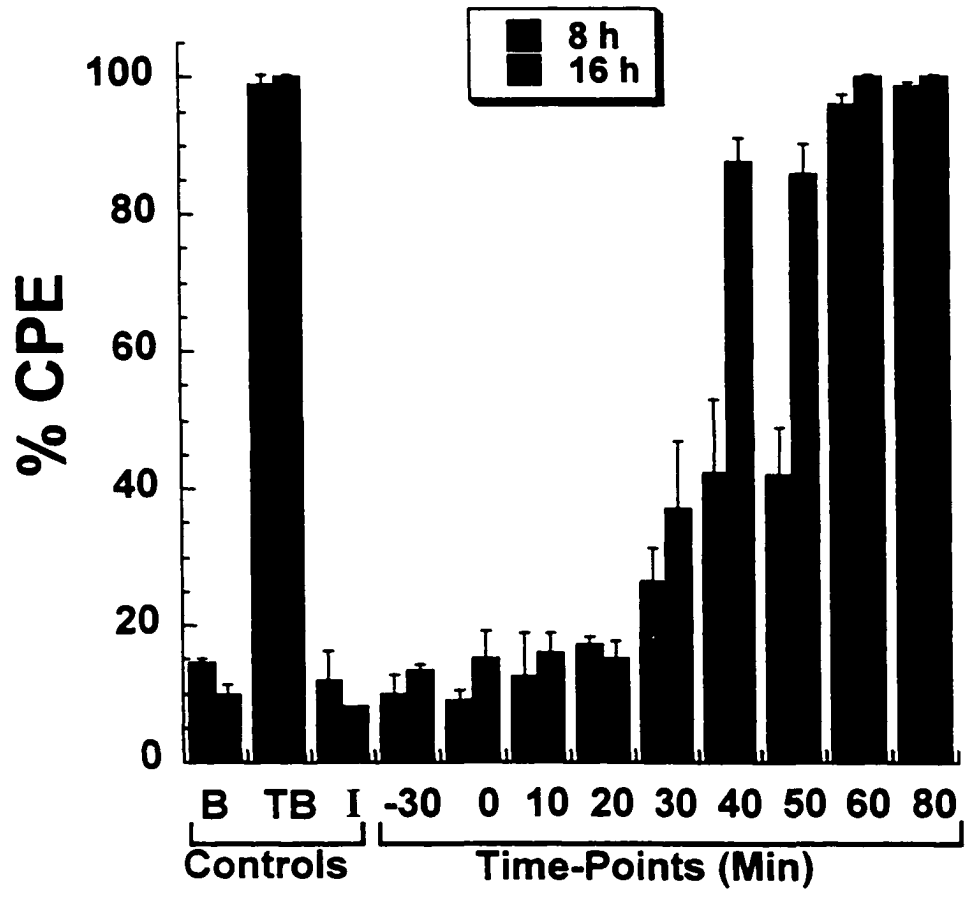


Figure 1. Bafilomycin A1 inhibition of Toxin B mediated cytopathic effects. In a 96-well plate CHO cells were incubated with toxin B (50 ng), and bafilomycin ($5x10^{-7}$ M) was added at 10 minute intervals from 0 to 80 min. Each sample was performed in triplicate and cytopathic effects were determined at 8 and 16 h. The error bars mark the standard deviation from the mean. Similar levels of inhibition were found in 2 subsequent repetitions of this experiment. B=PBS Buffer Control, TB=toxin B, I=bafilomycin A1.

For this reason we also investigated the effect brefeldin A (disrupts golgi and trans-golgi network) had on toxin entry. Treatment of cells with brefeldin A had no effect on toxin B activity (data not shown), indicating that toxic activity is not dependent on trafficking to the golgi.

Cellular intoxication following an acid pulse. In order to determine if the effects of bafilomycin A1 could be bypassed, cells were incubated with toxin B in the presence of the inhibitor and a brief acid pulse was provided. Following a 10 min acid pulse at pH 4.0, the cells were washed to remove unbound toxin B and the pH was raised back to neutrality. Subsequent cytopathic effects were followed for 8 h. As can be seen in figure 2, panel I, the lysosomotropic effects of bafilomycin A1 could be overcome by the acid pulse. This effect could be found in samples that were predialyzed to pH 4.0 or in samples at neutral pH.

Previous work had indicated toxin B could be delivered following an acid pulse, but only if the toxin was reduced with dithiothreitol(14). Since this previous work also involved using ammonium chloride instead of bafilomycin A1 as the inhibitor, we carried out this experiment in the presence of ammonium chloride. As can be seen in figure 2, panel II, the effects of ammonium chloride could be bypassed by providing an acid pulse. Furthermore, this bypass could be accomplished in the absence of any reducing agent.

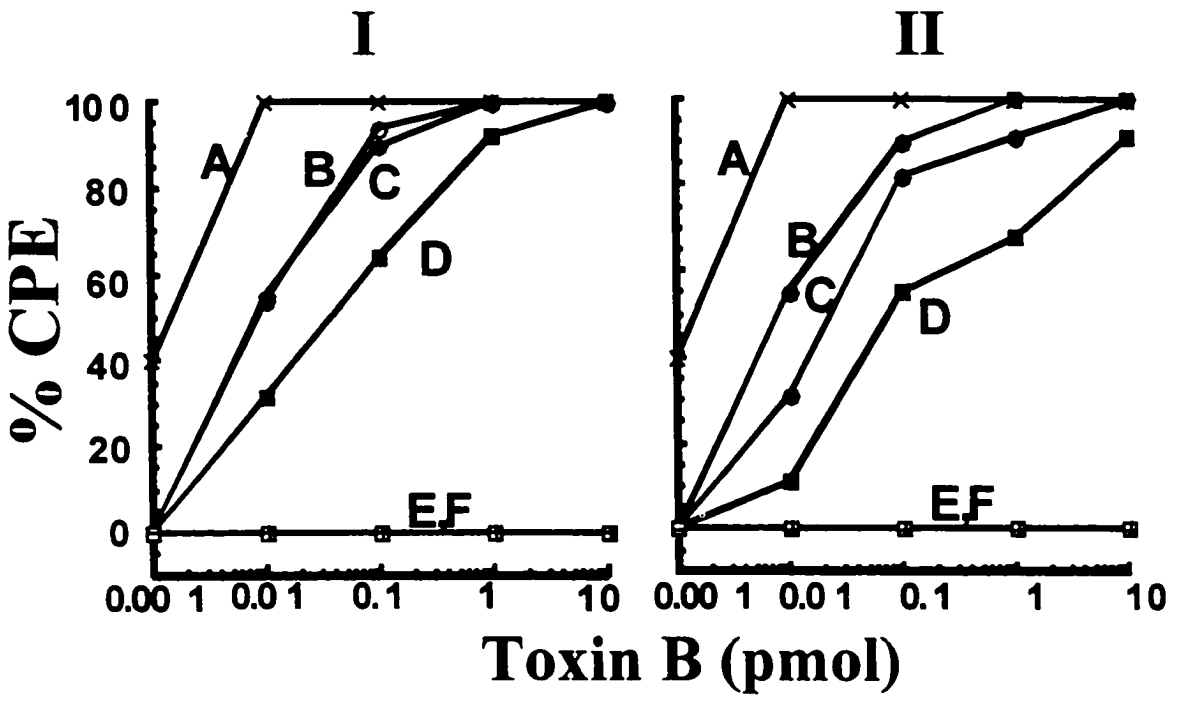


Figure 2. Acid Pulse Induced Entry of Toxin B. Endosomal acidification was inhibited with either ammonium chloride or bafilomycin A1. Cells were then subjected to a brief acid pulse at pH 4.0 followed by a return to neutral pH. Samples were followed for 8 h and cytopathic effects were determined by visualization. Panel I; Bafilomycin inhibitor and pH pulse. Panel II; Ammonium chloride inhibitor and pH pulse. A) Toxin B, pH 7.8, B) Toxin B pH 7.8, plus inhibitor, plus acid pulse, C) Toxin B predialyzed to pH 4.0, D) Toxin B pH 4.0, plus inhibitor, plus acid pulse, E) Toxin B pH 7.8, plus inhibitor, F) Toxin B pH 4.0, plus inhibitor

TNS fluorescence analysis of pH induced changes in toxin B hydrophobicity. TNS is a convenient probe for determining the exposure or sequestering of hydrophobic domains under varying conditions. To identify pH induced changes in toxin B hydrophobicity the protein was preincubated with 20 mM TNS for 20 min at either pH 7.0, 6.5, 6.0, 5.5, 5.0, 4.5 or 4.0. The samples were then analyzed for changes in TNS fluorescence. As shown in figure 3, toxin B exhibits a significant increase in hydrophobicity as pH declines. While there is little difference in the range of pH 5.5 to 7.0, at pH 5.0 there is a significant increase in fluorescence and the intensity continues to increase at pH 4.0. At the lowest pH, the fluorescent intensity has increased almost 100 fold over that of the neutral pH. This pH induced transition in hydrophobicity seems to be reversible since samples shifted from pH 4.0 to pH 7.0 demonstrate TNS fluorescence at background levels (figure 4).

Tryptophan fluorescence. Presumably the changes in hydrophobicity involve the movement of buried or less accessible hydrophobic regions into more aqueous environments. Since tryptophan fluorescence should be quenched under these conditions changes in the inherent fluorescence of the protein at neutral and acidic pHs should be revealed. In these experiments toxin B was incubated at 37°C at either pH 4.0 or pH 7.5. Environmental changes surrounding tryptophans were then followed by fluorescence

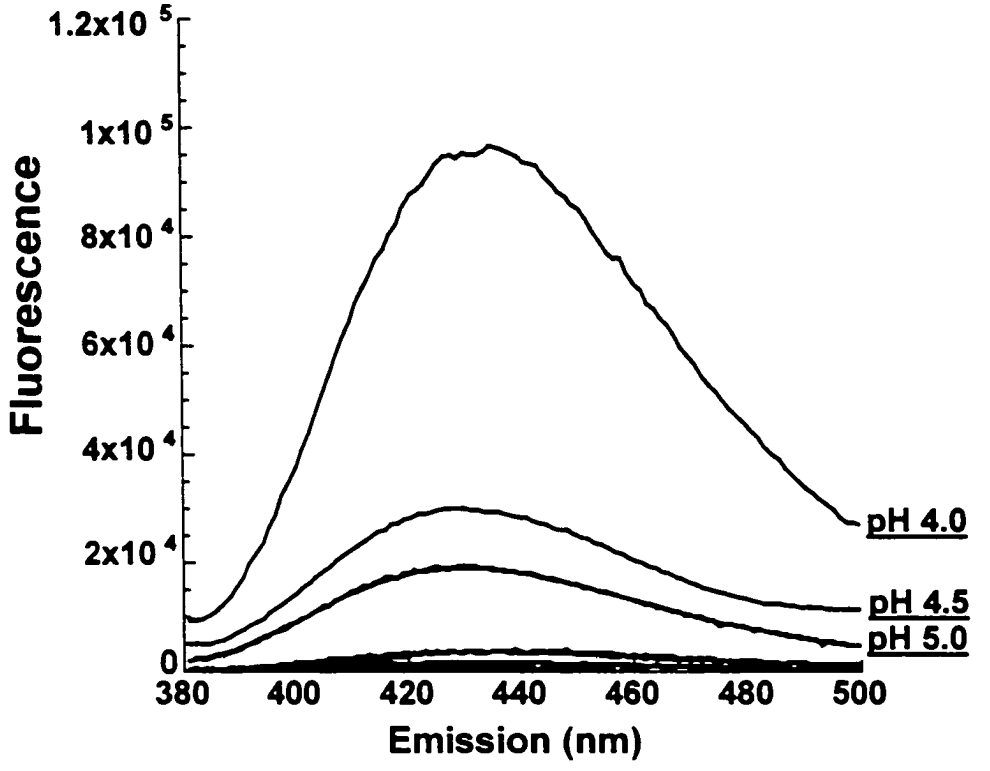


Figure 3. TNS analysis of pH induced hydrophobic transitions in toxin B. Twenty pmol of toxin B were incubated with 150 μM TNS for 20 min at 37°C. Samples were analyzed for changes in TNS fluorescence. The fluorescent spectra of each pH is shown as labeled. The spectra above represents the experimental sample with background (TNS and buffer alone) subtracted. TNS fluorescence for samples above pH 5.0 were not above background levels. Similar relative fluorescence was obtained in 2 consecutive repetitions of this experiment.

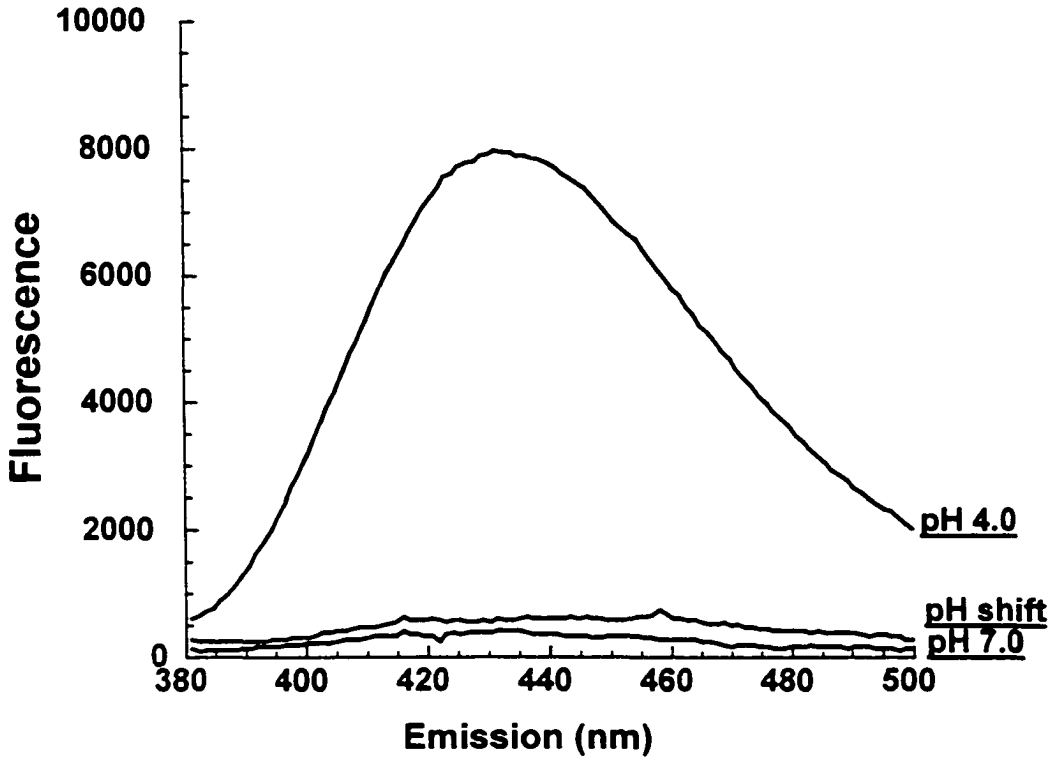


Figure 4. TNS analysis of toxin B hydrophobicity following pH shift. TNS was added to toxin B at pH 4.0, incubated for 20 min at 37°C, and the emission profile was determined. The pH was then raised to pH 7.0 and the TNS emission spectra was generated. The spectra above represent TNS-toxin B fluorescence after subtracting background (TNS plus buffer alone). Similar relative fluorescence was obtained in 2 consecutive repetitions of this experiment.

using an excitation of 270 nm and an emission scan from 300 nm to 400 nm. As can be seen in figure 5, there is a subtle shift in the fluorescent profile between pH 4.0 and pH 7.5. Tryptophan fluorescence is decreased at the lower pH, indicating that these residues are in a more solvent accessible environment.

V8 protease analysis. To further track the pH induced conformational changes in toxin B, we subjected the protein to protease digestion at pH 4.0 or pH 7.8. The *Staphylococcus aureus* derived V8 protease was selected since it maintains the same activity and specificity (peptide bond hydrolysis on the carboxylic side of glutamines) at both pHs (6, 9). In this experiment toxin B was incubated with V8 protease and the resulting digest was resolved by SDS-PAGE. As can be seen in figure 6, there is a difference in the proteolytic digest profile between the two pHs. We also made direct comparisons with different ratios of toxin to protease, to confirm that the effect was not due to varying degrees of activity at pH 4.0 and pH 7.8. Regardless of the ratio, we did not find a condition where the peptide profile was similar.

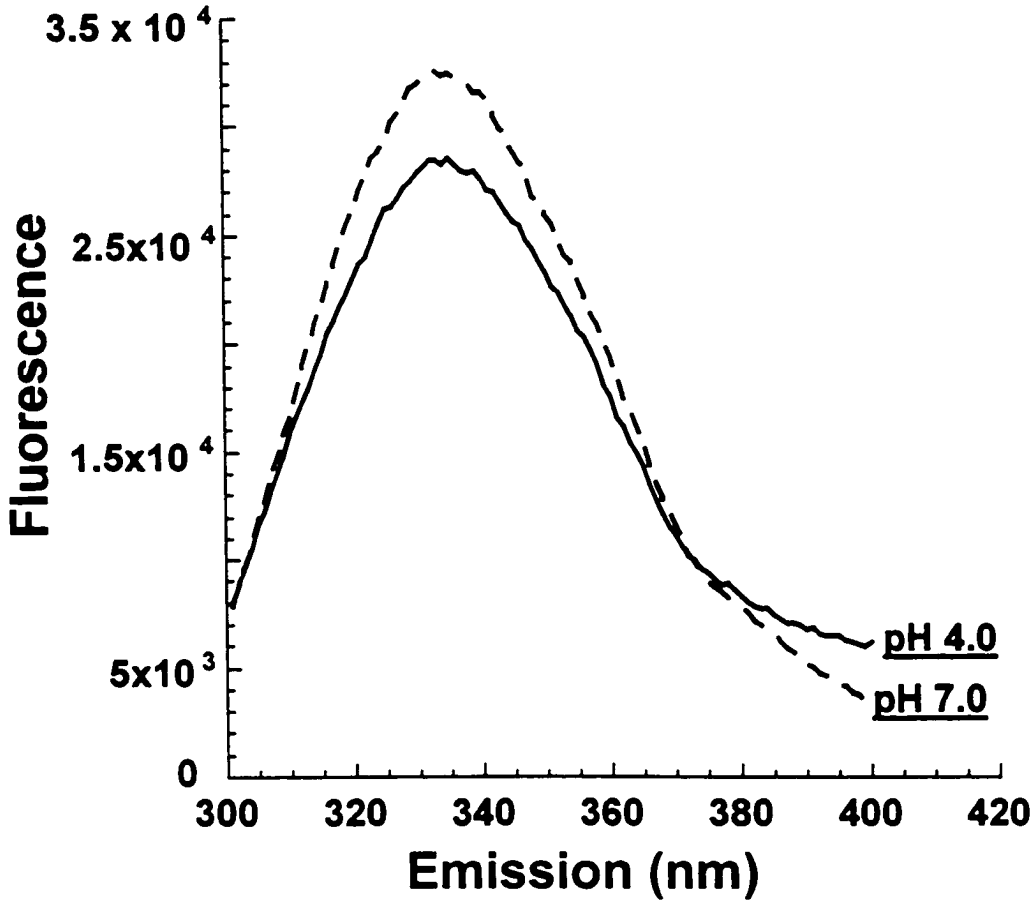


Figure 5. Tryptophan fluorescence of toxin B at acidic and neutral pH. Toxin B (20 pmol) was dialyzed to pH 4.0 or pH 7.0 and the tryptophan fluorescence was determined. The fluorescent spectra of each sample is shown and labeled above. The spectra above represents the experimental sample minus background. Similar relative fluorescence was obtained in 2 consecutive repetitions of this experiment.

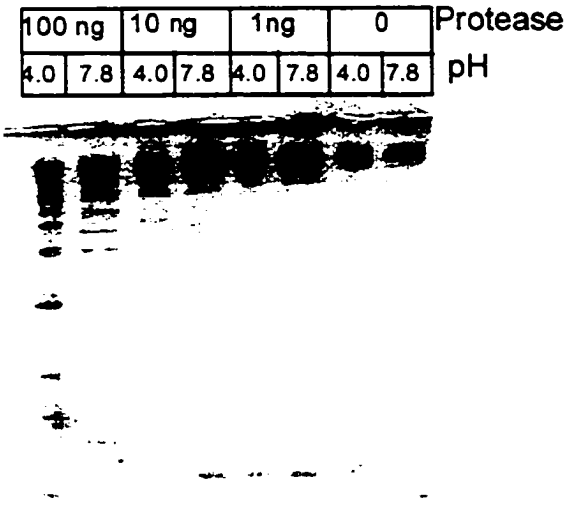


Figure 6. Relative susceptibility of toxin B to V8 protease at pH 4.0 and pH 7.8. Toxin B (75 pmol) was incubated with increasing dilutions of V8 protease at pH 4.0 or pH 7.8 for 1.5 h at 37°C. Controls of toxin B alone were included and incubated at the same pH and temperature. The samples were resolved by 10% SDS-PAGE and stained with commassie blue. The pH, amounts of V8 protease and controls are labeled above.

Discussion

Since intracellular bacterial toxins need to be relatively soluble following release from their host bacterium, they are not able to expose significant apolar domains. This presents a conundrum since the toxin must insert into a very hydrophobic environment, namely the phospholipid bilayer of the target cell membrane. For this reason intracellular bacterial toxins have had to evolve elegant mechanisms to alter their structure immediately prior to membrane insertion. By using pH as a signal, these proteins can exploit the natural processes of endocytosis and vacuolar acidification as a means to trigger the exposure of membrane insertable regions. Thus the hydrophilic molecule can remain soluble while outside the target cell and expose its membrane inserting domains when assured of having an accessible lipid bilayer. The purpose of this work was to determine if toxin B uses this type of mechanism for altering its structure and exposing hydrophobic regions.

Earlier work by Florin and Thelestam had addressed the issue of lysosomal involvement in intoxication by toxin B (7, 8). While this work focused on a cytotoxin from *C. difficile*, the reports indicated a protein of significantly different size to our isolated form of toxin B (440 kD instead of 270 kD). In a later paper these investigators report the amino terminal sequence and it matched the predicted sequence within toxin B. Interestingly, their protein seems to migrate as a larger form than ours and requires treatment with dithiothreitol for optimal toxic activity (14). Our purified form of toxin B shares some similar characteristics with this larger form. Like the larger form ours has an amino-terminal region matching predicted sequences, however reducing agents do not

appear to enhance the activity of our purified toxin B. These differences suggested I should confirm endosomal involvement in toxin B intoxication with my form before looking at the impact acidification has on toxin B structure. Using bafilomycin A1, an inhibitor of endosomal acidification, we found that acidification of the endosome is important for toxin B entry (figure 1). Additionally, I analyzed the temporal nature of entry and found that most of toxin B toxicity could be prevented up to 20 min following treatment. We were also able to circumvent this block by providing a brief acid pulse (figure 2). These results were in agreement with what was found by Thelestam and Florin with the larger, reductant dependent, form of toxin B. However, I was able to get pH pulse induced entry of toxin B from the cell surface in the absence of reducing agents. It remains unclear as to just what the actual differences, structurally, are between these two forms of the toxin. In spite of this, the data indicates that acid conditions have an impact on toxin B entry and that low pH alone seems to be sufficient for triggering translocation.

To identify the impact acidification has on toxin B structure, I followed pH induced structural changes by TNS fluorescence, tryptophan fluorescence and susceptibility to V8 protease. While toxin hydrophobicity at pHs 5.5 and above is not higher than background, beginning at pH 5.0 TNS fluorescence increases in the presence of toxin B (figure 3). TNS fluorescence continues to increase at pH 4.5 and pH 4.0. This increase in hydrophobicity appears to be reversible since raising the pH back to neutral conditions results in decreased fluorescence (figure 4). Whether the shift back to neutral pH causes refolding to the original conformation is currently being investigated. The toxin does

maintain toxic activity following acidification since toxin dialyzed to pH 4.0 still causes cell rounding (see figure 2). This toxic activity may be due to direct action of the pH 4.0 form or could be the result of the toxin refolding under the neutral conditions of the culture medium. Earlier reports suggested toxin B was inactivated by acid pH(15), which conflicts with our findings. The difference may be due to the fact that we slowly dialyzed toxin B into pH 4.0 buffer at 4°C, while the earlier work used a rapid dialysis method and incubation at room temperature.

The decreases in tryptophan fluorescence (figure 5) suggests tryptophan containing domains are moving into more aqueous environments or that hydrophobic pockets are moving away from tryptophans. In either case, the results suggest that toxin B is altering its structure in response to acidification. Finally, results from the V8 protease analysis further support our hypothesis that toxin B is going through pH induced structural changes (figure 6). Currently, I am investigating whether these structural changes and increases in hydrophobicity are in preparation for oligomerization and/or membrane insertion.

References

1.**Aktories, K.** 1997. Bacterial toxins that target Rho proteins. Journal of Clinical Investigation. **99**(5):827-9.

2.**Ayyagari, A., P. Sharma, Venkateswarlu, S. Mehta, and K. C. Agarwal.** 1986. Prevalence of Clostridium difficile in pseudomembranous and antibiotic-associated colitis in north India. Journal of Diarrhoeal Diseases Research. **4**(3):157-60.

3.**Ball, D. W., R. L. Van Tassell, M. D. Roberts, P. E. Hahn, D. M. Lyerly, and T. DWilkins.** 1993. Purification and characterization of alpha-toxin produced by Clostridium novyi type A. Infect Immun. **61**(7):2912-8.

4.**Boquet, P., P. Munro, C. Fiorentini, and I. Just.** 1998. Toxins from anaerobic bacteria: specificity and molecular mechanisms of action. Curr Opin Microbiol. **1**(1):66-74.

5.**Collier, R. J.** 1999. Mechanism of membrane translocation by anthrax toxin: insertion and pore formation by protective antigen. J Appl Microbiol. **87**(2):283.

6.**Drapeau, G. R., Y. Boily, and J. Houmard.** 1972. Purification and properties of an extracellular protease of Staphylococcus aureus. J Biol Chem. **247**(20):6720-6.

7.**Florin, I., and M. Thelestam.** 1983. Internalization of Clostridium difficile cytotoxin into cultured human lung fibroblasts. Biochim Biophys Acta. **763**(4):383-92.

8.**Florin, I., and M. Thelestam.** 1986. Lysosomal involvement in cellular intoxication with Clostridium difficile toxin B. Microbial Pathogenesis. **1**(4):373-85.

9.**Houmard, J., and G. R. Drapeau.** 1972. Staphylococcal protease: a proteolytic enzyme specific for glutamoyl bonds. Proc Natl Acad Sci U S A. **69**(12):3506-9.

10.**London, E.** 1992. Diphtheria toxin:membrane interaction and membrane translocation. Biochimica et Biophysica Acta. **1113**:25-51.

11.**Meador, J. d., and R. K. Tweten.** 1988. Purification and characterization of toxin B from Clostridium difficile. Infection & Immunity. **56**(7):1708-14.

12.**Menard, A., K. Altendorf, D. Breves, M. Mock, and C. Montecucco.** 1996. The vacuolar ATPase proton pump is required for the cytotoxicity of Bacillus anthracis lethal toxin. FEBS Lett. **386**(2-3):161-4.

13.**Pothoulakis, C., L. M. Barone, R. Ely, B. Faris, M. E. Clark, C. Franzblau, and J. T. LaMont.** 1986. Purification and properties of Clostridium difficile cytotoxin B. Journal of Biological Chemistry. **261**(3):1316-21.

14.**Shoshan, M. C., T. Bergman, M. Thelestam, and I. Florin.** 1993. Dithiothreitol generates an activated 250,000 mol. wt form of Clostridium difficile toxin B. Toxicon. **31**(7):845-52.

15.**Sullivan, N. M., S. Pellett, and T. D. Wilkins.** 1982. Purification and characterization of toxins A and B of Clostridium difficile. Infect Immun. **35**(3):1032-40.

Chapter II
pH Enhanced Cytopathic Effects of *Clostridium sordellii* Lethal Toxin

ABSTRACT

Clostridium sordellii lethal toxin (TcsL) is a large clostridial toxin (LCT) that glucosylates Ras, Rac and Ral. TcsL differs from other LCTs since it modifies Ras, which does not cycle from cytosol to membrane. Using a suite of inhibitors, steps in cell entry by TcsL were dissected and entry appears to be dependent on endosomal acidification, but in contrast to TcdB, TcsL was substantially slower in its time-course of entry. TcsL cytopathic effects (CPE) were blocked by bafilomycin A1 and neutralized by antiserum up to 2 h following treatment of cells with the toxin. This slow time course of intoxication and relatively high cytopathic dose were alleviated by exposing TcsL to acid pH resulting in a time-couse similar to TcdB. The optimal pH range for activation was pH 4.0 to pH 5.0, which increased the rate of intoxication over 5 fold, lowered the minimal intoxicating dose by over 100 fold, and allowed complete substrate modification within 2 h as shown by differential glucosylation. Fluorescence analysis of TcsL, using 2-(p-toluidinyl) naphthalene-6-sulfonic acid as a probe, suggested the acid pH stimulated a hydrophobic transition in the protein, a likely prelude to membrane insertion. Finally, acid entry by TcsL caused TcdB-like morphological changes on CHO cells, suggesting acid activation may be impacting substrate recognition profiles for TcsL.

INTRODUCTION

Clostridium sordellii, is an important veterinary pathogen, causing abosomal bloat, hemorrhage, ulcers, liver disease, myositis and sudden death in sheep(14, 21). *C. sordellii* has also been reported in human maternal deaths with a disease presenting as a toxic shock like syndrome (4, 15). Unfortunately, the etiology of *C. sordellii* disease remains poorly understood. Myonecrosis is apparently rather infrequent and death may be due to septicemia, as well as, the expression of several exotoxins. Like many of disease-causing clostridia, a single major virulence factor from *C. sordellii* has not been proposed and most of the *C. sordellii* toxins– including phosholipase-C, neuraminidase, and hemolysin- are largely uncharacterized (20). In contrast, two other *C. sordellii* extracellular toxins, hemorrhagic toxin (TcsH) and lethal toxin (TcsL), have garnished interest in recent years (6). Intrigue with TcsH and TcsL stems from both their unique mechanism of action as well as potential use as tools in cell biology (8, 16).

TcsH and TcsL are members of the large clostridial toxins (LCTs), which represent a novel group of exceptionally large (270 kD-304 kD) bacterial virulence factors with the capacity to inactivate multiple target substrates. Along with TcsH and TcsL, LCTs include *Clostridium difficile* toxins A and B (TcdA & TcdB), and *Clostridium novyi* alpha toxin (Tcnα). For recent reviews of LCTs see (1, 5, 6). LCTs target members of the Ras-superfamily of small GTP-binding proteins and, using UDP-glucose as a cosubstrate, TcsL, TcsH, TcdA and TcdB glucosylate Ras proteins with

varying substrate specificity. TcsH, TcdA and TcdB glucosylate Ras superfamily members Rho, Rac and Cdc42 whereas TcsL glucosylates Ras, Rac and Ral. Unlike other LCTs, Tcnα utilizes UDP-n-acetylglucosamine, rather than UDP-glucose, as a cosubstrate for glycosylation of Rho, Rac and Cdc42. In all cases the LCT glycosylates a threonine (T37 or T35) residue in loop 1 of the effector-binding region, thus blocking important downstream signaling events. For Rho, Rac and Cdc42, this inactivation may prevent effective membrane to cytosol cycling, regulation of actin polymerization, vesicular trafficking and transcriptional activation that ultimately causes extensive actin condensation, cell rounding, and cell death. Glucosylation of Ras prevents effective downstream signaling, such as phosphorylation of ERK1 and ERK2 MAP kinase (17).

As intracellular bacterial toxins, LCTs must enter or contact the cytosol to modify their target substrates. TcdB's mechanism of cell entry is the best characterized among LCTs and appears to require endosomal acidification and translocation from endocytic vesicles(10, 18). TcdB appears to translocate to the cytosol within 30 min following cell treatment, and at low pH the toxin exposes hydrophobic domains and forms ion-conducting channels(3, 18). Still, very little is known about the steps in cell entry for these remarkably large toxins, or if these steps in entry play any part in localization with particular substrates. The substrate targets of most LCTs cycle from the cytosol, where they are maintained in the GDP bound form, to the plasma membrane where the process of nucleotide exchange and activation can occur (11). In contrast, Ras, a target of TcsL, remains anchored at the cell membrane and does not cycle to the cytosol (2). Whether cellular localization plays a role in recognition of GTPase substrates by LCTs is not

known. In addition, it is not clear if the cellular glucosylation of Ras by TcsL is driven solely by substrate specificity or also involves a mechanism of cell entry different from other LCTs. In this study we investigated the mechanisms of cell entry by TcsL and report that TcsL CPE are dramatically enhanced by an extracellular acid pH, and blocked by lysosomotropic inhibitors. The acid pulsed entry increased the rate of TcsL intoxication, lowered the cytopathic dose, allowed complete substrate modification, and caused ultrastructrural effects similar to those of TcdB.

MATERIALS AND METHODS

Cell culture and media. Chinese hamster ovary (CHO)-K1 cells, human epitheloid carcinoma (HeLa) cells and mouse macrophage RAW cells were all obtained from ATCC (American Type Culture Collection Manassas, VA). These cell lines were maintained in RP-10 medium supplemented with 10% fetal bovine serum. Cultures were grown at 37°C in the presence of 6% CO_2. Unless otherwise noted all reagents and chemicals were purchased from Sigma (Sigma Chemical, St. Louis, MO).

Purification of TcsL and TcdB. *C. sordellii* strain 9714 (American Type Culture Collection Manassas, VA) or *C. difficile* strain 10463 (American Type Culture Collection Manassas, VA) were grown in cellulose ester dialysis tubing with a 10,000 to 12,000-molecular-weight-cutoff (Spectrum Medical Industries, Houston, Tex.) suspended in 1 L of 0.5X brain heart infusion broth (Becton Dickinson, Sparks, Md). Following growth at 37°C for 72 h the culture was centrifuged at 12,000 X g for 30 min, and the supernatant

was collected. TcsL and TcdB were subsequently purified at 4°C by sequential steps of high-resolution liquid chromatography as previously described (18). Each step in the purification was followed by cytotoxicity assays on CHO cells, Western blot analysis using TcdB polyclonal antiserum (a generous gift from Rodney Tweten), and visualization by sodium dodecyl sulfate-poly acrylamide gel electrophoresis (SDS-PAGE). Additionally, the activity of purified TcsL was confirmed based on its substrate recognition profile (glucosylation of Rac, but not Rho and Cdc42). Following the final step of purification, the protein concentration was determined by Bradford assay (Bio-Rad Laboratories, Hercules CA), and the sample was frozen at -80°C in 100 µl aliquots. Prior to use, samples of each toxin were thawed on ice and used immediately. Since repeated freeze thawing caused increased degradation, aliquots of TcsL and TcdB were thawed once, used in the appropriate experiment and discarded.

Inhibitor experiments. For inhibitor assays, CHO, HeLa, or RAW cells from a confluent monolayer were plated at 3 x 10^4 cells/well in a 96-well plate and incubated for 18 h. Cells were then preincubated for 30 min with 1 x 10^{-2} M ammonium chloride, 1 x 10^{-5} M monensin, or 1 x 10^{-7} M bafilomycin A1 at 37°C. One pmol of TcsL or TcdB was added to the inhibitor-treated cells the CPE were followed by visualization. For the time-course assay, CHO cells from a confluent monolayer were plated at 5 x 10^4 cells/well in a 96-well plate and incubated for 18 h, at which point 1 pmol of TcsL was added to the cells. At the indicated time points bafilomycin A1 was added to the treated cells to a final concentration of 5 x 10^{-7} M. Each sample was monitored for 16 h, and CPE were determined by visualization.

Acid pulse experiments. CHO, HeLa or RAW cells from confluent monolayers were plated at 5 x 10^4 cells/well in a 96-well plate, incubated for 18 h, then treated with either 5 x 10^{-7} M bafilomycin A1 or 100 mM ammonium chloride for 30 min. Following treatment with the lysosomotropic agents, TcsL was added to cells across 10 fold dilutions in amounts ranging from 10 pmol to 1 fmol in a total volume of 100 µl. One hour following toxin treatment at 37°C, an acid pulse was performed by exposing the cells to acidified medium (pH 4.0) for 10 min, and then replacing it with neutralized medium (pH 7.5). To determine the optimal pH for activation, cells were incubated with TcsL for 1 h 37°C, and then buffered media at was added to cells for 10 min, then removed and replaced with neutralized medium (pH 7.5). The buffers and pHs are as follows: 100 mM ammonium acetate for pHs 4.0, 4.5, 5.0, 5.5, 100 mM morpholineethanesulfonic acid (MES) for pHs 6.0 and 6.5, 100 mM Tris pHs 7.0 and 7.5. The treated cells were monitored for 11 h at 37°C and CPE was determined by visualization.

Fluorescent analysis of TcsL. Fluorescent analyis of TcsL was performed as previously described for TcdB (18). Briefly, 2-(p-toluidinyl) naphthalene-6-sulfonic acid, sodium salt [TNS] (Molecular Probes, Eugene, OR) solutions were prepared in the appropriate buffers for each of the pHs to be analyzed and used at final concentration of 150 µM. Twenty pmol of TcsL was added to each buffer in a final volume of 2 ml and incubated at 37°C for 20 min. Each sample was analyzed on a SLM 8100 photon counting

fluoremeter (Spectronic Instruments, Rochester, NY) with an excitation of 366 nm and an emission scan of 380 nm to 500 nm using a slit width of 2.0. For the pH shift experiments 20 pmol of TcsL was incubated with 150μM TNS, 50 mM TRIS, 1mM EDTA, 100 mM NaCl, pH 7.5. for 20 min and fluorescence was determined. The pH was adjusted to pH 4.0 by the gradual addition of 1 N HCl, and the emission spectrum was generated. The pH was then adjusted back to pH 7.5 by gradual addition of 1 N NaOH and the fluorescence spectrum was determined again.

TcsL neutralization assays. CHO cells and HeLa cells from a confluent monolayer were plated at 5 x 10^4 cells/well in a 96-well plate and incubated for 18 h, at which point TcsL or TcdB were added to cells at a final concentration of 2 x 10^{-9} M. At the indicated times, anti-TcdB antibody was added to the TcsL and TcdB treated cells, or cells were washed 4 times with 100 μl phosphate buffered saline. Cells were then monitored for 11 h and CPE were determined by visualization.

Scanning electron microscopy (SEM). SEM analysis was carried out at the Samuel Noble electron microscopy facility (The University of Oklahoma). CHO cells from a confluent monolayer were plated at 1 x 10^5 cells/well in a 24-well plate and incubated for 18 h, at which point cells were treated with TcsL, acid pulsed TcsL, or TcdB. After 11 h, cells were incubated with 2.5% gluteraldehyde 0.1 M cacodylate buffer at pH 7.3 for 30 min. Cells were then incubated with 0.1 M cacodylate buffer 1% osmium tetroxide pH 7.3 for 1 h. The cells were then washed 3 times with 1 ml/well cacodylate buffer at pH 7.3. Samples were then dehydrated in a graded series of ethanol ranging from 30% to

100%. Critical point drying followed using autosamdri-814 (Tousimis Research Corporation, Rockville, MD), at which point, samples were coated with gold up to 400 A in a Hammer VI sputter coating unit (Anatech LTD, Alexandria, VA). Observations were performed in a JEOL JSM-880 Scanning Electron Microscope.

Glucosylation Assay. Extracts from treated CHO cells were used as a source of substrate for TcsL glucosylation. To prepare these extracts, CHO cells were grown in 75 cm^2 tissue culture flasks until confluent at a density of ~$1x10^7$ cells/flask. The cells were treated with 20 pmol TcsL in the presence of bafilomycin A1, with or without an acid-pulse. Two hours following treatment the cells were then washed three times in ice cold PBS followed by mechanical removal in the presence of lysis buffer (1 mM $MgCl_2$, 1 mM $MnCl_2$, 0.1 mM phenylmethylsulfonyl fluoride (PMSF), 10 μg/ml leupeptin, 25 mM triethanolamine-HCl (pH 7.5)) similar to a previously described method (13). Cells were sonicated on ice 5 times for 30 sec intervals and the resulting extract was centrifuged at 40K x g for 8 h. The supernatant was removed and concentrated in a centricon concentrator with a 10 kD mwco (Millipore, Bedford, MA) until the extract reached a final volume of 0.5 ml.

For the glucosylation assay, CHO extracts (2 mg/ml) were added to a glucosylation mix containing 50 mM HEPES, 100 mM KCl, 1 mM $MnCl_2$, 1 mM $MgCl_2$ 100 μg/ml BSA, 35 μM[^{14}C]UDP-glucose (308 Ci/mol; ICN Pharmaceuticals Inc., Irvine, CA) and 10 μg/ml TcsL in a final reaction volume of 20 μl. The reaction was incubated for 2 h at 37°C and resolved by SDS-PAGE on a 15% acrylamide gel and

imaged on a Packard electronic autoradiograph instant imager (Packard Instrument Company, Meriden, CT) similar to previously described methods (12).

RESULTS

Effects of lysosomotropic agents and time-course of cell entry by TcsL. The steps in cell entry for TcdA and TcdB have been documented by others and our group (9, 10, 18). While TcsL is genetically similar to TcdA and TcdB, the toxin targets different substrates, and the extent to which cell entry contributes to this difference in target recognition is not known. Since TcsL is known to interact with cytosolic targets, the toxin may exploit vesicular trafficking to gain access to substrates. In the first set of experiments we directly compared the impact inhibitors of endosomal acidification or inhibiting conditions had on TcsL and TcdB entry. Using CHO, HeLa and RAW cell lines, I tested monensin, bafilomycin A1 and ammonium chloride for the ability to block TcsL CPE and found, similar to previous reports, (3, 17) that TcsL induced CPE were blocked by the inhibitors of endosomal and lysosomal acidification. Similar to earlier reports on TcdB, cellular intoxication was blocked by monensin, bafilomycin A1 and ammonium chloride (data not shown).

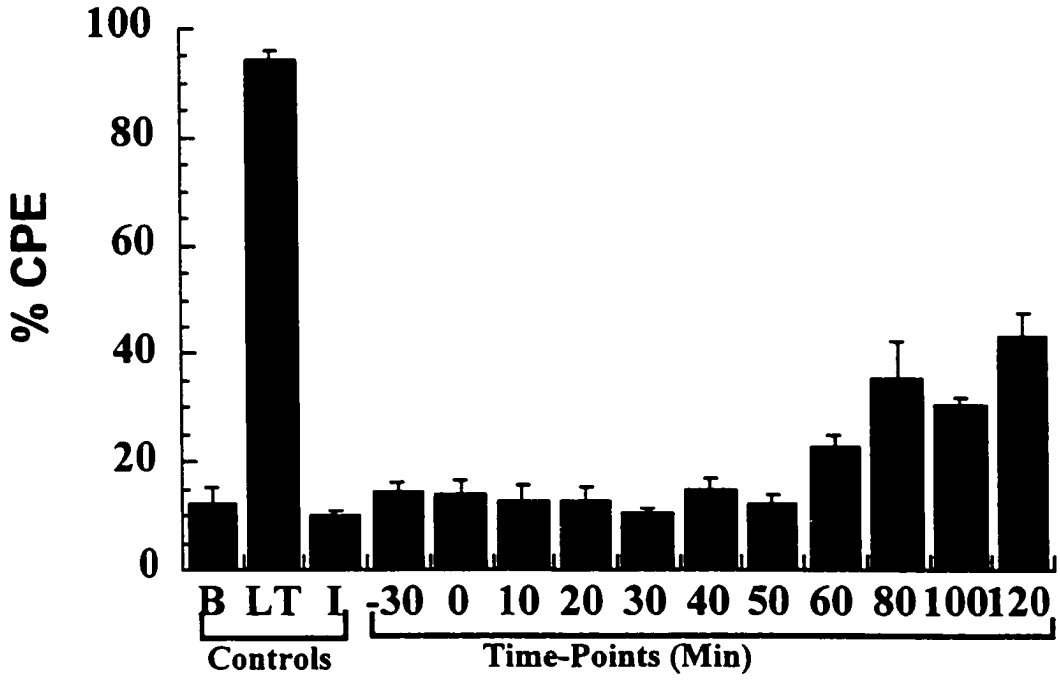


Fig. 1. Time course of TcsL cytosolic entry. In a 96-well plate CHO cells (5 X 10^4 cells/well) were incubated with TcsL (1 pmol) in a final volume of 100 µl, and bafilomycin A1 (1 x 10^{-7} M) was added at 10-min intervals from 0-180 min. Each sample was tested in triplicate, and CPE were determined at 16 h. The error bars mark the standard deviation from the mean. Similar levels of inhibition were found in two subsequent repetitions of the same experiment. B, PBS control; LT, TcsL; I, bafilomycin.

Using bafilomycin A1, we were also able to estimate the time-course of cytosolic entry by TcsL and make comparison with the known time-course of entry for TcdB. In this experiment, target cells (CHO, HeLa and RAW) were treated with bafilomycin A1 at various times prior to and following toxin treatment. If the toxin enters the cytosol, adding bafilomycin A1 should no longer block CPE. As shown in figure 1, unlike previous work with TcdB where we reported entry was almost complete within 30 min, we found that adding bafilomycin A1 up to 2 h following TcsL treatment blocked more than 60% of TcsL cytotoxicity. These results suggested TcsL entry into the cytosol was significantly slower than had been reported for TcdB and might account differences in the time-course of intoxication between the two toxins.

Extracellular pH pulse bypasses the bafilomycin A1 block. To determine whether the blocking effects of bafilomycin A1 could be bypassed, cells, preteated with bafilomycin A1, were treated with TcsL for 1 h at 37°C and then acid pulsed (pH 4.0) for 10 min. Interestingly, as shown in figures 2 and 3, the acid pulse entry of TcsL not only relieved the bafilomycin A1 block, but also dramatically increased the rate of intoxication, as well as significantly reducing the minimal cytopathic dose. Treatment with acid pulsed TcsL

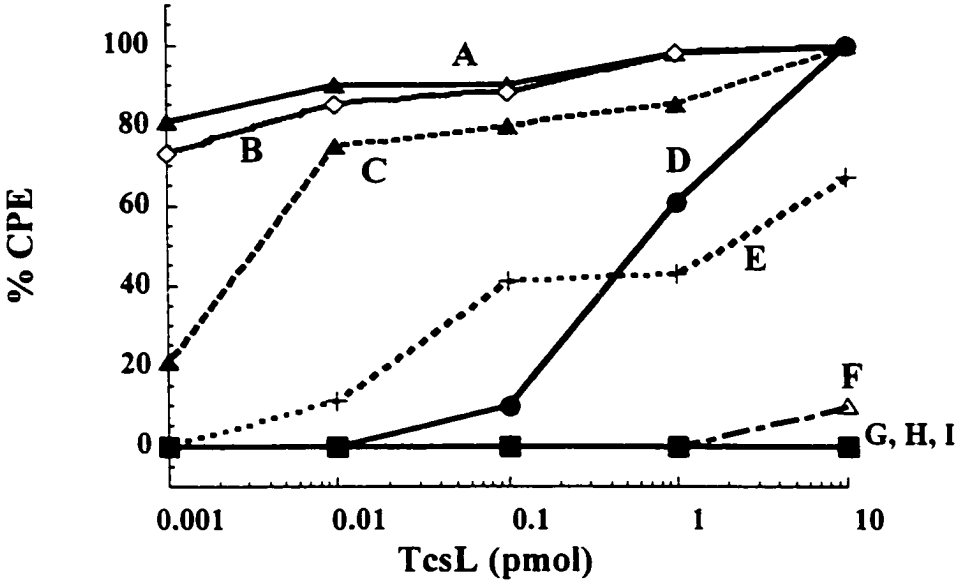


Fig. 2. pH range of acid pulse induced entry of TcsL. In a 96-well plate, CHO cells ($5x10^4$ cells /well) were incubated with bafilomycin A1 (5×10^{-7} M) in a final volume of 100 µl for 30 min. The cells were then treated with TcsL (1 pmol) for 1 h at 37°C and subjected to a 10 min pH pulse across a range of pHs and finally returned to the pH 7.8 by addition of neutralized medium. Samples were followed for 11 h, and CPE were determined by visualization. Similar effects were determined for CHO, HeLa and RAW cells. Curves: (A) pH 4.0; (B) pH 4.5; (C) pH 5.0; (D) TcsL (no pulse); (E) pH 5.5; (F) pH 6.0; (G) pH 6.5; (H) pH 7.0; (I) pH 7.5.

resulted in toxic effects within less than 1 h and reached 100% within 2 h. In contrast the first CPE from TcsL treatment at neutral pH are not evident until 6 h and did not reach maximum until after 10 h. At neutral pH the amount of TcsL yielding 50% cytopathic dose was 500 fmol, whereas the acid pulse 50% cytopathic dose was less than 1 fmol. The CPE was not a reflection of cell necrosis since at 2 h all the cells appeared viable by trypan blue exclusion assay (data not shown).

I also investigated whether the acid pulsed TcsL effect could be initiated by preincubating the toxin at pH 4.0 prior to treating cells. When TcsL was preincubated for 30 min at pH 4.0 then added to cells in neutral pH media, there was no enhanced cytopathic effect. however, when TcsL pretreated at acid pH was added to cells with acidified media the CPE were similar to acid pulsed TcsL (data not shown).

The optimal pH for TcsL activation was determined by pH pulsing the toxin in the presence of cells at pHs ranging from pH 8.0 to pH 4.0. As can be seen in figure 2, pH 5.5 appears to be the highest pH at which the rate of intoxication increases dramatically.

Acid pH stimulates hydrophobic transitions in TcsL. TNS is a convenient probe for determining the exposure or sequestering of hydrophobic domains under varying conditions. In an earlier report we had shown that TcdB goes through low pH-induced structural changes which stimulate an increase in TNS fluorescence (18). To determine whether acid pH was having a similar impact on TcsL structure, we carried out a set of TNS fluorescence experiments. As shown in figure 4, and in line with our previous report on TcdB, we found that as TcsL is exposed to lower pH the protein begins to expose more hydrophobic regions. Furthermore, and also similar to TcdB, this hydrophobic transition is reversible since raising the pH back to neutrality results in a decrease in TNS fluorescence.

Neutralization of extracellular TcsL. While TcdB and TcsL appear to be similar in some aspects of cell entry and acid-induced structural changes, the two proteins are set apart by the long delay in cytosolic entry by TcsL at neutral pH. This slow entry might be explained by a slow rate of effective cell binding or relatively slow entry under test conditions. To address these possibilities we used a washing procedure and antibody neutralization assay to determine at which time-point TcsL has been endocytosed under neutral pH conditions. In one experiment cells were treated with TcsL and washed 3

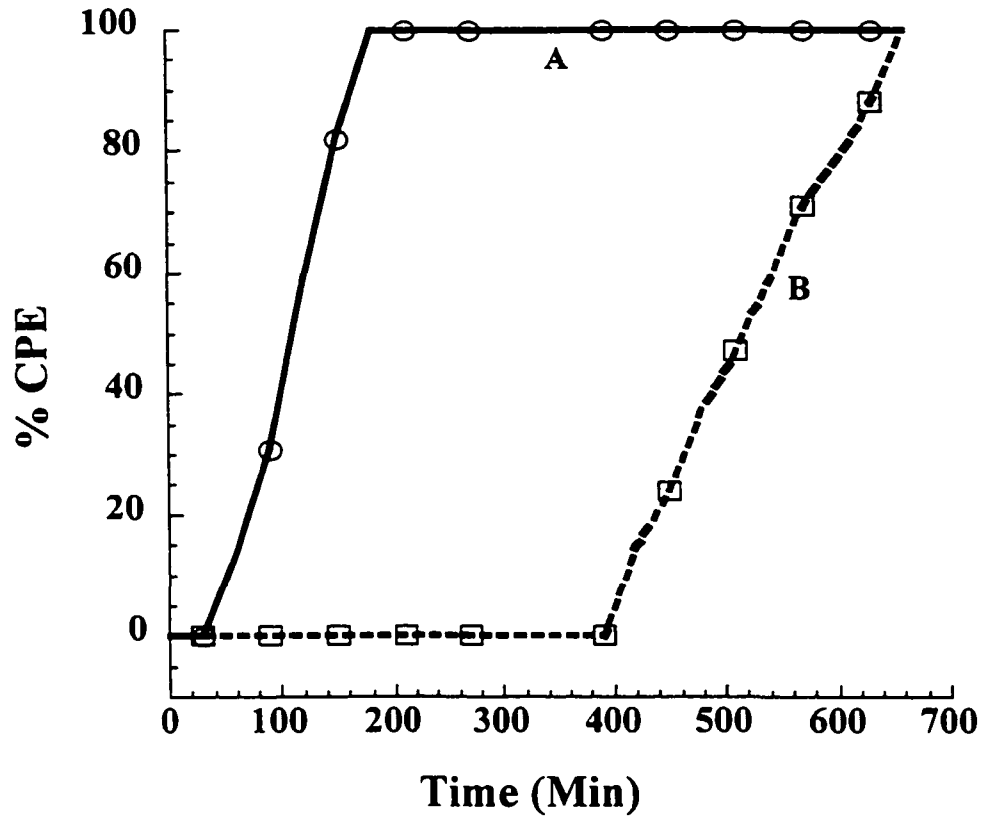


Fig. 3. pH enhanced rate of intoxication by TcsL. . In a 96-well plate CHO cells (5 X 10^4 cells/well) were treated with either 1 pmol of TcsL or acid pulsed TcsL (pH 4.0) in the presence of bafilomycin A1 (1 x 10^{-7} M) in a final volume of 100 µland then observed for 11 h. CPE were determined by visualization. Curves: A, acid pulsed TcsL; b, TcsL. Similar rates were obtained for HeLa and RAW cells.

times vigorously at specific time-points to remove accessible toxin, then followed for 18 h to determine CPE. As shown in panel A of figure 5, TcsL CPE could be depleted by washing the cells up to 3 h after treatment, indicating a majority of TcsL was still accessible at the cell surface and, apparently not tightly bound. For comparison, TcdB was subjected to the same wash experiment and, as shown in figure 4, by 20 min the CPE could not be reduced by washing the cells.

Neutralizing antibody had a similar effect on treated cells. The addition of anti-TcdB polyclonal serum, which cross neutralizes TcsL, also blocked the CPE of TcsL 3 hours following the addition of TcsL to target cells (figure 4 panel B). When cells were acid pulsed with TcsL, the effects of washing and antibody neutralization were similar to TcdB. The delay in TcsL activity did not appear to be due to extracellular activation, since preincubating TcsL with culture media did not increase the rate of intoxication (data not shown).

SEM analysis of CHO cells treated with acid pulsed TcsL. In addition to adopting a time-course of intoxication similar to TcdB, acid pulsed TcsL also appeared to confer morphological changes similar to TcdB. When examined under an inverted light microscope, cells treated with acid pulsed TcsL demonstrated a different morphology than cells treated with TcsL at neutral pH (data not shown). Furthermore, the cells

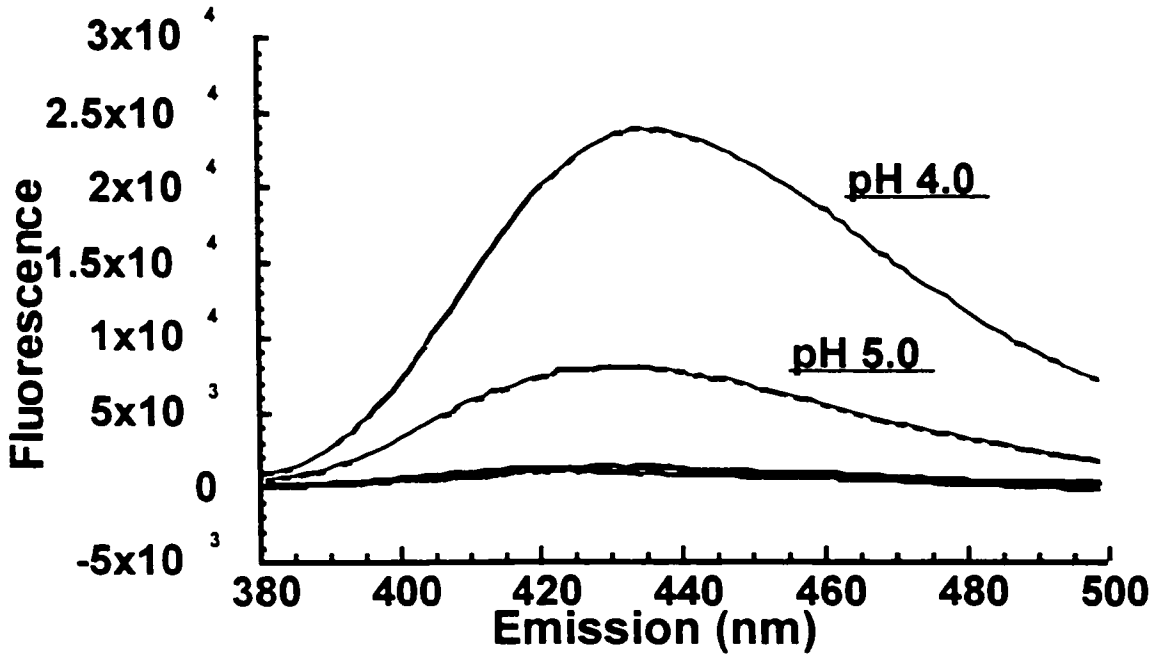


Fig. 4. (A) TNS fluorescent analysis of TcsL. The analysis of pH-induced conformational changes in TcsL was carried out using the fluorescent probe, TNS. Each spectrum represents the experimental sample with background (TNS and buffer alone) subtracted. For the pH shift condition, the toxin was treated with TNS at pH 7.5, the solution was then titrated to pH 4.0 by gradual addition of 1 N HCl and returned to neutrality by addition of 1 N NaOH. TcsL hydrophobicity across a range of pHs. TNS fluorescence for samples above pH 5.0 were not above background levels. Emission from pHs 6.0, 7.0 and 8.0 were not detectable above background.

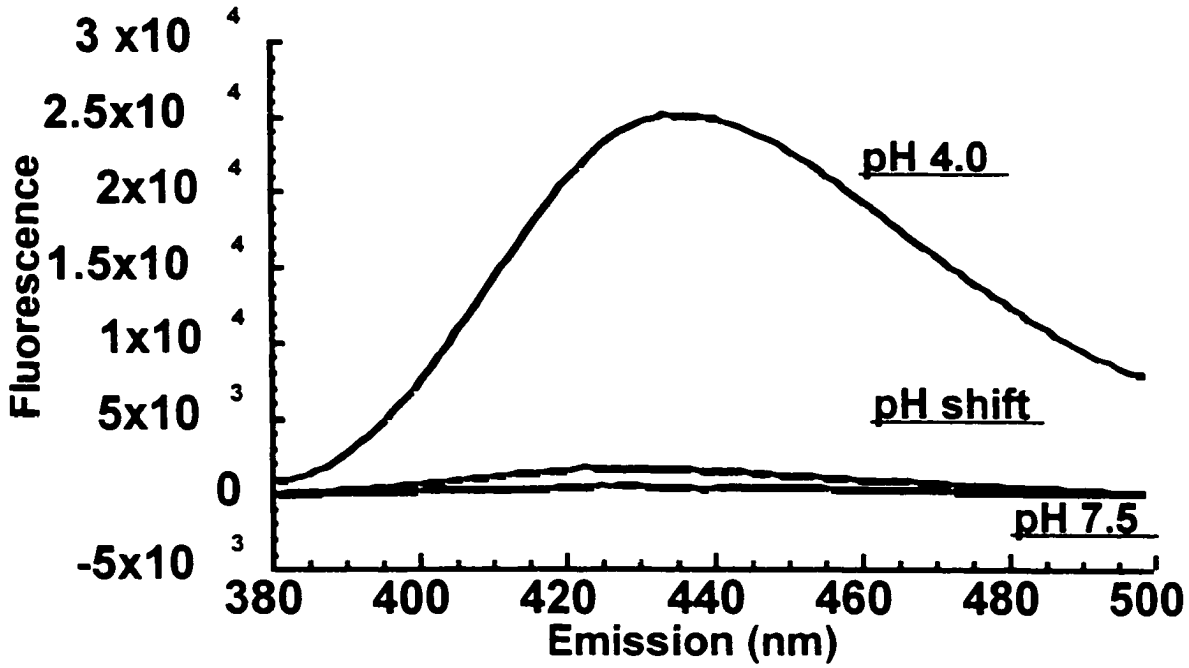


Fig. 4 (B) TNS analysis of TcsL hydrophobicity following pH shift.

treated with acid pulsed TcsL looked remarkably similar to TcdB treated cells (data not shown). To better characterize these changes in morphology we analyzed the treated cells by SEM. Since the time-course of intoxication is different between acid pulsed TcsL and TcsL at neutral pH, we attempted to normalize the effect by examining the cells at time points when rounding was complete but cell death, assayed by trypan-blue exclusion, had not occurred. In the case of TcdB and acid-pulsed TcsL this time point was 2 h and for TcsL at neutral pH this time point was 11 h. As shown in figure 5, SEM analysis of CHO cells treated with acid pulsed TcsL appeared similar to TcdB treated cells, with rounding and smooth cell surfaces. This morphology was clearly different from cells treated with TcsL at neutral pH, where rounding and extensive cell surface blebbing had occurred.

Differential glucosylation in extracts from cells treated with acid pulsed TcsL. Recently, Barth et al. (3) reported on the pH induced channel forming activity of TcdB and TcsL. Therefore it was possible that the CPE of cells treated with acid pulsed TcsL were due to the formation of channels at the cell surface and not related to cytosolic entry. To address this possibility we examined lysates from cells treated with TcsL at neutral pH or with an acid pulse to determine the relative amount of glucosylated substrate. CHO cells were treated with TcsL under the two conditions and incubated for 2 h at which point the cells were collected and lysates were prepared. The lysates from these samples were then used in glucosylation assays to determine whether acid pulsed entry allowed TcsL access to the substrate targets. As can be seen in figure 7, lysates from cells treated with acid pulsed TcsL did not have accessible substrate, whereas cells treated with TcsL at neutral pH were still able to present substrate for glucosylation. These results suggest that while channels may be formed during the acid pulse entry, the observed CPE are more likely a result of substrate modification.

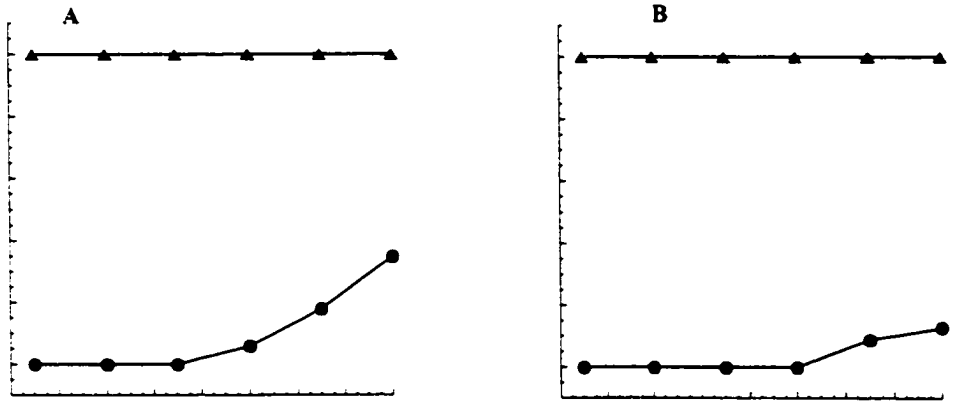


Fig. 5. Time-course of TcsL extracellular neutralization. In a 96-well plate CHO cells ($5x10^4$ cells/well) were treated with either 1 pmol of TcdB, TcsL or acid pulsed TcsL in a final volume of 100 µl. At the indicated time points cells were then subjected to neutralizing antiserum or wash treatments. (A) Treated cells were washed vigorously with PBS four times at the indicated time points; (B) Neutralizing antiserum (10 µl) was added to cells at the indicated time-points. In both experiments cells were then followed for 11 h, and CPE were determined by visualization. Curves: TcdB (triangle); TcsL (circles).

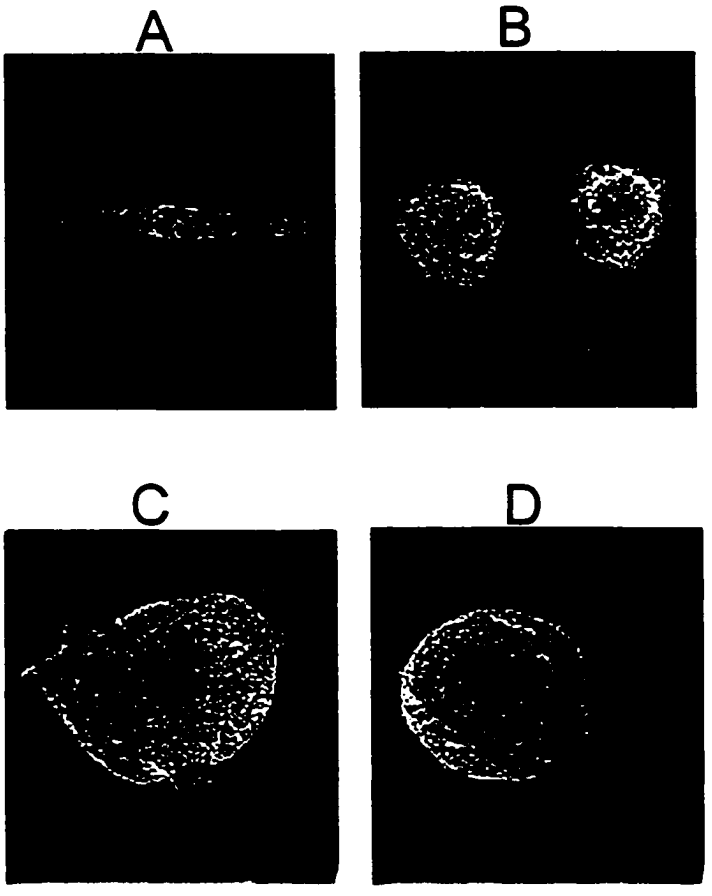


Fig. 6. SEM analysis of TcdB, TcsL and acid pulsed TcsL treated CHO cells. CHO cells were grown on cover slips and treated 1 pmol of either TcdB, TcsL, or acid pulsed TcsL in a final volume of 100 µl. After detecting changes in morphology, cells were fixed, dried, and mounted for SEM analysis and visualization. (A) PBS control (magnification, X 1,600); (B) TcsL (magnification, X 3,300); (C) TcdB (magnification, X 7,500); (D) acid pulsed TcsL (magnification, X 7,500).

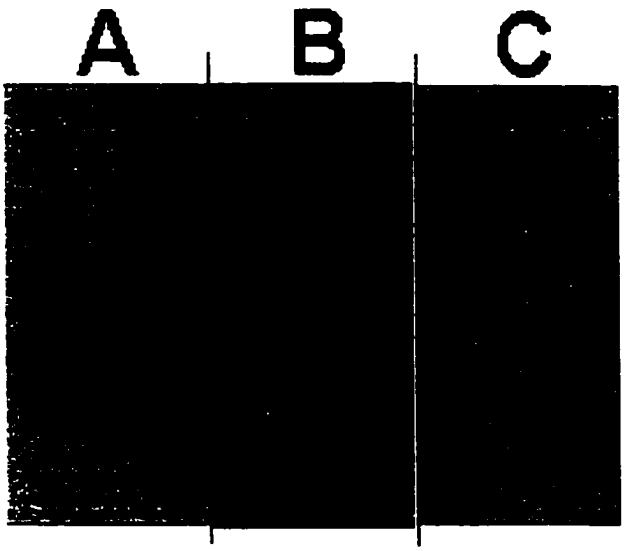


Fig 7. TcsL differential glucosylation of extracts from TcsL and acid-pulsed TcsL treated cells. Extracts from CHO cells which had been treated with 1 pmol of acid-pulsed TcsL or TcsL were used in glucosylation assay to determine if pretreatment under these conditions blocks substrate. Glucosylation assays were carried out using [^{14}C]UDP-Glucose and TcsL with the extracts as target substrates. Incorporation of the radiolabeled glucose was determined by autoradiography. (A) Glucosylation of extracts from PBS-treated CHO cells; (B) Glucosylation of extracts from TcsL-treated CHO cells; (C) Glucosylation of extracts from TcsL (acid pulsed; pH 4.0) treated CHO cells.

DISCUSSION

Although TcsL and TcdB are genetically similar (83% identity), these toxins target different sets of substrates (5). Interestingly, TcsL targets Ras which, unlike other LCT substrates, remains anchored at the inner plasma membrane and, following farnesylation, does not cycle from this site to the cytosol. Whether TcsL also differs from TcdB in its mechanism of entry has not been investigated. Based on the results from our inhibitor assays, TcsL entry appeared to be similar to TcdB entry. Furthermore, acid pH appears to have similar effect on TcdB and TcsL structure, stimulating the exposure of hydrophobic regions. The possibility that these two toxins are temporally different in their entry pathways became evident to us from the bafilomycin A1 time-course studies. In a previous study we found that treatment with bafilomycin A1 was ineffective at blocking TcdB activity when added to cells 30 min after toxin treatment (18). Results from the washing and antibody neutralization experiments suggest the lag in cell entry could be accounted for, at least in part, by a slow initiation of endocytosis or low affinity for the tested cells at neutral pH. All of these effects-slow entry, low rate of intoxication, and high cytopathic dose-could be alleviated by providing a brief acid pulse at the cell surface.

The increase in cytopathic activity for acid pulsed TcsL differs from our previous report on TcdB (18). In the earlier TcdB experiments the blocking effects of lysosomotropic agents could be bypassed using an extracellular acid pulse; however, acid pulse entry did not dramatically reduce the cytopathic dose. While different from TcdB, acid pulsed

TcsL entry does appear to be similar to the activity reported for diphtheria toxin almost 20 years ago (19). In the case of diphtheria toxin, while presumably not the natural mode of entry, bypassing time-consuming steps in vesicular trafficking with an acid pulse increases the rate of inhibition of protein synthesis. As a further comparison, *Helicobacter pylori* VacA requires extracellular acid pH for activation and is optimally active under these conditions (7). For VacA the acid enhanced activity appears to be part of the natural mode of action for this toxin, since *H. pylori* may face an acidified environment. In the case of TcsL, whether the acid pH conditions reflect a natural mechanism of activation or simulation of the endocytic vesicle is unclear.

Finally, there is only limited information on *C. sordellii* disease and very little is known about the tissue or cell type that this organism targets. In this study I selected three cell lines (CHO, HeLa, RAW) to use as targets in our assays and each of these cell lines gave similar data. Since the receptor for TcsL is not known, I can not dismiss the possibility that low receptor number might account for the slow entry, as well as account for the results from the wash and antibody neutralization experiments. Low receptor number would not account however for the blocking activity of lysosomotropic inhibitors and the acid pulse effects. Taken together these data certainly suggest endosomal trafficking and acid pH are important to the entry and cytopathic activity of TcsL.

REFERENCES

1. **Aktories, K., G. Schmidt, and I. Just** 2000. Rho GTPases as targets of bacterial protein toxins Biol Chem. **381:**421-6.

2. **Bar-Sagi, D., and A. Hall** 2000. Ras and Rho GTPases: a family reunion Cell. **103:**227-38.

3. **Barth, H., G. Pfeifer, F. Hofmann, E. Maier, R. Benz, and K. Aktories** 2001. Low pH-induced formation of ion channels by Clostridium difficile toxin B in target cells J Biol Chem. **276:** 10670-6

4. **Bitti, A., P. Mastrantonio, P. Spigaglia, G. Urru, A. I. Spano, G. Moretti, and G. B. Cherchi** 1997. A fatal postpartum Clostridium sordellii associated toxic shock syndrome J Clin Pathol. **50:**259-60.

5. **Boquet, P.** 1999. Bacterial toxins inhibiting or activating small GTP-binding proteins Ann N Y Acad Sci. **886:**83-90.

6. **Boquet, P., P. Munro, C. Fiorentini, and I. Just** 1998. Toxins from anaerobic bacteria: specificity and molecular mechanisms of action Curr Opin Microbiol. **1:**66-74.

7. **de Bernard, M., E. Papini, V. de Filippis, E. Gottardi, J. Telford, R. Manetti, A. Fontana, R. Rappuoli, and C. Montecucco** 1995. Low pH activates the vacuolating toxin of Helicobacter pylori, which becomes acid and pepsin resistant J Biol Chem. **270:**23937-40.

8. **Doussau, F., S. Gasman, Y. Humeau, F. Vitiello, M. Popoff, P. Boquet, M. F. Bader, and B. Poulain** 2000. A Rho-related GTPase is involved in Ca(2+)-dependent neurotransmitter exocytosis J Biol Chem. **275:**7764-70.

9. **Fiorentini, C., and M. Thelestam** 1991. Clostridium difficile toxin A and its effects on cells Toxicon. **29:**543-67.

10. **Florin, I., and M. Thelestam** 1986. Lysosomal involvement in cellular intoxication with Clostridium difficile toxin B Microb Pathog. **1:**373-85.

11. **Hall, A., and C. D. Nobes** 2000. Rho GTPases: molecular switches that control the organization and dynamics of the actin cytoskeleton.[In Process Citation] Philos Trans R Soc Lond B Biol Sci. **355:**965-70.

12. **Hofmann, F., C. Busch, and K. Aktories** 1998. Chimeric clostridial cytotoxins: identification of the N-terminal region involved in protein substrate recognition Infect Immun. **66:**1076-81.

13. **Just, I., G. Fritz, K. Aktories, M. Giry, M. R. Popoff, P. Boquet, S. Hegenbarth, and C. von Eichel-Streiber** 1994. Clostridium difficile toxin B acts on the GTP-binding protein Rho J Biol Chem. **269:**10706-12.

14. **Lewis, C. J., and R. D. Naylor** 1998. Sudden death in sheep associated with Clostridium sordellii Vet Rec. **142:**417-21.

15. **McGregor, J. A., D. E. Soper, G. Lovell, and J. K. Todd** 1989. Maternal deaths associated with Clostridium sordellii infection Am J Obstet Gynecol. **161:**987-95.

16. **Palsson, E. M., M. Popoff, M. Thelestam, and L. A. O'Neill** 2000. Divergent roles for Ras and Rap in the activation of p38 mitogen- activated protein kinase by interleukin-1 J Biol Chem. **275:**7818-25.

17. **Popoff, M. R., E. Chaves-Olarte, E. Lemichez, C. von Eichel-Streiber, M. Thelestam, P. Chardin, D. Cussac, B. Antonny, P. Chavrier, G. Flatau, M. Giry, J. de Gunzburg, and P. Boquet** 1996. Ras, Rap, and Rac small GTP-binding proteins are targets for Clostridium sordellii lethal toxin glucosylation J Biol Chem. **271:**10217-24.

18. **Qa'Dan, M., L. M. Spyres, and J. D. Ballard** 2000. pH-induced conformational changes in Clostridium difficile toxin B Infect Immun. **68:**2470-4.

19. **Sandvig, K., and S. Olsnes** 1981. Rapid entry of nicked diphtheria toxin into cells at low pH. Characterization of the entry process and effects of low pH on the toxin molecule J Biol Chem. **256:**9068-76.

20. **Smith, L.** 1975. *Clostridium sordellii. In* L. Smith (ed.), The Pathogenic Anaerobic Bacteria. CC Thomas, Springfield, IL.

21. **Vatn, S., M. A. Tranulis, and M. Hofshagen** 2000. Sarcina -like bacteria, Clostridium fallax and Clostridium sordellii in lambs with abomasal bloat, haemorrhage and ulcers J Comp Pathol. **122:**193-200.

Chapter III
Clostridium difficile toxin B activates dual caspase-dependent and caspase-independent apoptosis in intoxicated cells

Abstract

Clostridium difficile toxin B (TcdB) inactivates small GTPases Rho, Rac and Cdc42 during intoxication of mammalian cells. In the current work, we show that TcdB has the potential to stimulate caspase-dependent and caspase-independent apoptosis. The apoptotic pathways became evident when caspase-3-processed-vimentin was detected in TcdB-treated HeLa cells. Caspase-3 activation was subsequently confirmed in TcdB-intoxicated HeLa cells. Interestingly, caspase inhibitor delayed TcdB-induced cell death, but did not alter the time-course of cytopathic effects. A similar effect was also observed in MCF-7 cells, which are deficient in caspase-3 activity. The time course to cell death was almost identical between cells treated with TcdB plus caspase inhibitor and cells intoxicated with the TcdB enzymatic domain ($TcdB^{1-556}$). Unlike TcdB treated cells, intoxication with $TcdB^{1-556}$ or expression of $TcdB^{1-556}$ in a transfected cell line, did not stimulate caspase-3 activation yet cells exhibited cytopathic effects and cell death. Although $TcdB^{1-556}$ treated cells did not demonstrate caspase-3 activation these cells were apoptotic as determined by differential annexin-V/propidium iodide staining and nucleosomal DNA fragmentation. These data indicate TcdB triggers caspase-independent apoptosis as a result of substrate inactivation and caspase-dependent apoptosis due to a second, yet undefined, activity of TcdB. This is the first example of a bacterial virulence factor with the potential to stimulate multiple apoptotic pathways in host cells.

Introduction

Clostridium difficile – the leading cause of hospital acquired diarrhea (Mylonakis et. al, 2001) - produces two large clostridial toxins (LCTs), TcdA (~304 kD) and TcdB (~270 kD). As an intracellular bacterial toxins TcdA and TcdB glucosylate Rho, Rac, and Cdc42, causing changes in cell physiology (Boquet et. al, 1999). Like many intracellular toxins, LCTs can be roughly divided into enzymatic, translocation and receptor binding domains. Proceeding from the amino to carboxy terminus, the first ~550 amino acids contain the enzymatic region, which is followed by a putative translocation region and receptor-binding domain located within the remaining two-thirds of the toxin. Domains outside of the enzymatic region remain largely uncharacterized in LCTs.

Cell rounding is an accentuated feature of cells intoxicated by TcdA or TcdB, and may result from blocking Rho's ability to regulate actin polymerization. In addition to cell rounding, there are diverse changes in cell physiology during intoxication by TcdA and TcdB. TcdA has been shown to stimulate substance P release and initiate inflammation (McVey et. al, 2001), as well as, induce COX-2 expression and increase prostaglandin levels (Alcantara et. al, 2001). A series of reports indicate TcdB is capable of inhibiting IL-2 expression, reducing Bcl-2 levels, disrupting tight junctions, activating MMP-2, inducing NO production and down regulating endocytosis (Hausding et. al, 2000); (Koike et. Al, 2000); (Lombet et. al, 2001); (Nusrat et. al, 2001); (Garrett et. al, 2000).

Despite the list of morphological and physiological changes in TcdB intoxicated cells, there are conflicting reports on the ultimate fate of cells targeted by this toxin. Rho

prevents apoptosis by regulating expression of apoptotic factors such as Bcl-2 (Gomez et. al, 1997), thus its inactivation by TcdB could trigger apoptosis. To this end, TcdB has been used to induce apoptosis in a variety of cell types and TcdB has been used to dissect steps in apoptosis for neuronal cell survival and renal cell function (Anderson et. al, 2000); (Linseman et. al, 2001). In the case of neuronal cell survival studies TcdB was shown to activate caspase-3 at later time-points, suggesting a process of caspase-dependent apoptosis occurred in these intoxicated cells. In agreement with this observation, Gall et al. (Le Gall et. al, 2000) reported PARP cleavage in cells treated with TcdB, further suggesting caspase activation during TcdB induced apoptosis. Interestingly, Warny et al. reported finding necrotic cell death in TcdB-treated THP-1 monocytes (Warny et. al, 1999), while Fiorentini et al. reported that TcdB was a potent inducer of apoptosis in IEC-6 intestinal cells (Fiorentini et. al, 1998). In both of these experiments it is difficult to make a clear distinction between complete apoptosis and necrosis. In fact the data suggest a mixture of necrotic and apoptotic events. For example, THP-1 cells appeared necrotic when treated with TcdB, but also were protected by a broad-spectrum caspase inhibitor. Conversely, in the studies on IEC-6 cells, while complete rounding occurs, less than half of the cells show markers of apoptosis. In the case of TcdA, there is evidence to suggest apoptosis, or at least perturbation of the mitochondria, occurs as a result of activities other than inactivation of Rho, Rac and Cdc42 and may be initiated prior to substrate glucosylation (He et. al, 2000). Clearly, there are a variety of events occurring in LCT-intoxicated cells, all of which may not necessarily be due to inactivation of small GTPases.

In current experiments, while analyzing the proteome of HeLa cells treated with TcdB, we identified a differentially processed form of the intermediate filament vimentin, which appeared to be cleaved by caspase-3. Degradation of intermediate filaments may contribute to the gross morphological changes in TcdB intoxicated cells, a process previously attributed only to actin condensation. The observations of vimentin processing in TcdB intoxicated cells prompted a detailed analysis of caspase-3 activation, and its contribution to apoptosis in TcdB intoxicated HeLa cells. Using a combination of experimental approaches, we delineated the role of Rho, Rac and Cdc42 inactivation as an initiator of apoptosis in TcdB intoxication. These studies identified dual, caspase-3 dependent and independent, apoptotic events in TcdB intoxicated cells, and indicate specific inactivation of Rho, Rac and Cdc42 triggers apoptosis in a caspase-independent manner.

Materials and Methods

Cell culture, reagents, wild type and recombinant toxins.

Unless otherwise noted, all reagents and chemicals were purchased from Sigma. Human epitheloid carcinoma (HeLa) cells, human adenocarcinoma mammary gland cells (MCF-7) and Chinese hamster ovary cells (CHO) were obtained from the American Type Culture Collection. HeLa cells were maintained in RP-10 medium supplemented with 10% fetal bovine serum, while MCF-7 cells were maintained in RP-10 medium supplemented with 10% fetal bovine serum plus 0.01 mg/ml bovine insulin. Cultures were grown at 37°C in the presence of 6% CO_2 and all cells were used between passages

6 and 10. TcdB, PA and $LFnTcdB^{1-556}$ were isolated as previously described (Qa'Dan et. al, 2000) (Spyres et. al, 2001). Cell viability assays were carried out using WST-8 (2-(2-methoxy-4-nitrophenyl)-3-(4-nitrophenyl)-5-(2,4-disulfophenyl)-2H-tetrazolium, monosodium salt) (Dojindo Laboratories) according to manufacturer's instructions.

Cell extracts and two-dimensional gel analysis.

HeLa cells were grown to confluence in a T-75 flask (~1 X 10^7 cells) and treated with TcdB (50 ng/ml) for 24 h, along with control cells mock treated with PBS in a final volume of 20 ml. Cell extracts were prepared as previously described (Just et. al, 1994). The extract was concentrated and protein concentration was determined by Bradford assay (Life Technologies).

For 2-dimensional gel analysis, 200 μg of cell extract was loaded on 7 cm IPG strips, pH range 3-10 non-linear (Pharmacia). Rehydration solution containing 8M urea, 2% CHAPS, 1% DTT, and 0.5% IPG buffer was added with the extract to a final volume of 120 μL. Isoelectric focusing (IEF) was carried out on an IPGphor system (Pharmacia) according to manufacturer's instructions. Following IEF, proteins were resolved in the second dimension on strips were then loaded on 15% polyacrylamide SDS-PAGE gel. After coomassie staining, gels were compared visually and candidate spots were prepared as described by *Devreese et al.* (Devreese et. al, 2001).

Nano-electrospray MS-MS/MS analysis.

Candidate proteins were analyzed by nano-electrospray MS and MS/MS on a Q-TOF mass spectrometer (Micromass) similar to previously described conditions *Devreese et al* (Devreese et. al, 2001). *In situ* digests were washed using Millipore C18 Ziptips and prepared extracts were loaded into a coated fused silica capillary (New Objective), and placed into the nanospray source. Spectra were collected in the 100-1000 mass range using 2 sec scans with data collected for 2 min. Prominent doubly charged molecular ions were identified and selected for collision induced dissociation fragmentation. MassLynx software (Micromass) was used to interpret MS/MS spectra. The MaxEnt3 tool was used to convert multiply charged ions to singly charged species and the PepSeq tool was used to determine the amino acid sequence after delineating the fragment ion series. Sequence comparisons were performed using the BLAST algorithm (Altschul et. al. 1997) against the *Homo sapiens* database.

Immunoblot and immunostain analysis of cellular vimentin.

Immunoblot analysis was carried out on extracts from HeLa cells treated with TcdB. HeLa cells, grown to confluence (3 X 10^6 cells) in a T-25 flask, were treated with 1 pmol of TcdB and at the indicated time-points extracts were collected as previously described (Just et. al, 1994). Extracts were probed with anti-vimentin monoclonal antibody V-9 (Santa Cruz Biotechnology), and developed by ECL luminescence (Amersham Pharmacia). For immunostaining vimentin, HeLa cells were plated on 12 mm coverslips at a density of 1 X 10^5 cells/coverslip and allowed to grow for 24 h, at which point cells

were treated with 1 pmol of TcdB in a final volume of 0.5 ml. At the indicated time-points cells were fixed and immunostained with anti-vimentin V-9 antibody and TRITC-labeled secondary antibody as previously described (Safiejko-Mroczka et. al, 1998). Cells were viewed using a Zeiss Universal epifluorescence microscope equipped with Olympus oil immersion in DApo UV objectives.

Caspase-3 activation and caspase inhibitor assays.

To test for caspase-3 activity, HeLa cells were grown in 25-cm^2 tissue culture flasks until confluent at a density of 3 X 10^6 cells/flask, at which point 1 pmol of TcdB, or 30 pmol PA plus 100 pmol $LFnTcdB^{1-556}$, was added to the cells in a final volume of 5 ml. At the indicated time points, cells were scraped and centrifuged at 1000 X g for 5 min at 4°C. Treated cells were suspended in lysis buffer (50 mM HEPES, 100 mM NaCl, 0.1% CHAPS, 1mM DTT, 0.1 mM EDTA, pH 7.4) and incubated for 10 min on ice, and cell debris was removed by centrifugation at 10000 X g for 5 min at 4°C. Eighty microliters of assay buffer (50 mM HEPES, 100 mM NaCl, 0.1% CHAPS, 10 mM DTT, 0.1 mM EDTA, 10% glycerol, pH 7.4) was then added to 10 µl of Caspase-3-Substrate I (CPP32/apopain colorimetric substrate, Ac-Asp-Glu-Val-Asp-*p*NA) (Calbiochem) and 20 µl of cell extract. Readings were then recorded every 5 min using a PowerWavex plate reader (BIO-TEK) at 405 nm for 24 h at 37°C. Caspase-3 specific-activity, was calculated per manufacturer's instructions. Caspase inhibitor assays were performed according to manufacturer's instructions using 50 µM caspase inhibitor cocktail III (Calbiochem).

Generation of TcdB$^{1-556}$-expressing CHO cells.

A DNA sequence coding for the enzymatic domain of TcdB (TcdB$^{1-556}$) placed downstream and in-frame with a Kozak sequence (GNNATGG) was cloned between the *Hind*III and *Eco*RI sites of plasmid pGene/V5-His version B (Invitrogen) multiple cloning site. The recombinant plasmid was linearized with *Sap*I and introduced into GeneSwitch-CHO cells (Invitrogen) by lipofection according to the protocol supplied with the LipofectAMINE PLUS Reagent Kit (Gibco Life Technologies). Stably transfected cells were selected on growth medium consisting of complete F-12 (HAM) medium plus zeocin (300 μg/ml) and hygromycin (100 μg/ml). Single clone lineages of the transfected cells were established by limiting dilution. Expression of TcdB was induced in the different cell lineages of transfected CHO cells by the addition of mifepristone (10^{-8}M), to the selective medium. GeneSwitch-CHOpGene/TcdB1-556 a lineage of transfected cells showing nearly 100 % rounding in 24 h in the presence of mifepristone was identified and chosen for the experiments reported herein.

Propidium iodide and Annexin-V staining.

For differential propidium and annexin-V staining experiments, HeLa cells were grown in 25-cm^2 tissue culture flasks at a density of 3 X 10^6 cells/flask for 16 h, at which point 10 pmol of TcdB, or PA plus LFnTcdB$^{1-556}$, were added to the cells in a final volume of 5 ml. At the indicated time points, cells were trypsinized and pelleted at 100 X g for 10 min at 4°C. Cells were then resuspended in cold PBS and pelleted at 100 X g for 10 min at 4°C. Annexin binding buffer (10 mM HEPES, 140 mM NaCl, 2.5 mM $CaCl_2$, pH 7.4) was used to resuspend cells at a density of 1 X 10^6 cells/ml. Cells were then labeled with

5 μl of Annexin-V Alexa Flour 488 dye and propidium iodide (Molecular Probes) according to the manufacturer's protocol. Labeled cells were analyzed using a FACSCalibur system (BD Biosiences). The probe was excited with a laser at 488 nm (250 mW), and emission was measured at 530 nm and > 575 nm; logarithmic amplification was used for fluorescence detection.

Analysis of nucleosomal fragmentation.

HeLa cells were grown in 25-cm^2 tissue culture flasks until confluent at a density of 3 X 10^6 cells/flask, at which point 10 pmol of TcdB, or PA plus $LFnTcdB^{1-556}$, were added to the cells in a final volume of 5 ml. At the indicated time points, cells were mechanically removed and centrifuged at 1000 X g for 5 min at 4°C. The cells were then resuspended in PBS at 1-2 X 10^6 cells/ml, and then pelleted by brief centrifugation. Nucleosomal DNA was extracted using an ApoptoticLADDER Kit (Geno Technology) according to manufacturer's instructions. The DNA sample was then loaded and analyzed on a 1.8 % agarose gel.

Statistical analysis.

Statistical determinations were made using the statistics component of Microsoft Excel 2001. Significance was determined by students t-test ($p<0.01$) and error bars in respective plots represent the standard deviation from the mean.

Results

Protein profiles of TcdB-treated HeLa cells.

While recent studies have defined mechanisms of cell entry and substrate modification by TcdB, there remains a dearth of information on the downstream effects of these activities. To better understand the physiological results of TcdB intoxication, I analyzed the proteome of TcdB-intoxicated cells for differential protein profiles. Protein extracts from TcdB-intoxicated HeLa cells were resolved by 2-dimensional gel electrophoresis and visualized by coomassie blue staining (see Fig. 1). Under these conditions, one protein was noticeably increased in TcdB-treated samples compared to control. The differential protein was trypsinized, extracted from the gel, and the tryptic fragments were analyzed by tandem mass spectroscopy in which candidate ions were subjected to amino-acid sequencing (see Fig. 2A). Three candidate peptides (QDVDNASLAR, EEAESTLQSFR, FSLADALNTEFK) were identified (see Fig. 2B) by MS/MS analysis. BLAST comparisons of these peptides revealed 100% homology with the human intermediate filament vimentin. Interestingly, the differential protein did not migrate at the size predicted for human vimentin (~ 57 kD). Instead, the candidate protein migrated at ~ 20 kD, suggesting protein might be a modified or truncated form of vimentin. Thus, to determine the fate of vimentin in intoxicated cells, samples were examined by

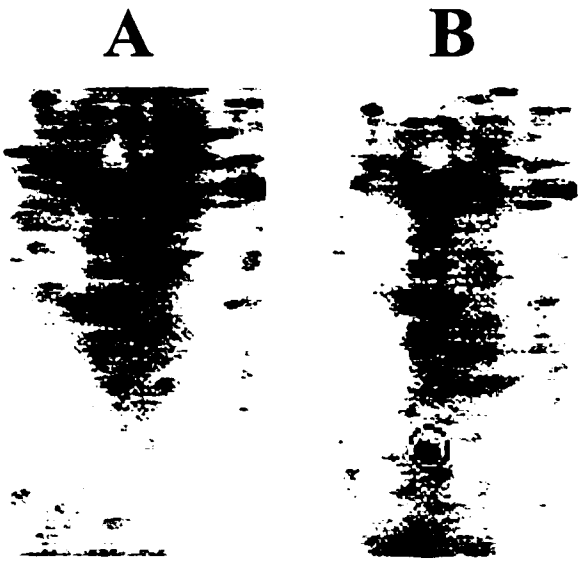
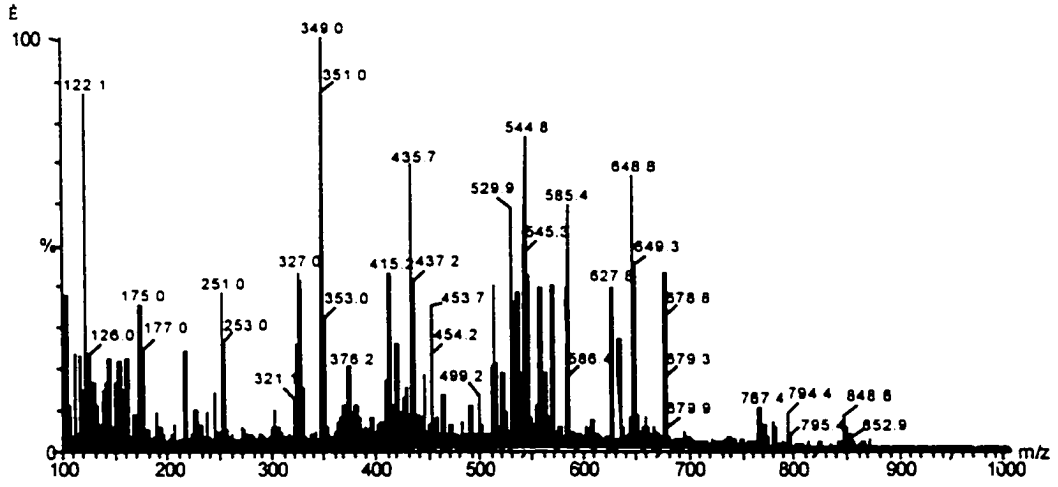


Fig. 1. Two-dimensional gel analysis of extracts from TcdB-treated HeLa cells. HeLa cells ($1x10^7$) were treated with TcdB or PBS for 24 h, soluble protein was collected and 200 μg was loaded on pH 3-10 non-linear focusing strips then separated on a IPGphor IEF apparatus. Following IEF, samples were resolved in the second dimension by SDS-PAGE and stained with coomassie brilliant blue. Panel A) Two-dimensional protein profile from PBS treated HeLa cells, Panel B) Two-dimensional protein profile from TcdB treated HeLa cells.

Fig. 2

A



B

678.8 m/z	FSLADALNTEFK
648.8 m/z	EEAESTLQSFR
544.8 m/z	QDVDNASLAR

```
1    mstrsvssssyrrmfggpgtsrpsssrsyvttstrtyslgsalrpstsrslyasspggv
61   yatrssavrlrssvpgvrllqdsvd  fsladaintefk  ntrtnekvelqelndrfanyidk
121  vrfleqqnkillaeleqlkgqgksrlgdlyeeemrelrrqvdqltndkarveverdnlae
181  dimrlreklqeemlqr  eeaentlqsfrqdvdnaslar  ldlerkveslqeeiaflkklhee
241  eiqelqaqiqeqhvqidvdvskpdltaalrdvrqqyesvaaknlqeaeewykskfadlse
301  aanrnndalrqakqesteyrrqvqsltcevdalkgtneslerqmremeenfaveaanyqd
361  tigrlqdeiqnmkeemarhlreyqdllnvkmaldieiatyrkllegeesrislplpnfss
421  lnlretnldslplvdthskrtlliktvetrdgqvinetsqhhddle
```

Fig. 2. Mass-spectrometry and sequence analysis of differential protein. Candidate protein was trypsinized and extracted from the 2-dimensional gel, prepared and analyzed by nano-spray MS/MS on a Q-TOF mass spectrometer. Spectra were collected across a 100-1000 mass range and the amino-acid sequence was determined for prominent doubly charged peptides. Sequence comparisons were made by BLAST analysis against the *Homo sapiens* database. Panel A) Mass-spectrum profile of tryptic fragments from candidate protein, Panel B) Sequence of 3 candidate peptides and sites of homology with the human intermediate filament vimentin.

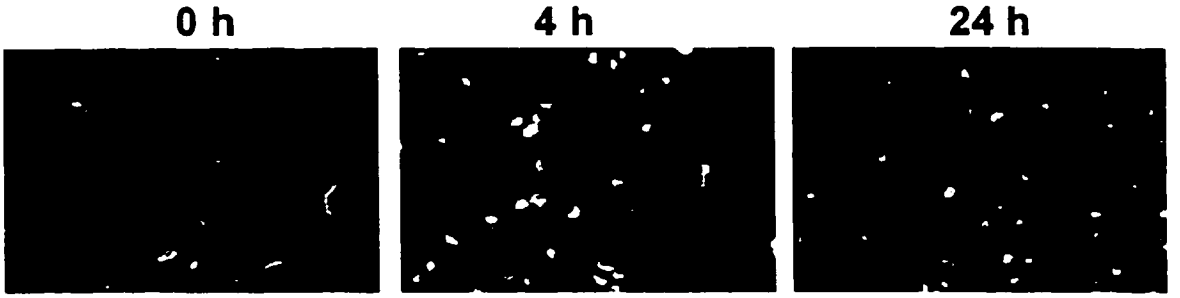
immunostaining or immunoblotting vimentin in TcdB treated HeLa cells. As shown in Fig. 3A, vimentin demonstrates both temporal and spatial changes in TcdB intoxicated cells. Early in the intoxication, vimentin is concentrated around the perinuclear region and over time vimentin become less prominent. In line with this observation, as shown in Fig. 3B, vimentin is cleaved in intoxicated cells and migrates at a size similar to that of cleaved vimentin from staurosporine (an inducer of vimentin degradation) treated cells. These results suggested vimentin was reorganized and degraded in TcdB-intoxicated cells.

Caspase activation in TcdB-intoxicated HeLa cells.

Several candidate peptides from vimentin were analyzed and sequenced via tandem mass spectrometry. Since the protein is trypsinized prior to MS/MS sequencing all candidate

Fig. 3

A



B

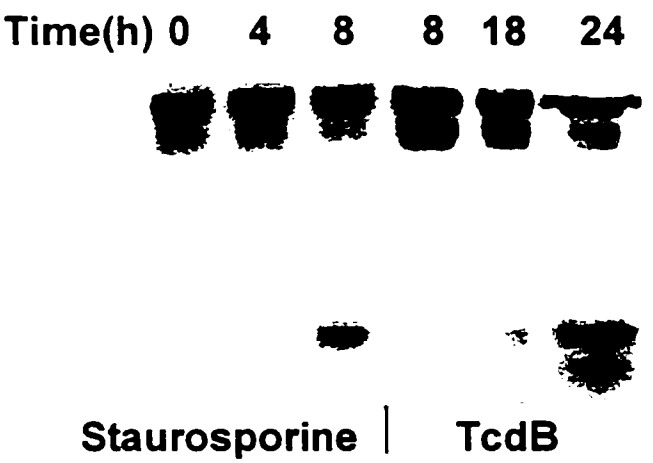


Fig. 3. Immunostain and immunoblot analysis of vimentin in TcdB-treated HeLa cells. HeLa cells, treated with TcdB, were fixed and stained with anti-vimentin monoclonal antibody V-9 or extracts were collected from intoxicated cells and subjected to immunoblot analysis also using the V-9 primary antibody. In the fixed cells immunoreactivity was detected using TRITC-labeled secondary antibody and viewed under an epifluorescence microscope. ECL luminescence was used for vimentin detection during immunoblot analysis. Panel A) Vimentin staining in control and TcdB-treated HeLa cells at the indicated time-points; Panel B) Immunoblot of extracts from staurosporine or TcdB treated HeLa cells at the indicated time-points.

peptides should contain carboxy and amino terminal trypsin sites. Interestingly, ^{86}FSLADALNTEFK^{97} revealed only one recognizable trypsin cleavage site at K^{97}N^{98}, yet the amino terminal region of this peptide between D^{85}F^{86} did not contain a trypsin recognition site. Further sequence analysis revealed a proteolytic cleavage site (DSVD) at the amino-terminal side of the sequenced peptide. DSVD matches an established DXXD recognition motif for caspase-3, and processing at this site suggested caspase-3 may be activated in this system. Furthermore, recent reports have shown that caspase-3, along with other caspases, is capable of cleaving vimentin during apoptosis (Byun et. al, 2001). To confirm caspase-3 activation in this system, HeLa cells were treated with TcdB and at various time-points cells were analyzed for caspase-3 activity using the colorimetric substrate Ac-Asp-Glu-Val-Asp-*p*NA. As shown in Fig. 4, active caspase-3 is detected as early as 4 h following treatment with TcdB and is maximal between 16 h and 24 h.

The role of caspases in TcdB intoxication.

To determine the contribution of caspase activation to cell death in TcdB intoxicated cells, TcdB toxic effects were analyzed in the presence of a broad-spectrum caspase inhibitor. As shown in Fig. 5A, treatment with caspase inhibitor slowed the killing effects of TcdB. Comparisons were also made between the full-length toxin and the enzymatic domain of TcdB (TcdB$^{1-556}$). To focus on the enzymatic domain of TcdB we

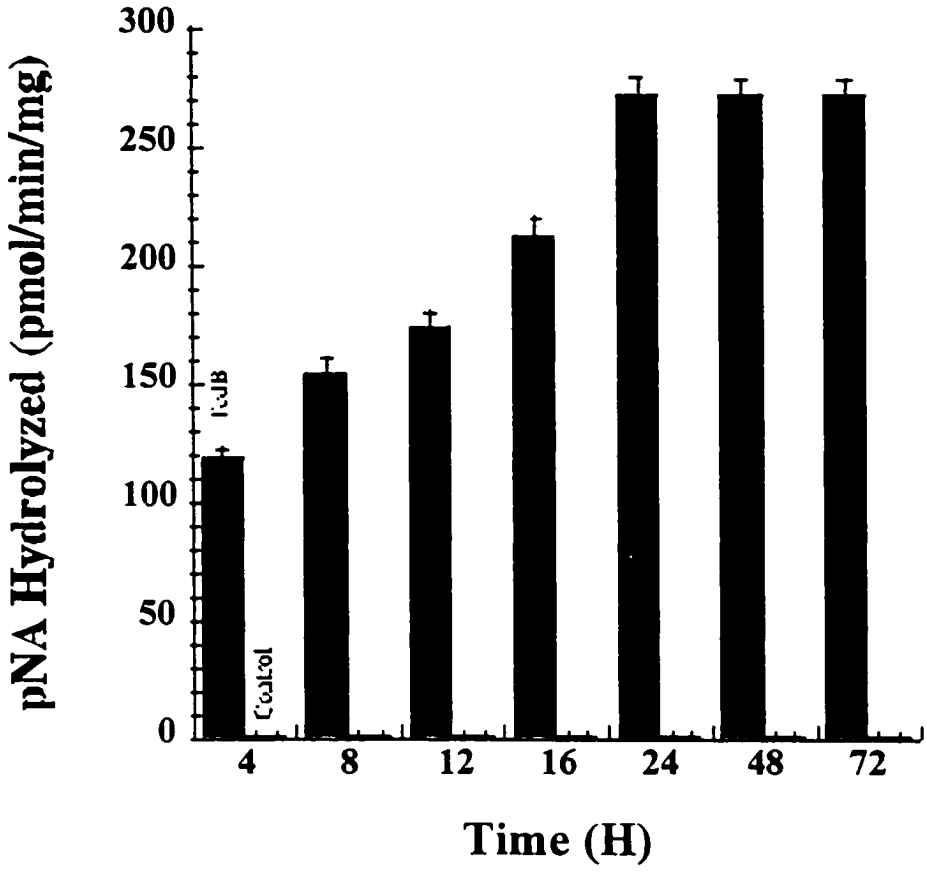


Fig. 4. Caspase-3 activation in TcdB-treated HeLa cells. HeLa cells were treated with TcdB (50 ng/ml) and extracts were collected at the indicated time-points. Extracts were assayed for caspase-3 activity using the CPP32/apopain colorimetric substrate. The assay was maintained at 37°C and A_{405} was collected every 5 min for 24 h. The change in absorbance was plotted and the slope of the line was used to calculate the rate of caspase-3 activity in each sample. Time-points and samples are labeled on the bar-chart.

took advantage of a protein-based cell delivery system from an attenuated form of anthrax toxin. This anthrax toxin derivative consists of anthrax protective antigen (PA), and a truncated form of anthrax lethal toxin (LFn), to which heterologous fusions are made. PA then mediates the cell entry of the LFn fusion via anthrax toxin's normal mode of cell penetration. We have used the system in the past as a tool to analyze the toxic effects of $TcdB^{1-556}$ and for a more detailed description *Spyres et. al.* Interestingly, $TcdB^{1-556}$ specific intoxication was remarkably similar to that observed in cells treated with TcdB plus caspase inhibitor (see Fig. 5B) and addition of the caspase inhibitor did not change the rate of cytotoxic effects for $TcdB^{1-556}$ (see Fig. 5C). Furthermore, in contrast to differences in viability, the caspase inhibitor did not alter the time-course of cytopathic effect in TcdB intoxicated cells (data not shown). Taken together these results suggested early TcdB cytopathic effects are not the result of caspase-3 activation, and are more likely due to modification of Rho, Rac and Cdc42. Later effects, involving cell death, may be accelerated by activities that occur in addition to substrate modification. Furthermore, intoxication by $TcdB^{1-556}$ does not appear to require caspase activation.

We also examined the susceptibility of a caspase-3 deficient cell line (MCF-7) to TcdB intoxication. As shown in Fig. 6A, MCF-7 cells also demonstrated a slower time-course of death compared to cells with normal caspase-3. In line with the caspase inhibitor assay, the rate of MCF-7 intoxication was also very similar to the rate of cell death for

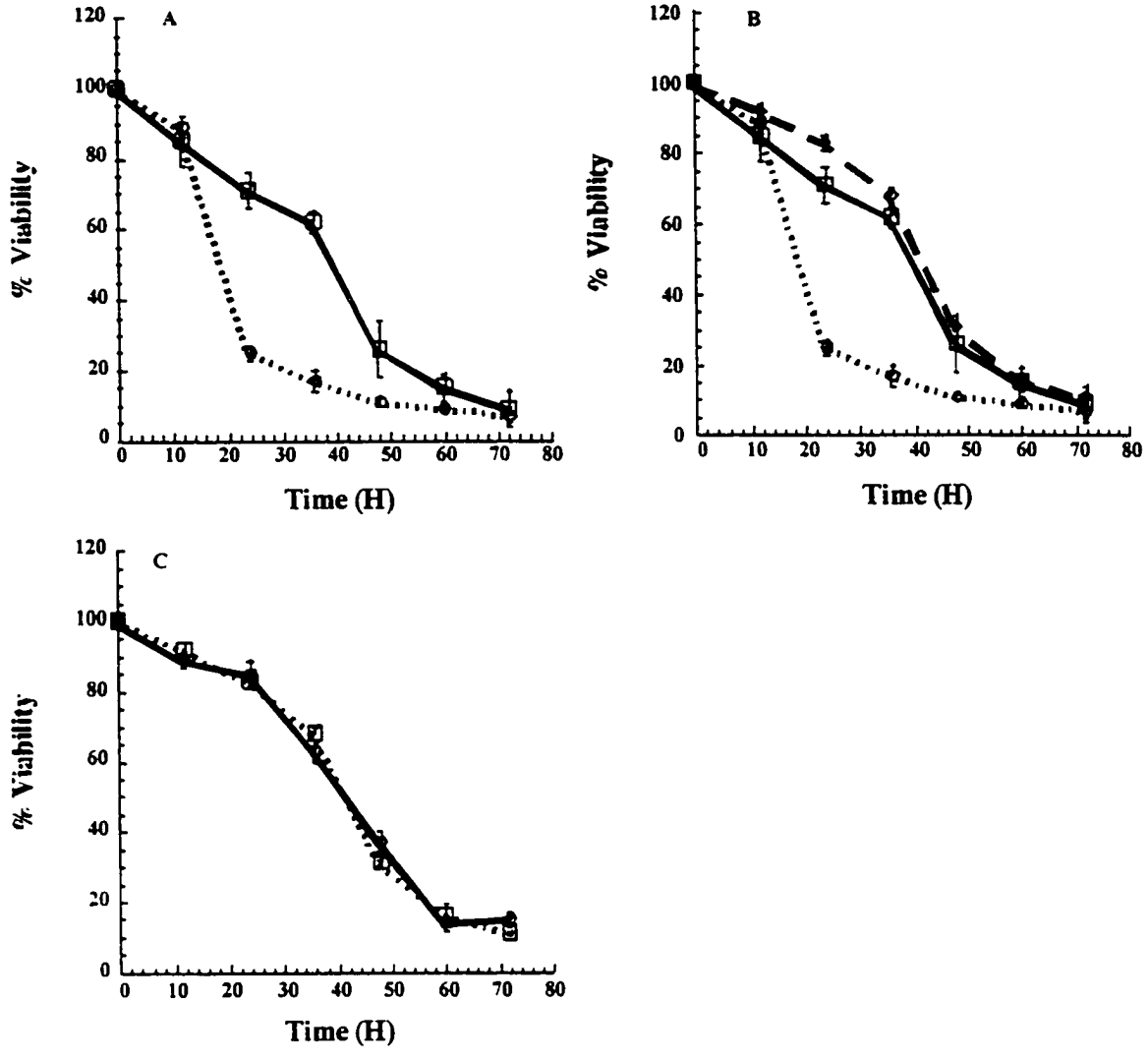


Fig. 5. Effect of pancaspase inhibitor on TcdB and TcdB$^{1-556}$ intoxication. HeLa cells were treated with TcdB or TcdB$^{1-556}$ (via PA,LFn) in the presence of a broad spectrum caspase inhibitor and cell viability was determined by WST-8 staining. Panel A) Comparison of TcdB mediated intoxication in the presence and absence of inhibitor. Open circles, TcdB; Open Squares TcdB plus caspase inhibitor. Panel B) Comparison between TcdB$^{1-556}$ treated cells and cells treated with TcdB plus caspase inhibitor. Open circles, TcdB; Open Squares, TcdB plus caspase inhibitor; Open diamonds, TcdB$^{1-556}$. Panel C) Impact of caspase inhibitor on TcdB$^{1-556}$ intoxication. Open squares, TcdB$^{1-556}$; Open circles TcdB$^{1-556}$ plus caspase inhibitor.

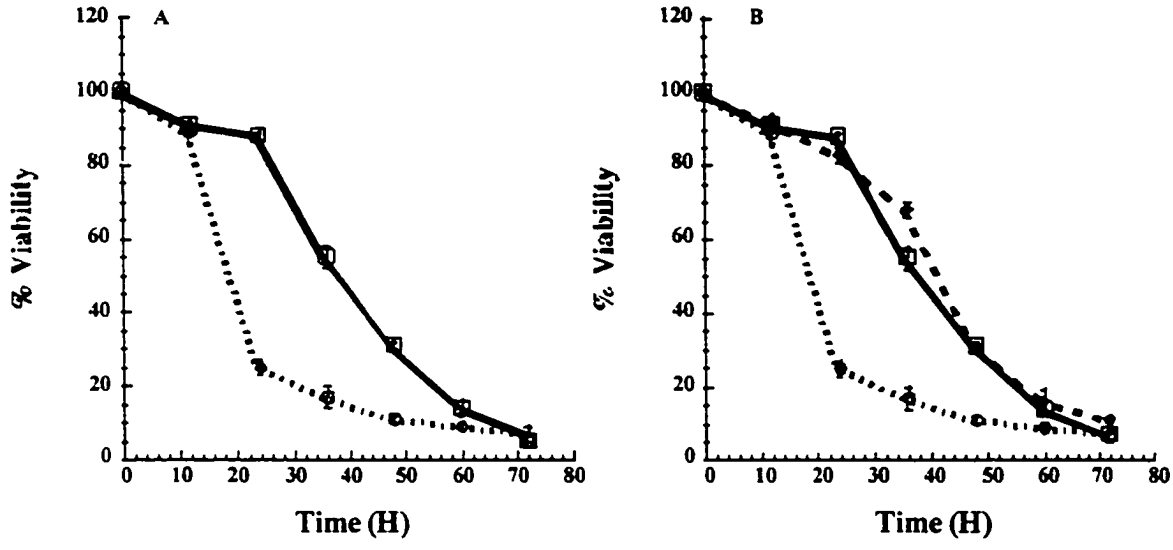


Fig. 6. Effects of TcdB on a caspase-3 deficient cell line. MCF-7 or HeLa cells were treated with TcdB and cell viability was determined by WTS-8 cell staining at the indicated time-points. Comparisons were also made between MCF-7 cells treated with TcdB, HeLa cells treated with TcdB, and HeLa cells treated with PA, $LFnTcdB^{1-556}$. Panel A) Rate of cell death in MCF-7 versus HeLa cells. Open circles, TcdB treated HeLa cells; Open squares, TcdB treated MCF-7 cells. Panel B) Comparison of the rate of cell death for $TcdB^{1-556}$ treated HeLa cells versus TcdB treated MCF-7 cells. Open circles, TcdB treated HeLa cells; Open squares, TcdB treated MCF-7 cells; Open diamonds, PA, $LFnTcdB^{1-556}$ treated HeLa cells.

HeLa cells intoxicated with TcdB$^{1-556}$ (see Fig. 6B). These results further suggested caspase-3 activation is a part of the TcdB intoxication process and might be conferred by an activity of the toxin other than substrate modification.

Caspase-3 Activity in TcdB$^{1-556}$ Intoxicated Cells.

Since the results from the caspase inhibitor and MCF-7 experiments suggested caspase-3 might not be involved in substrate specific intoxication, we assayed cells intoxicated with the TcdB$^{1-556}$ for caspase-3 activation. HeLa cells were treated with TcdB$^{1-556}$ -delivered via the PA,LFn system- and extracts were assayed for caspase-3 activity at selected time-points. While TcdB$^{1-556}$ can confer cytopathic effects and cell death there is no detectable activated caspase-3 in these cells (see Fig. 7A). This result suggested that, corresponding to the caspase inhibitor data, inactivation of Rho, Rac and Cdc42 was not sufficient to evoke caspase-3 activation in TcdB intoxicated cells.

It was also possible that the absence of caspase-3 activation was due to lower activity from TcdB$^{1-556}$ compared to TcdB. Futhermore, caspase-independent apoptosis can be triggered through cell surface death receptors such as TNFR-1 and Fas (Leist et. al, 2001), and it was plausible that TcdB$^{1-556}$ was capable of activating these receptors during PA, LFn mediated cell entry. To contend with these possibilities we generated a CHO cell line capable of inducible expression of TcdB$^{1-556}$. In this case the gene

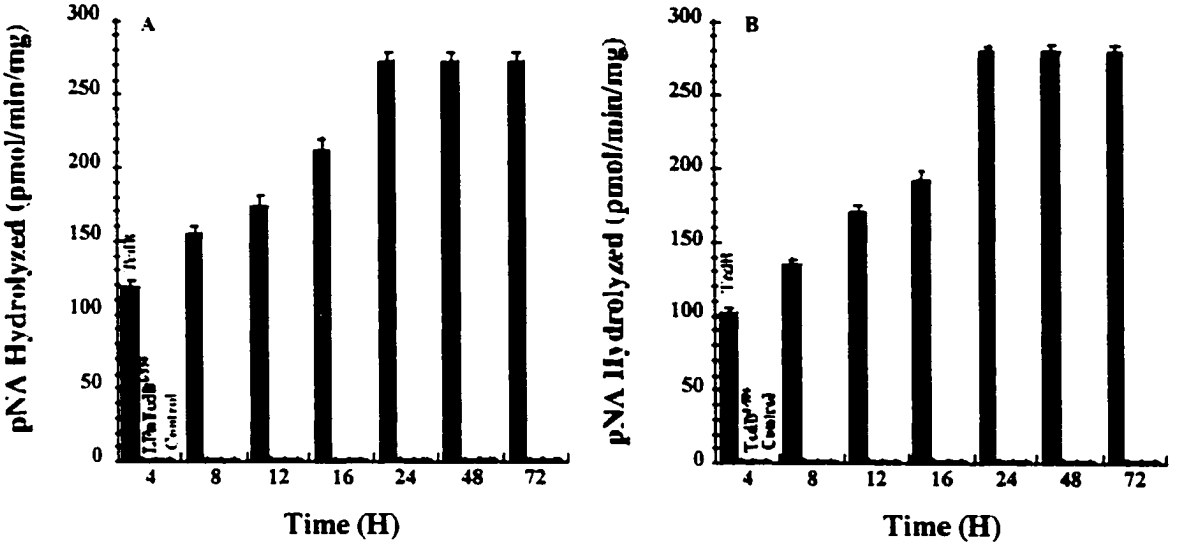


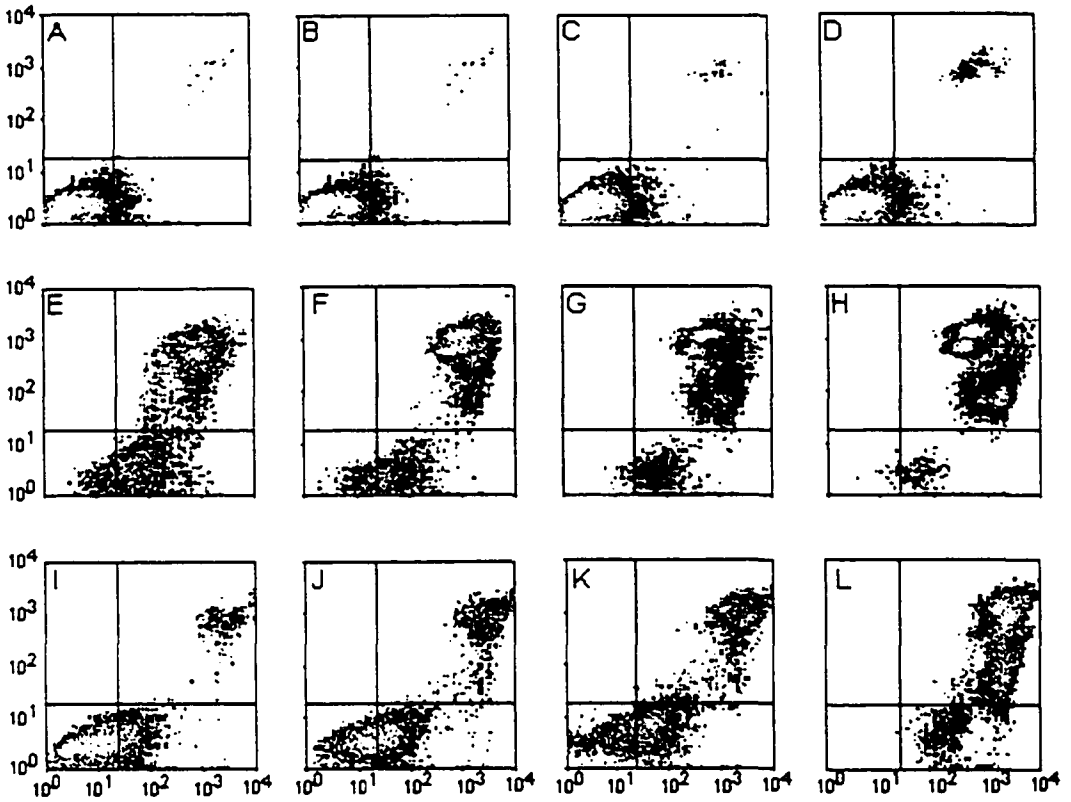
Fig. 7. Caspase-3 activity in $TcdB^{1-556}$ treated cells and in a $TcdB^{1-556}$-expressing cell line. HeLa cells were treated with PA, $LFnTcdB^{1-556}$ or CHO cells stably transfected with the $TcdB^{1-556}$- encoding DNA fragment was induced with mifepristone. Samples were collected from these cells and compared with extracts from TcdB treated cells for caspase-3 activation. Extracts were assayed for caspase-3 activity as described early. Panel A) Caspase-3 activity in TcdB or $PA.LFnTcdB^{1-556}$ treated HeLa cells over the course of 72 h. Panel B) Caspase-3 activity in CHO cells treated with TcdB or cells expressing $TcdB^{1-556}$ over the course of 72 h.

fragment encoding for $TcdB^{1-556}$ was cloned into the mifepristone inducible expression system pGene and transfected into the pSwitch CHO cell line, thus providing a tool for sustained enzymatic activity. As shown in Fig. 7B, in line with the $TcdB^{1-556}$ results, the mifepristone-induced cells did not contain activated caspase-3. Also similar to the $TcdB^{1-556}$ results these cells showed cell rounding and cell death (data not shown). These data further suggested inactivation of Rho, Rac and Cdc42 does not stimulate caspase-3 activation in TcdB intoxicated cells.

Apoptosis in $TcdB^{1-556}$ Treated Cells.

Although caspase-3 activity was not detected in cells treated with or expressing $TcdB^{1-556}$, according to cell staining and trypan-blue exclusion assays these cells eventually died. The mechanism of cell death for these cells was not clear, so we carried out experiments to determine if cells treated with $TcdB^{1-556}$ go through apoptosis. In this assay, HeLa cells were treated with TcdB or $TcdB^{1-556}$ and assayed by dual annexin-V and propidium iodide (PI) staining. The number of annexin-V and PI positive cells was determined by FACS analysis. As shown in Fig. 8, cells treated with TcdB show hallmarks of apoptosis by 12 h and also show significant PI staining at this relatively early time-point. Conversely, $TcdB^{1-556}$ treated cells are slower to demonstrate annexin-V staining, but this clearly proceeds any PI staining. In all, by 12 h 39% of the cells were annexin-V positive (apoptotic) in the TcdB treated samples and 51% were PI positive (interpreted as necrotic or late-apoptotic). By 24 h, 65% had become PI positive and the number of annexin-V positive had decreased to 24%.

Fig. 8



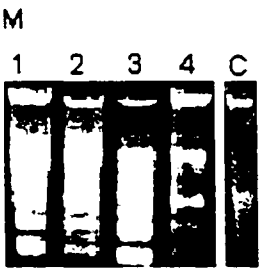


Fig. 8. Markers of apoptosis in TcdB and $TcdB^{1-556}$ treated cells. HeLa cells were treated with TcdB or $TcdB^{1-556}$ (delivered via PA, LFn) and analyzed for differential annexin-V /propidium iodide staining or nucleosomal DNA laddering. For FACS analysis, at the indicated time-points following TcdB treatment, cells were collected and labeled with annexin V- Alexa Fluor 488 and propidium iodide. Cells were analyzed at 12 h, 24 h, 36 h, and 48 h following treatment. Panels A-D, Mock-treated buffer control cells; Panels E-H, TcdB treated HeLa cells; Panels I-L $TcdB^{1-556}$ treated HeLa cells; Panel M, DNA laddering in TcdB and $TcdB^{1-556}$ treated cells. At 24 h and 36 h following TcdB or $TcdB^{1-556}$ treatment, nucleosomal DNA was collected from cells and analyzed on a DNA agarose gel. Lane 1, TcdB 24 h; Lane 2, $TcdB^{1-556}$ 24 h; Lane 3, TcdB 36 h; Lane 4, $TcdB^{1-556}$ 36 h.

By the final time point greater than 90% of the TcdB treated cells were PI positive. In contrast to this, at 12 h only 10% of $TcdB^{1-556}$ treated cells were PI positive and 28% were annexin-V positive. The percentage of both PI positive and annexin-V positive cells increased by the next two time-points in $TcdB^{1-556}$ treated cells and by the final time point a majority of the cells had become PI positive. As a confirmation of apoptosis in $TcdB^{1-556}$ treated cells, nucleosomal fragmentation was examined in TcdB and $TcdB^{1-556}$ treated cells. As shown in Fig. 8M, both TcdB and $TcdB^{1-556}$ treated cells show fragmentation of nucleosomal DNA, further demonstrating apoptosis induced by TcdB and $TcdB^{1-556}$. These results demonstrate that $TcdB^{1-556}$ treated cells are capable of going through apoptosis, yet this process is slower than that observed in TcdB treated cells.

Discussion

Results from this current work identify important new aspects of TcdB intoxication. First, TcdB intoxication causes the degradation of intermediate filaments, which contributes to changes in cell morphology. Second, there are dual caspase-dependent and caspase-independent apoptotic processes occurring in TcdB-intoxicated cells, and caspase-independent apoptosis appears to be due to substrate modification. This data also suggests TcdB may have an activity, encoded outside of the enzymatic domain, that triggers caspase-3 activation. Alternatively, intact TcdB may traffic to a site within the cell that is not accessed by $TcdB^{1-556}$ alone.

Intermediate filaments -such as vimentin- provide strength and structure to cells, thus reorganization and processing of vimentin may be necessary during some types of cell rounding. Based on the immunostaining experiments, vimentin appeared to first reorganize around the nucleus in TcdB intoxicated cells and this was followed by degradation of vimentin at later time-points. The immunoblot results are completely in-line with the observations from the cell immunostaining. While immunostaining revealed changes in vimentin by 4 h after intoxication, processed forms of vimentin was not detected by immunoblot until almost 24 h after toxin treatment. In the past, morphological changes in TcdB-intoxicated cells have been attributed to inactivation of Rho and thus disrupting actin polymerization. Reorganization and modification of

intermediate filaments also contributes to changes in the cell morphology during TcdB intoxication.

By blocking caspase-activity I was able to slow the rate of cell death in cells treated with TcdB. I became increasingly interested in this event when we found that the rate of cell death in cells treated with TcdB plus caspase inhibitor is remarkably similar to that observed in cells treated with $TcdB^{1-556}$. A similar intoxication effect was also observed on MCF-7 cells that lack caspase-3. This suggested that caspase activation, or at least caspase-3 activation, contributed to cytotoxicity and might not be related to substrate inactivation. This possibility was confirmed by showing that cells intoxicated by $TcdB^{1-556}$ did not exhibit activated caspase-3. These data also imply early cytopathic effects result from the substrate specific activity of TcdB, since the rate of cell rounding did not change in the presence of the inhibitor. It is worth noting that later cytopathic effects could be attributed to the activation of caspase-3. The evidence for caspase-3 modulation of the cytoskeleton is compelling. Interestingly, the pathway for caspase-3 regulation of the cytoskeleton is linked to Rac and Cdc42. Caspase-3 has been shown to degrade Rac and Cdc42 (Tu et. al, 2001), thus activation of caspase-3 may directly impact Rac and Cdc42 activity regardless of glucosylation by TcdB. While caspase-3 activation does not appear to lead to Rho cleavage, caspase-3 has been shown to cleave Rho-GDIs suggesting Rho may be modulated by caspase-3 during apoptosis (Essmann et. al, 2000). Indeed, activities other than glucosylation of Rho, Rac and Cdc42 may contribute to TcdB intoxication.

$TcdB^{1-556}$ apoptosis and cell death occur in the absence of caspase-3 activation but at a slower rate. At the concentration tested, apoptosis is detected as early as 12 h in TcdB treated cells. PI staining also occurs at early time-points and suggests some cells from this population could be going through necrotic cell death or late apoptosis. These results may explain earlier conflicting reports regarding cell necrosis versus apoptosis in TcdB intoxicated cells (Warny et. al, 1999); (Fiorentini et. al, 1998). The time-course of $TcdB^{1-556}$ induced apoptosis was different from that of TcdB. Treatment with $TcdB^{1-556}$ caused a different dual annexin-V, PI staining pattern, with a majority of cells staining early with annexin-V, then at later time points more cells became PI positive. These results suggested substrate-specific, and thus caspase-3 independent, apoptosis occurs slower than TcdB-induced, caspase-3 dependent apoptosis. Also, $TcdB^{1-556}$ apoptosis profiles did not show early signs of necrosis like that observed in TcdB intoxication. The mechanism of substrate specific apoptosis is not entirely clear and we are currently dissecting the role of other factors, such as Bcl-2 family members that may be involved in the caspase independent apoptosis. In addition, the region of TcdB that contributes to caspase dependent apoptosis is not defined and identification of this domain will significantly add to our understanding of this LCT.

Results from the $TcdB^{1-556}$-specific studies presented here, as well as, studies from other groups, clearly show that the enzymatic domain is capable of causing cell death. However, there is a growing body of data, including this report, that suggest LCTs have activities other than glucosylation that contribute to cell death. To my knowledge there are two reports that most directly implicate Rho inactivation as the sole cause of cell

death. First, work by Giry et al. (Giry et. al, 1995) showed that overexpression of Rho isoforms protected CHO cells from TcdB's toxic effects. Secondly, work by Chaves-Olarte (Chaves-Olarte et. al, 1996) showed that a cell line deficient in UDP-glucose was resistant to TcdB. It is interesting that Rho has been shown to regulate the expression of Bcl-2 and overexpression of Rho could prevent cells from going through apoptosis. In the case of the UDP-glucose deficient cell lines, while these cells were protected against TcdB's toxic effects, the cells did succumb to the toxin after extended incubation or exposure to increased doses of the toxin, and this could be a result of TcdB's nonsubstrate related activities.

Numerous studies have been carried out using TcdB as an inhibitor of Rho, Rac and Cdc42. We contend that data from such studies must be considered in the light of other possible intracellular activities of TcdB. TcdB (~270 kD) is a remarkably large intracellular bacterial toxin, and may have maintained this size to carry multiple functions within the cell. Finally, while TcdB is not unique as a virulence factor capable of stimulating apoptosis, TcdB does appear to be unusual since to our knowledge this is the first report of a single virulence factor capable of activating dual apoptotic pathways.

References

1. **Alcantara, C., Stenson, W.F., Steiner, T.S., and Guerrant, R.L.** (2001) J Infect Dis **184,** 648-652.
2. **Altschul, S.F., Madden, T.L., Schaffer, A.A., Zhang, J., Zhang, Z., Miller, W., and Lipman, D.J.** (1997) Nucleic Acids Res **25,** 3389-3402.
3. **Anderson, R.J., Ray, C.J., and Popoff, M.R.** (2000) *Kidney Int* **58,** 1996-2006.
4. **Boquet, P.** (1999) Ann N Y Acad Sci **886,** 83-90.
5. **Byun, Y., Chen, F., Chang, R., Trivedi, M., Green, K.J., and Cryns, V.L.** (2001) Cell Death Differ **8,** 443-450.
6. **Chaves-Olarte, E., Florin, I., Boquet, P., Popoff, M., von Eichel-Streiber, C., and Thelestam, M.** (1996) J Biol Chem **271,** 6925-6932.
7. **Devreese, B., Vanrobaeys, F., and Van Beeumen, J.** (2001) Rapid Commun Mass Spectrom **15,** 50-56.
8. **Essmann, F., Wieder, T., Otto, A., Muller, E.C., Dorken, B., and Daniel, P.T.** (2000) Biochem J **346 Pt 3,** 777-783.
9. **Fiorentini, C., Fabbri, A., Falzano, L., Fattorossi, A., Matarrese, P., Rivabene, R., and Donelli, G.** (1998) Infect Immun **66,** 2660-2665.
10. **Garrett, W.S., Chen, L.M., Kroschewski, R., Ebersold, M., Turley, S., Trombetta, S., Galan, J.E., and Mellman, I.** (2000) Cell **102,** 325-334.

11. **Giry, M., Popoff, M.R., von Eichel-Streiber, C., and Boquet, P.** (1995) Infect Immun **63,** 4063-4071.

12. **Gomez, J., Martinez, C., Giry, M., Garcia, A., and Rebollo, A.** (1997) Eur J Immunol **27,** 2793-2799.

13. **Hausding, M., Witteck, A., Rodriguez-Pascual, F., von Eichel-Streiber, C., Forstermann, U., and Kleinert, H.** (2000) Br J Pharmacol **131,** 553-561.

14. **He, D., Hagen, S.J., Pothoulakis, C., Chen, M., Medina, N.D., Warny, M., and LaMont,** J.T. (2000) Gastroenterology **119,** 139-150.

15. **Just, I., Fritz, G., Aktories, K., Giry, M., Popoff, M.R., Boquet, P., Hegenbarth, S., and von Eichel-Streiber, C.** (1994) J Biol Chem **269,** 10706-10712.

16. **Koike, T., Kuzuya, M., Asai, T., Kanda, S., Cheng, X.W., Watanabe, K., Banno, Y., Nozawa, Y., and Iguchi, A.** (2000) Biochem Biophys Res Commun **277,** 43-46.

17. **Le Gall, M., Chambard, J.C., Breittmayer, J.P., Grall, D., Pouyssegur, J., and Van Obberghen-Schilling,** E. (2000) Mol Biol Cell **11,** 1103-1112.

18. **Leist, M., and Jaattela, M.** (2001) Nat Rev Mol Cell Biol **2,** 589-598.

19. **Linseman, D.A., Laessig, T., Meintzer, M.K., McClure, M., Barth, H., Aktories, K., and Heidenreich, K.A.** (2001) J Biol Chem **276,** 39123-39131.

20. **Lombet, A., Zujovic, V., Kandouz, M., Billardon, C., Carvajal-Gonzalez, S., Gompel, A., and Rostene, W.** (2001) Eur J Biochem **268,** 1352-1362.

21. **McVey, D.C., and Vigna, S.R.** (2001) Peptides **22,** 1439-1446.

22. **Mylonakis, E., Ryan, E.T., and Calderwood, S.B.** (2001) Arch Intern Med **161,** 525-533.

23. **Nusrat, A., von Eichel-Streiber, C., Turner, J.R., Verkade, P., Madara, J.L., and Parkos, C.A.** (2001) Infect Immun **69,** 1329-1336.

24. **Qa'Dan, M., Spyres, L.M., and Ballard, J.D.** (2000) Infect Immun **68,** 2470-2474.

25. **Safiejko-Mroczka, B., and Bell, P.B., Jr.** (1998) Exp Cell Res **242,** 495-514.

26. **Spyres, L.M., Qa'Dan, M., Meader, A., Tomasek, J.J., Howard, E.W., and Ballard, J.D.** (2001) Infect Immun **69,** 599-601.

27. **Tu, S., and Cerione, R.A.** (2001) J Biol Chem **276,** 19656-19663.

28. **Warny, M., and Kelly, C.P.** (1999) Am J Physiol **276,** C717-724.

Chapter IV
Multiple Death Pathways Are Triggered By *Clostridium sordellii* Lethal Toxin

ABSTRACT

Clostridium sordellii lethal toxin (TcsL) glucosylates Ras, Rap, Ral, and Rac during intoxication of mammalian cells. In this study we show that TcsL has the capacity to activate multiple death pathways in intoxicated cells. Initially, we generated a fusion protein encoding the TcsL enzymatic domain (residues 1-556) with a truncated version of anthrax toxin lethal factor (LFn). When delivered to the cytosol of the cell with anthrax protective antigen (PA), LFnTcsL$^{1-556}$ caused cytopathic effects at a rate faster than wild-type TcsL; however, cell death in fusion treated cells was delayed compared to TcsL. In light of this disparity in cytotoxicity between LFnTcsL$^{1-556}$ and TcsL, we analyzed a death pathway in treated cells by quantifying caspase-3 activation. In contrast to TcsL, PA plus LFnTcsL$^{1-556}$ did not stimulate any detectable caspase-3 activation under conditions that caused cell rounding and cell death. Furthermore, a broad-spectrum caspase inhibitor delayed cell death in HeLa cells intoxicated with TcsL, but the inhibitor did not afford the same protection to PA, LFnTcsL$^{1-556}$ treated cells. In addition, a caspase-3 deficient cell line (MCF-7), treated with TcsL, showed delayed cell death, but an almost identical time-course of cytopathic effects compared to HeLa cells. Interestingly, nucleosomal DNA fragmentation and annexin-V positive staining was detected in cells treated with TcsL or PA, LFnTcsL$^{1-556}$ suggesting both are capable of triggering apoptosis. These data suggest TcsL uses multiple functional domains to activate more than one death pathway in intoxicated cells

INTRODUCTION

Clostridium sordellii is an important veterinary pathogen, and causes liver disease, myositis, and sudden death in sheep (17, 22). In humans, *C. sordellii* has been implicated in post-partum deaths and, recently, as the causative agent of death in patients undergoing knee surgery (3, 14). *C. sordellii* has also been involved in a shock-like disease among intravenous drug users (2). *C. sordellii* disease appears to be on the rise in humans, and unfortunately we have a poor understanding of the mechanisms of pathogenesis for this organism. Two *C. sordellii* virulence factors, lethal toxin (TcsL) and hemorrahgic toxin (TcsH), have been analyzed in some detail, and toxoids of these proteins are effective vaccines against *C. sordellii* (1). Thus, TcsL and TcsH are important to the disease process and may be major *C. sordellii* virulence factors.

TcsL and TcsH are members of the family of large clostridial toxins (LCTs), which is composed of at least 5 sizable (250 kDa-308 kDa) glycosyltransferase toxins from the clostridia (4). In addition to TcsL and TcsH, LCTs include toxin A (TcdA) and toxin B (TcdB) from *Clostridium difficile*, and α-toxin (Tcnα) from *Clostridium novyi*. Each of these toxins causes pronounced cytopathic effects (CPE) in cultured mammalian cells, and these effects are apparently a prelude to cell death. To cause CPE, LCTs enter cells via receptor mediated endocytosis and require acidified endosomes for translocation to the cytosol where target substrates are modified. TcsL causes delayed CPE compared to TcdB and TcdA, and this appears to be due to TcsL's relatively slow time-course of cell entry (6, 20). The differences in cytotoxicity might also be due to TcsL's substrate targets, which differ from those of TcdA and TcdB.

LCTs glycosylate members of the Ras family of small GTPases. In particular, TcdA, TcdB, TcsH, and Tcnα preferentially target Rho, Rac and Cdc42, while TcsL inactivates Ras, Ral, Rap, and Rac. Since Rho, Rac, and Cdc42 are responsible for cytoskeleton organization and cell signaling, their inactivation leads to the inhibition of actin polymerization, vesicular trafficking, and transcriptional activation (8, 13, 16). Ras, a target of TcsL, plays a key role in a mitogen activated protein kinase pathway (MAPK), and its inactivation leads to the inhibition of signal transduction to key downstream effectors like extracellular-signal regulated kinases 1 and 2 (10, 12, 19). Despite this list of targets and physiological impacts on cell biology, little is known about how or why these cells ultimately succumb to the intoxication. There are two primary modes of cell death, necrosis and programmed cell death. TcsL appears to involve the latter to cause cell death, and reportedly triggers caspase-3 activation and apoptosis (18).

Recently, work by He et al. indicated TcdA is capable of initiating processes within the cell prior to substrate modification, suggesting LCTs may have other activities unrelated to glucosylation and these contribute to changes in cell physiology (9). In light of this, and in order to better define TcsL intoxication, we analyzed the impact of the TcsL enzymatic domain, in the absence of other regions of the toxin, on cell physiology. In particular, I examined the ability of the TcsL enzymatic domain to cause cytotoxic effects and trigger apoptosis during intoxication. Herein, I report that unlike full-length toxin, which causes caspase-dependent cell death, the TcsL enzymatic domain triggers apoptotic cell death in a caspase-independent fashion.

MATERIALS AND METHODS

Cell culture, reagents, wild type and recombinant toxins. Unless otherwise noted, all reagents and chemicals were purchased from Sigma Chemical Co., St. Louis, Mo. Human epitheloid carcinoma (HeLa) cells, human adenocarcinoma mammary gland cells (MCF-7) and Chinese hamster ovary cells (CHO) were obtained from the American Type Culture Collection (Manassas, Va). HeLa cells were maintained in RP-10 medium supplemented with 10% fetal bovine serum, while MCF-7 cells were maintained in RP-10 medium supplemented with 10% fetal bovine serum plus 0.01 mg/ml bovine insulin. Cultures were grown at 37°C in the presence of 6% CO_2 and all cells were used between passages 6 and 10. TcsL, PA and $LFnTcdB_{1\text{-}556}$ were isolated as previously described (20, 21).

Glucosylation, Cell Viability and Quantification of Cytopathic Effects. Differential glucosylation assays were similar to those previously described (20), except PA (300 pmol) plus $LFnTcsL^{1\text{-}556}$ (300 pmol) was substituted for acid pulsed TcsL. Cell viability assays were carried out using WST-8 (2-(2-methoxy-4-nitrophenyl)-3-(4-nitrophenyl)-5-(2,4-disulfophenyl)-2H-tetrazolium, monosodium salt) (Dojindo Laboratories, Gaithersburg, MD) according to manufacturer's instructions. The following formula was used to determine % viability $\{(A_{test}\text{-}A_{background})/(A_{control}\text{-}A_{background})*100\}$, wherein A=absorbance at OD_{405}, background=SDS treated sample, and control=cells treated with media alone. Percent cytopathic effects (% CPE) were calculated by counting a

minimum of 100 cells in 3 fields from each sample. Fully rounded cells were scored positive for CPE and the final % CPE was calculated as % rounded $cells_{test}$ - % rounded $cells_{control}$, wherein control sample= cells treated with media alone. In a standard assay, cells were treated with 100 fmol of TcdB or TcsL in a volume of 100 µl. For assays with the fusion proteins cells were treated with 30 pmol of PA and 1 pmol of either $LFnTcsL_{1-556}$ or $LFnTcdB_{1-556}$.

Construction, expression, and isolation of $LFnTcsL_{1-556}$. The region encoding for TcsL enzymatic domain was amplified from *Clostridium sordellii* strain 9714 genomic DNA by PCR using the forward primer 5'-GCGCGCGGATCCATGAACTTAGTTAACAAAGCCCAA-3' and the reverse primer 5'-GCGCGCGGATCCTTATTATAATATTTTTTTAGAAACATAATC-3' to generate $tcsL_{1-1668}$ with 5' and 3' *Bam*HI site. $tcsL_{1-1668}$ was then restricted with *Bam*HI, and *lfn* was genetically fused to $tcsL_{1-1668}$ by ligation overnight at 16°C with *Bam*HI restricted pABII, a derivative of pET15b containing *lfn*. This construct generated an in-frame fusion of *lfn* and $tcsL_{1-1668}$ and the resulting plasmid, pMQ101. The correct genetic fusion resulted in joining the 3' end of *lfn* at the codon TCC encoding S254, followed by sequences within the multiple cloning site that encoded the linker region and a string of residues (PGGGGGS), with the 5' end of $tcsL_{1-1668}$ at the ATG codon encoding M1. pMQ101 was then transformed into *Escherichia coli* DH5α (CLONTECH, Palo Alto, Calif.), and candidate clones were screened by mini-prep analysis. In-frame, correctly oriented, clones were identified by restriction analysis and DNA sequencing, and then

transformed into *E. coli* BL-21(DE3) (Stratagene, La Jollla, Calif.). For expression, cells were grown at 37°C until 0.8 OD_{600} density was reached, and induced with 0.1 mM IPTG (Isopropyl-B-D-Thiolgalactopyranoside) (Denville Scientific Inc., Metuchen, NJ) at 16°C for 12-16 h. $LFnTcsL^{1-556}$ was purified by Ni^{2+} affinity chromatography according to manufacturer's instructions (Novagen, Madison, Wis.). The purified protein migrated within the predicted size range (~94 kDa) by sodium dodecyl sulfate-poly-acrylamide gel electrophoresis (SDS-PAGE) analysis and was reactive to both anti-LF and TcsL polyclonal antisera.

Caspase-3 activation and caspase inhibitor assays. To test for caspase-3 activity, HeLa cells were grown in 25-cm^2 tissue culture flasks until confluent at a density of 3 X 10^6 cells/flask, at which point 1 pmol of TcsL, or 30 pmol PA plus 100 pmol $LFnTcsL_{1-556}$, was added to the cells in a final volume of 5 ml. At the indicated time points, cells were scraped and centrifuged at 1000 X g for 5 min at 4°C. Treated cells were suspended in lysis buffer (50 mM HEPES, 100 mM NaCl, 0.1% CHAPS, 1mM DTT, 0.1 mM EDTA, pH 7.4) and incubated for 10 min on ice, and cell debris was removed by centrifugation at 10000 X g for 5 min at 4°C. Eighty microliters of assay buffer (50 mM HEPES, 100 mM NaCl, 0.1% CHAPS, 10 mM DTT, 0.1 mM EDTA, 10% glycerol, pH 7.4) was then added to 10 µl of Caspase-3-Substrate I (CPP32/apopain colorimetric substrate, Ac-Asp-Glu-Val-Asp-*p*NA) (Calbiochem, La Jolla, Calif.) and 20 µl of cell extract. Readings were then recorded every 5 min using a PowerWavex plate reader (BIO-TEK,Winooski,VT) at 405 nm for 24 h at 37°C. Caspase-3 specific-activity, was calculated per manufacturer's instructions. Caspase inhibitor assays were performed

according to manufacturer's instructions using 50 μM caspase inhibitor cocktail III (Calbiochem, La Jolla, Calif.).

Analysis of nucleosomal fragmentation. HeLa cells were grown in 25-cm^2 tissue culture flasks until confluent at a density of 3 X 10^6 cells/flask, at which point 10 pmol of TcsL, or PA plus $LFnTcsL^{1-556}$, were added to the cells in a final volume of 5 ml. At the indicated time points, cells were mechanically removed and centrifuged at 1000 X g for 5 min at 4°C. The cells were then resuspended in PBS at 1-2 X 10^6 cells/ml, and then pelleted by brief centrifugation. Nucleosomal DNA was extracted using an Apoptotic LADDER Kit (Geno Technology, St. Louis, MO) according to manufacturer's instructions. The DNA sample was then loaded and analyzed on a 1.8 % agarose gel.

Propidium iodide and Annexin-V staining. For differential propidium and annexin-V staining experiments, HeLa cells were grown in 25-cm^2 tissue culture flasks at a density of 3 X 10^6 cells/flask for 16 h, at which point 10 pmol of TcsL, or PA plus $LFnTcsL^{1-556}$, were added to the cells in a final volume of 5 ml. At the indicated time points, cells were trypsinized and pelleted at 100 X g for 10 min at 4°C. Cells were then resuspended in cold PBS and pelleted at 100 X g for 10 min at 4°C. Annexin binding buffer (10 mM HEPES, 140 mM NaCl, 2.5 mM $CaCl_2$, pH 7.4) was used to resuspend cells at a density of 1 X 10^6 cells/ml. Cells were then labeled with 5 μl of Annexin-V Alexa Fluor 488 dye and propidium iodide (Molecular Probes, Eugene, Oreg.) according to the manufacturer's protocol. Labeled cells were analyzed using a FACSCalibur system (BD Biosiences, San Diego, Calif.) at the University of Oklahoma Health Sciences Center FACS core facility.

The probe was excited with a laser at 488 nm (250 mW), and emission was measured at 530 nm and > 575 nm; logarithmic amplification was used for fluorescence detection.

Statistical analysis. Statistical determinations were made using the statistics component of Microsoft Excel 2001.

RESULTS

Comparison of LFnTcsL$^{1-556}$ plus PA and TcsL cytotoxic effects. Under normal cell culture conditions TcsL causes cell death at a rate substantially slower than TcdB. In earlier work, we reported that providing an extracellular acid pH pulse quickened TcsL's otherwise slow time-course of intoxication (20). Acid pulsed entry of TcsL also caused CPE similar to that of TcdB. This suggested the limitation to intoxication by TcsL, relative to TcdB, could be at the stage of cell entry and not due to differing substrate targets. Chaves-Olarte et al. have also suggested this possibility (6). It is also possible that domains outside of the enzymatic region, which could function within the cytosol, contribute to differences in toxicity between TcsL and TcdB. Thus an approach to normalize entry for the enzymatic domains of TcsL and TcdB was investigated. In past studies on TcdB, we have utilized an anthrax toxin derived delivery system to facilitate entry of the TcdB enzymatic domain into target cells (21). I have now generated a

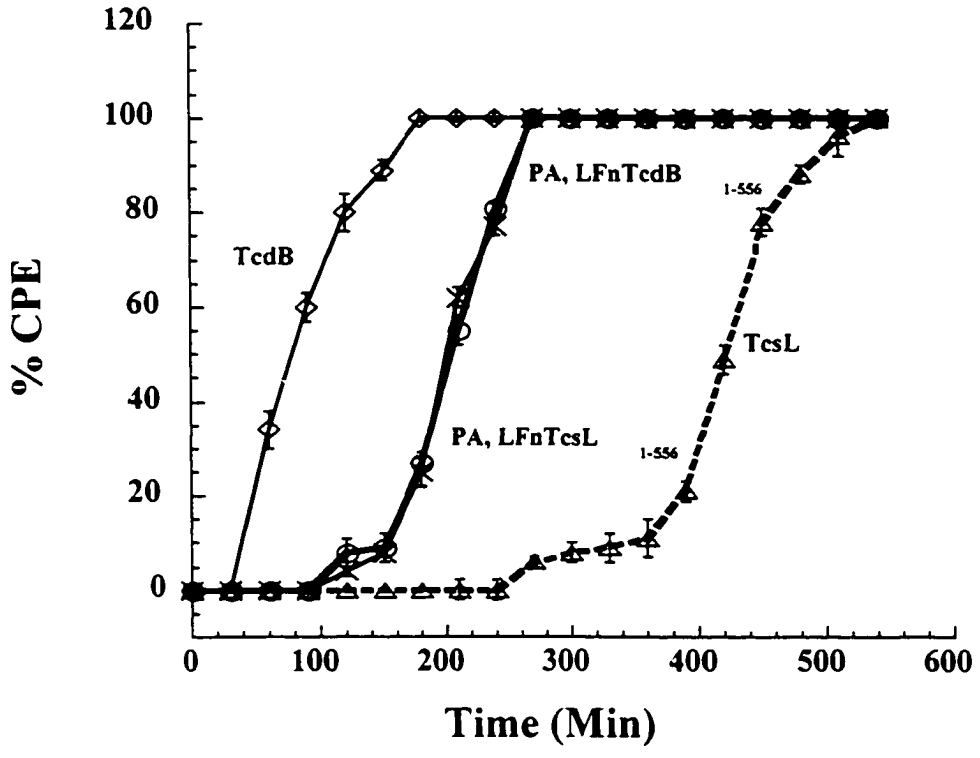


FIG. 1. Time course of CPE in TcsL and LFnTcsL$^{1-556}$ treated cells. HeLa cells were grown to confluence in a 96-well plate to approximately 5 x 10^4 cells/well. Cells were treated with either TcdB (100 fmol), TcsL (100 fmol), LFnTcsL$^{1-556}$ (1 pmol) or LFnTcdB$_{1-556}$ (1 pmol) in a volume of 100 µl. PA (30 pmol) was included with the fusion proteins. Control cells were treated with media, heat-inactivated toxin or PA-LFn alone. Following treatment, the cells were followed for 10 h and % CPE was calculated by visualizing the number of rounded cells from a field of at least 100 cells. The final % CPE was then calculated by subtracting the % CPE in test samples from % CPE in the appropriate controls. The corresponding lines for each sample are labeled within the figure.

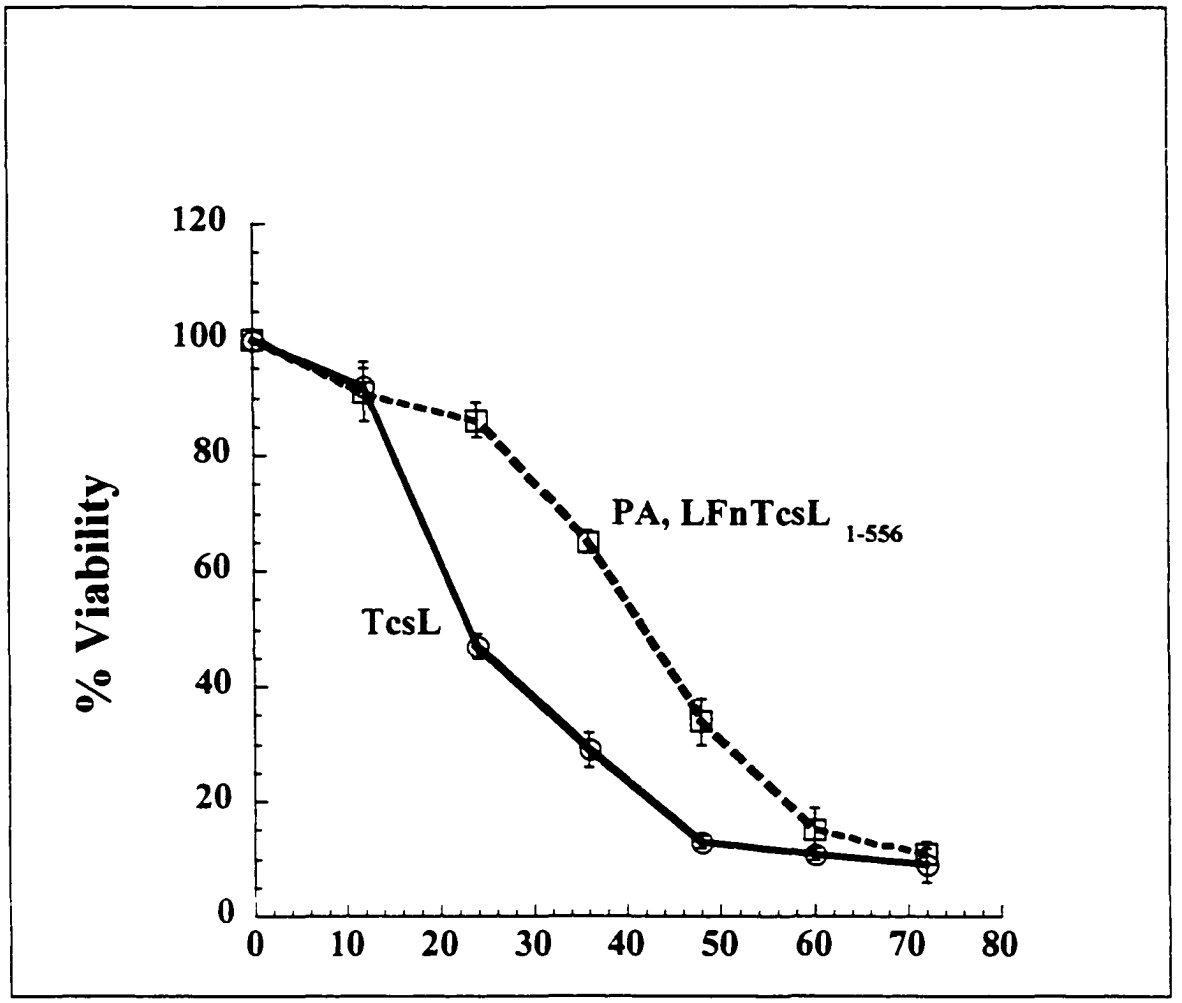


FIG. 2. Cell viability after treatment with TcsL or LFnTcsL$^{1-556}$. HeLa cells were grown to confluence in a 96-well plate to approximately 5 x 10^4 cells/well. Cells were treated with TcsL (100 fmol) or LFnTcsL$^{1-556}$ (1 pmol) plus PA (30 pmol) in a final volume of 100 µl. Following toxin treatment, cells were treated with the viability stain WST-8 at the indicated time points. Percent viability was determined by subtraction of background and comparison with untreated samples as described in the materials and methods. The corresponding lines for each sample are labeled within the figure. Samples were analyzed in triplicate and the error bars represent the standard deviation from the mean.

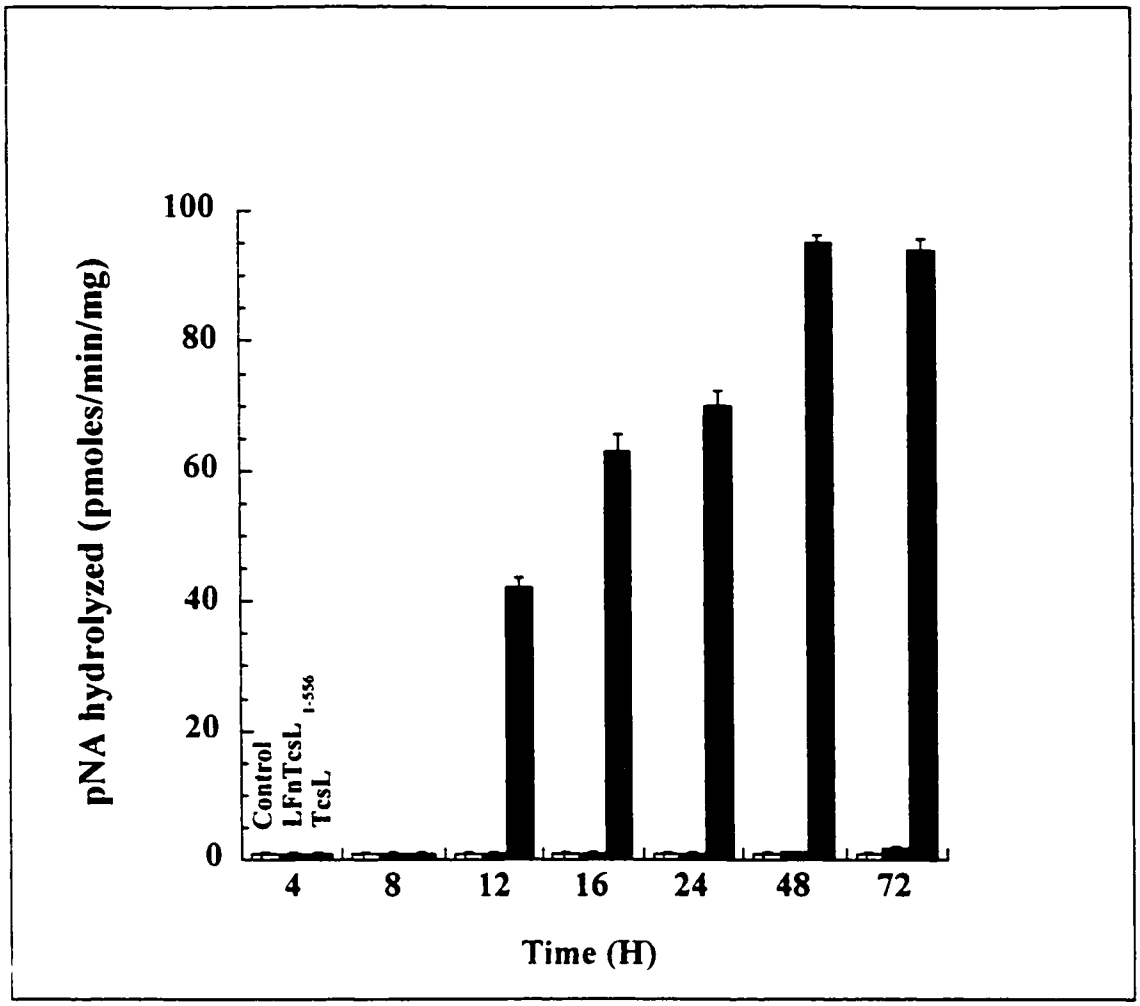


FIG. 3. Caspase-3 activation in TcsL treated cells. HeLa cells were grown in 25-cm^2 tissue culture flasks until confluent at a density of 3 X 10^6 cells/flask. Cells were then treated with TcsL (100 pmol), or $LFnTcsL^{1-556}$ (100 pmol) plus PA (300 pmol) in a final volume of 5 ml. At the indicated time-points cells were lysed and extracts were collected. Extracts from the various samples were assayed for hydrolysis of the caspase-3 substrate, Ac-Asp-Glu-Val-Asp-*p*NA. The corresponding bars for each sample are labeled within the figure. Each assay was performed in triplicate and the error bars represent the standard deviation from the mean.

similar construct with the TcsL enzymatic domain. This anthrax toxin delivery system consists of anthrax protective antigen (PA), and a truncated form of anthrax lethal factor (LFn), to which heterologous fusions are made. PA then mediates the cell entry of the LFn fusion via anthrax toxin's normal mode of cell penetration. Like the LFnTcdB$^{1-556}$ fusion, LFnTcsL$^{1-556}$ is expressed in recombinant form with a His_6 tag and can be isolated in a single step of Ni^{2+} affinity chromatography. Similar to our report on acid pulsed entry of TcsL(20), glucosylation profiles from extracts of cells treated with LFnTcsL$^{1-556}$ plus PA showed that all TcsL substrates were modified by the fusion (data not shown). Thus the fusion appeared suitable for making comparisons between the enzymatic domains of TcsL and TcdB.

As shown in Fig. 1, LFnTcdB$^{1-556}$ and LFnTcsL$^{1-556}$ delivered with PA demonstrate a similar time-course of cytopathic effects (CPE) on HeLa cells. Wild-type TcdB causes CPE more rapidly than the fusions or TcsL. In comparison to TcsL, LFnTcsL$^{1-556}$ plus PA caused CPE more quickly than wild-type toxin. Interestingly, there was not a connection between the rates of CPE and cell death in the fusion treated cells. As shown in Fig. 2, ~ 55% of TcsL treated cells lose viability after 24 h compared to 12% of cells treated with LFnTcsL$^{1-556}$ plus PA. After 48 h, almost 90% of TcsL treated cells are nonviable compared to about 75% of LFnTcsL$^{1-556}$ plus PA treated cells. By 72 h complete cell death had occurred in each of the conditions. These results suggested the enzymatic domain is capable of evoking early cytopathic effects, but activities dependent on regions outside of this part of the toxin contribute to a more rapid cell death.

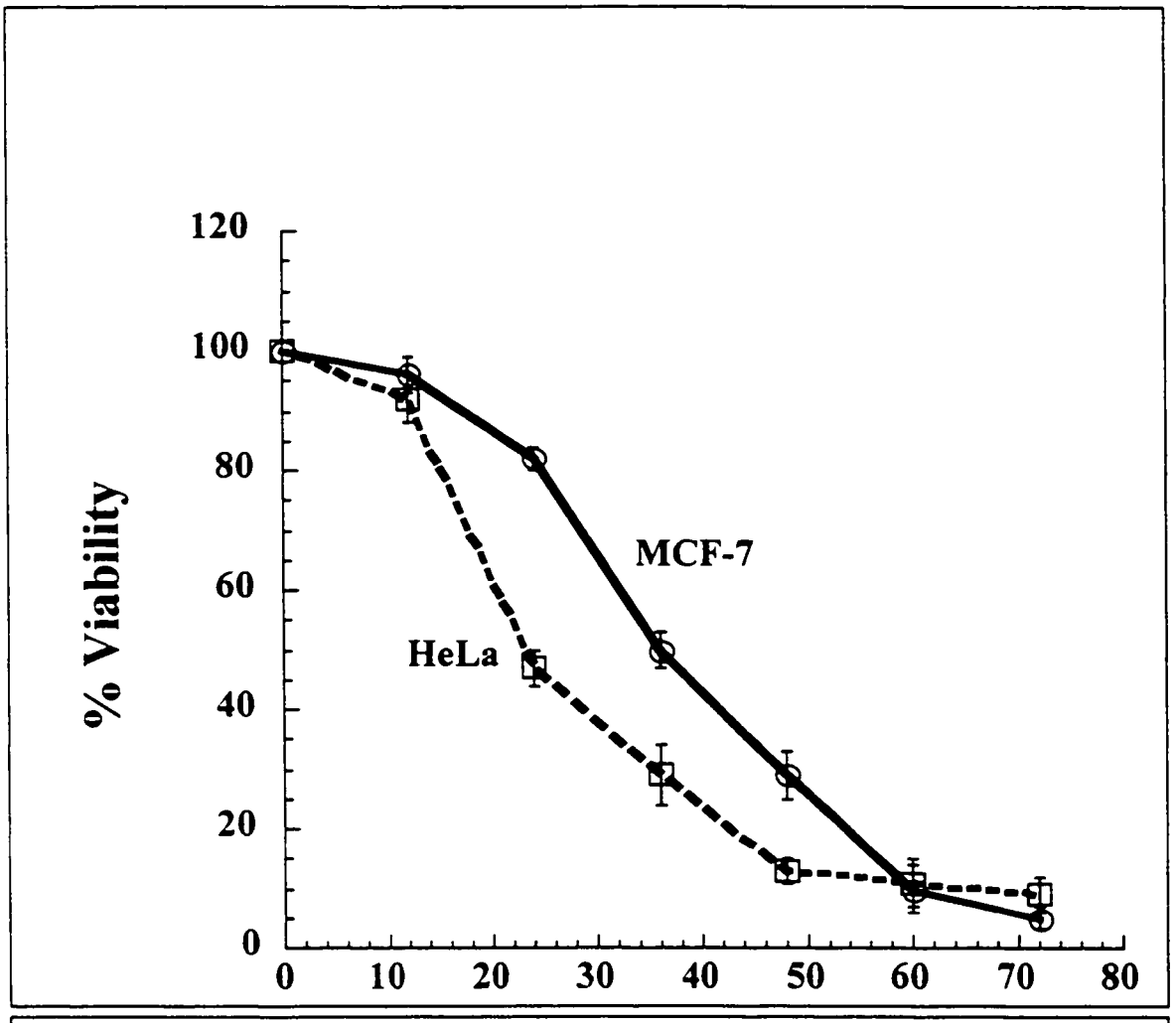


FIG. 4. Effect of TcsL on Caspase-3 deficient cells. A caspase-3 deficient cell line (MCF-7), or HeLa cells, was grown to confluence in a 96-well plate at final density of 5 x 10^4 cells/well. Both cell lines were then treated with TcsL (100 fmo) in a final volume of 100 µl. Cell viability was determined using WST-8 staining at the indicated time points. The lines corresponding to the appropriate sample are labeled within the figure. Each sample was analyzed in triplicate and the error bars represent the standard deviation from the mean.

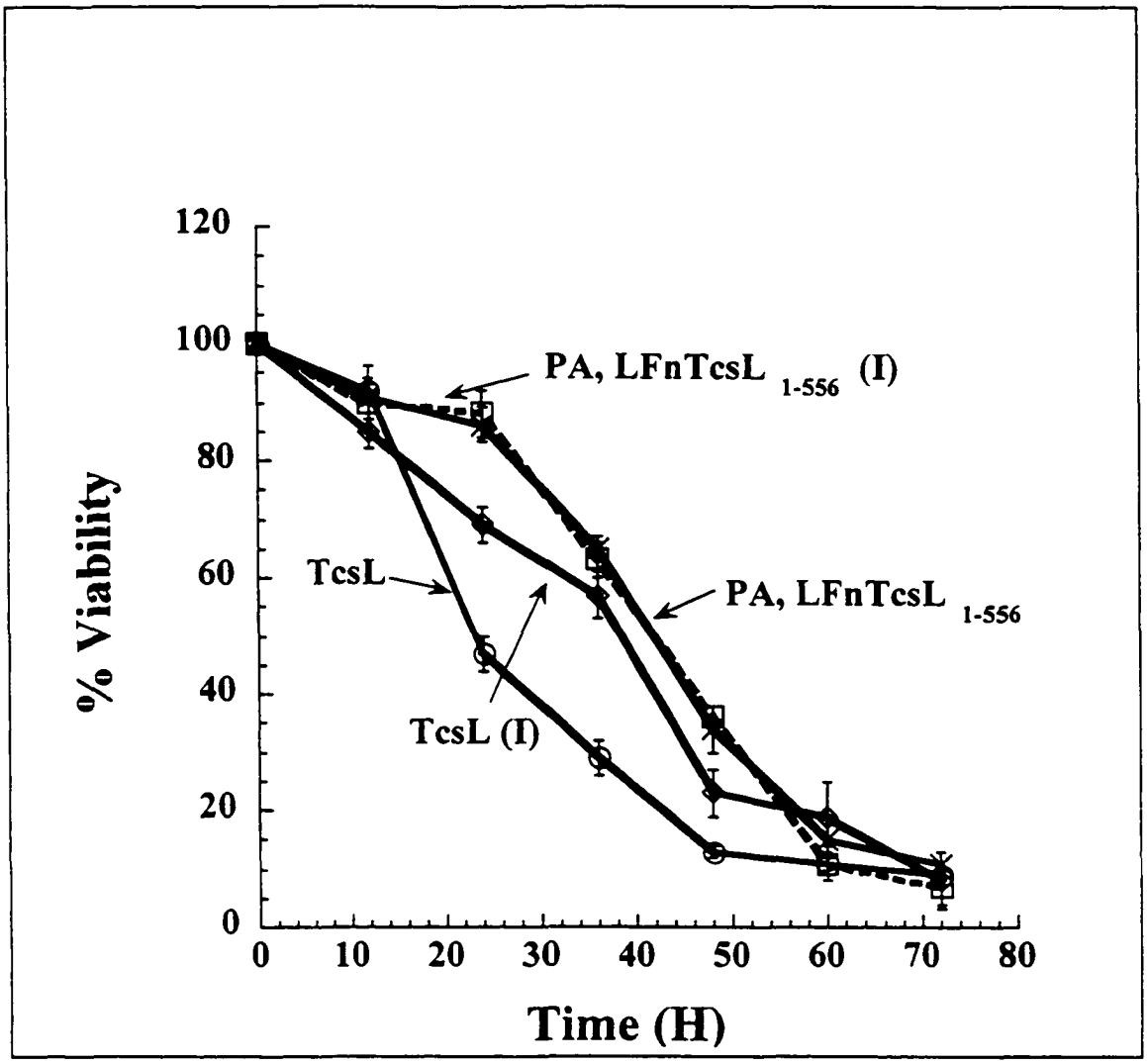


FIG. 5. Effect of pancaspase inhibitor on TcsL and LFnTcsL$^{1-556}$ intoxication. HeLa cells were grown to confluence in a 96-well plate to approximately 5 x 10^4 cells/well. Cells were then treated with TcsL (100 fmol) or with LFnTcsL$^{1-556}$ (1 pmol) plus PA (30 pmol) in a final volume of 100 µl. Samples were assayed at the indicated time-points and cell viability was determined by WST-8 staining. The lines corresponding to the appropriate samples are labeled within the figure. Each sample was analyzed in triplicate and the error bars represent the standard deviation from the mean.

Caspase activation in toxin and LFnTcsL$^{1-556}$ plus PA treated cells. In an effort to define the differing mechanisms of cell death between cells treated with TcsL and LFnTcsL$^{1-556}$ plus PA, we first analyzed the impact these proteins have on caspase activation in intoxicated cells. Work by Linseman et al. suggested caspase-3 was activated during toxin-induced apoptosis (18), consequently we analyzed the enzymatic domain for the ability to activate this protein. HeLa cells were treated with TcsL or the fusion protein plus PA, and extracts from various time-points in intoxication were analyzed for caspase-3 activation. Using a colorimetric substrate, Ac-Asp-Glu-Val-Asp-*p*NA, the specific activity for caspase-3 was determined. As shown in Fig. 3, although caspase-3 was clearly activated in TcsL treated cells, there was no detectable caspase-3 activation in cells treated with LFnTcsL$^{1-556}$ plus PA. In line with this observation we also found that a caspase-3 deficient cell line (MCF-7), demonstrated a slower time-course to cell death in comparison to HeLa cells when treated with TcsL (see Fig. 4). Although, MCF-7 cells show a delay in cell death compared to HeLa cells when treated with TcsL, the cells demonstrate almost identical time-courses for CPE (data not shown). This further suggested that factors other than those inducing CPE contribute to death of the cell.

The role of caspase activity in TcsL cytotoxicity was investigated further by determining the impact of a broad-spectrum caspase inhibitor on intoxication. As shown in Fig. 5, inhibition of caspase activity slowed the killing effect of TcsL. Addition of the caspsase inhibitor did not change the rate of CPE in TcsL treated cells (data not shown). Furthermore, also shown in Fig.5, the caspase inhibitor was unable to alter the time-course for CPE or death in cells treated with LFnTcsL$^{1-556}$ plus PA. Addition of the

caspase inhibitor caused cell death in TcsL treated cells to occur at rate very similar to that of LFnTcsL$^{1-556}$ plus PA. This result further suggested that caspase activation contributes to cell death, but is instigated by a region of the toxin outside of the enzymatic domain.

Analysis of apoptosis in TcsL and LFnTcsL$^{1-556}$ plus PA treated cells. The caspase analysis indicated activation of these proteases contributes to the death of TcsL intoxicated cells. Clearly, in the absence of caspase activity, the cells eventually die. It was not evident if cells died from necrosis or an alternative, caspase-independent form of apoptosis. Hence, cells treated with TcsL or LFnTcsL$^{1-556}$ plus PA were analyzed for hallmarks of apoptotic cell death. Initially, cells were analyzed for nucleosomal fragmentation as a result of intoxication. As shown in Fig. 6, cells treated with TcsL or LFnTcsL$^{1-556}$ plus PA caused nucleosomal fragmentation, suggesting both forms of the toxin caused apoptosis.

The nucleosomal fragmentation assay does not exclude the possibility that a mixed population of necrotic and apoptotic cells could be present in the treated cells. Therefore, to analyze the characteristic of cell death within individual cells, a FACS analysis was carried out using differential annexin-V/propidium iodine (PI) staining. Apoptotic cells stain positive for annexin-V, and PI staining can occur in necrotic cells or late course apoptotic cells. As shown in the panels of Fig. 7, HeLa cells treated with TcsL or

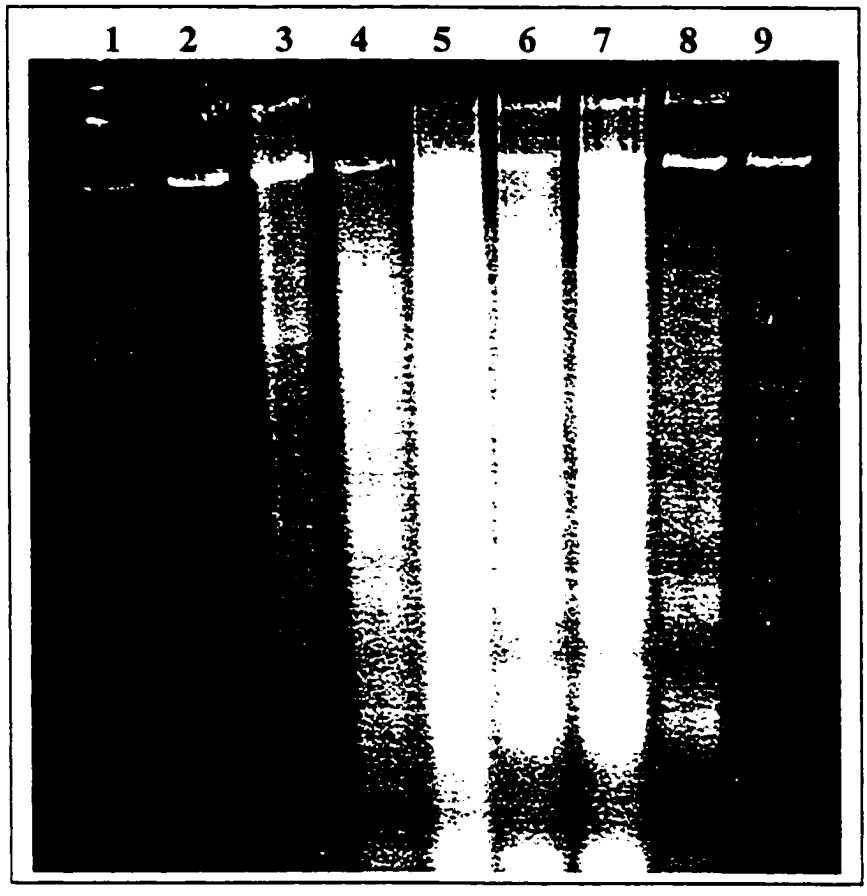


FIG. 6. Nucleosomal DNA fragmentation following treatment with TcsL or LFnTcsL$^{1-556}$. HeLa cells were grown in 25-cm^2 tissue culture flasks until confluent at a density of 3 X 10^6 cells/flask. Cells were then treated with TcsL (100 fmol), or LFnTcsL$^{1-556}$ (100 fmol) plus PA (300 pmol) in a final volume of 5 ml. Nucleosomal DNA was then extracted and analyzed on a 1.8% agarose gel. lane 1, Control; lane 2, PA, LFnTcsL$^{1-556}$ 12 h; lane 3, TcsL 12 h; lane 4, PA, LFnTcsL$^{1-556}$ 24 h; lane 5, TcsL 24 h, lane 6, PA, LFnTcsL$^{1-556}$ 36 h; lane 7, TcsL 36 h, lane 8, PA, LFnTcsL$^{1-556}$ 48 h; lane 9, TcsL 48 h.

Fig. 7

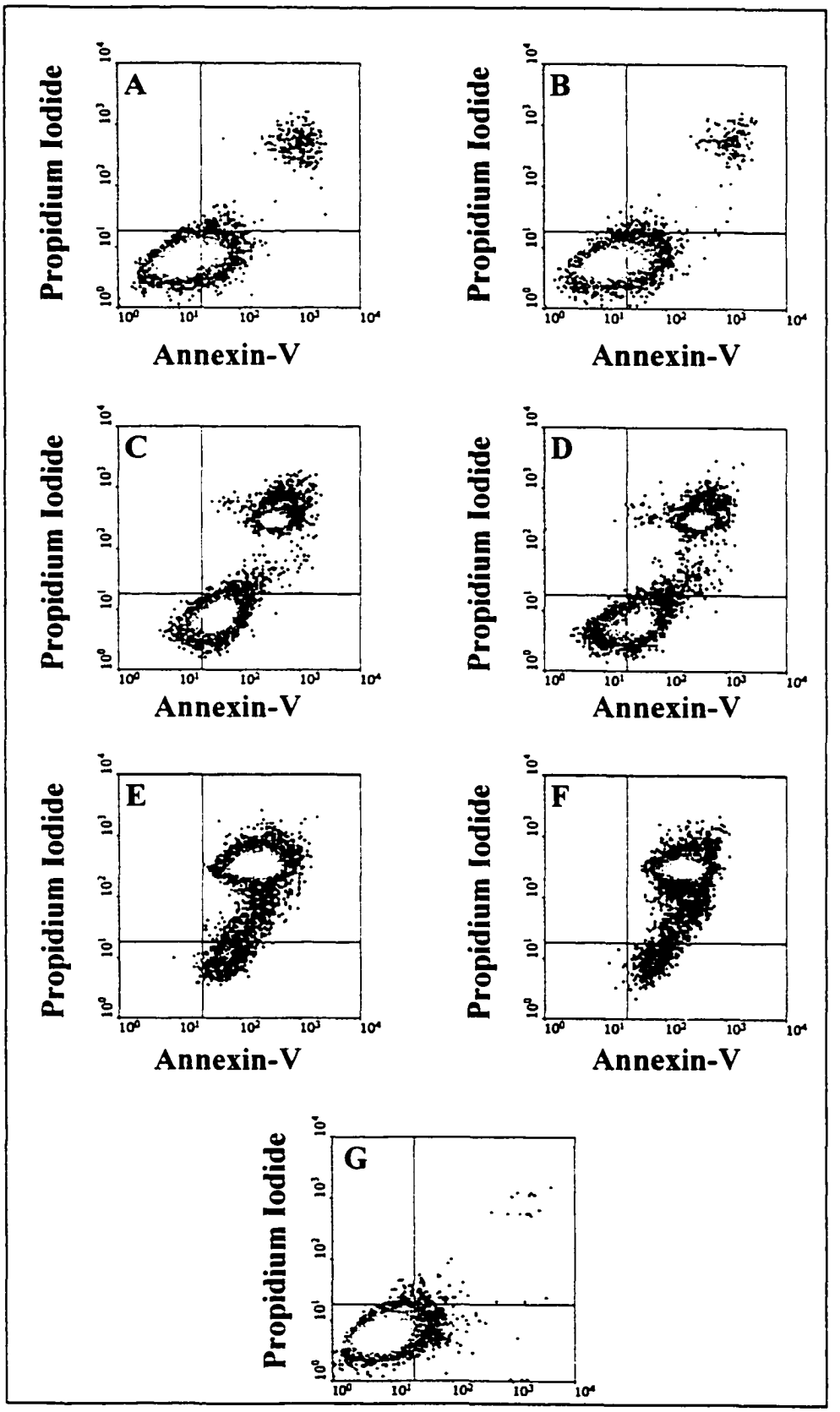


FIG. 7. Differential annexin-V/propidium iodide staining of cells treated with TcsL or LFnTcsL$^{1-556}$ plus PA. HeLa cells were grown in 25-cm^2 tissue culture flasks until confluent at a density of 3 X 10^6 cells/flask. Cells were then treated with TcsL (100 pmol) or LFnTcsL$^{1-556}$ (100 pmol) plus PA (300 pmol) in final volume of 5 ml. Control samples were treated with media alone. Cells were collected at the indicated time points and labeled with annexin-V Alexa flour 488 and propidium iodide. Panel A, TcsL 12 h; panel B, LFnTcsL$^{1-556}$ 12 h; panel C, TcsL 24 h; panel D, LFnTcsL$^{1-556}$ 24 h, panel E, TcsL 36 h; panel F, LFnTcsL$^{1-556}$ 36 h; panel G, control.

LFnTcsL$^{1-556}$ plus PA stained annexin-V positive as early as 12 h, with a low number of cells staining positive with PI. By 24 h, close to 40% of cells treated with TcsL or LFnTcsL$^{1-556}$ plus PA were annexin-V positive (apoptotic), and about 40% stained annexin-V/PI positive. By 36 h, ~ 85% of the cells stained positive for annexin-V/PI. These results strongly suggest, LFnTcsL$^{1-556}$ plus PA treated cells, while incapable of activating caspases, go through a process of apoptotic cell death.

DISCUSSION

In this work, I report on two previously undefined aspects of TcsL intoxication. First, TcsL's capacity to intoxicate cells is limited at the stage of cell entry. Second, TcsL activates caspase-dependent and caspase-independent cell death, and distinct regions of the protein initiate these pathways.

In earlier studies I found that by providing an extracellular acid pH pulse TcsL cytotoxic activity could be enhanced (20). I also found that acid pulse entry of TcsL causes CPE similar to that of TcdB. In line with that report, I have now shown that normalized entry of the enzymatic domains of TcdB and TcsL results in an intoxication profile that is almost identical between the enzymatic domains. Although the substrate recognition profile is different between the toxins, this does not dramatically impact the rate of CPE. It is possible that TcsL is slower at entering cells than TcdB and that acid pulse or PA, LFn delivery is not a fair reflection of CPE for this toxin. There are two other plausible explanations for TcsL's slow entry at neutral pH. First, the enhanced activity at acid pH may suggest the toxin is optimally active within an acidified environment, such as that found in many clostridial infections. Second, the appropriate target cell has not yet been identified. Clearly, a more detailed analysis of TcsL's role in pathogenesis and preferred cell targets is needed to better understand how this toxin functions during the disease process.

The size of LCTs suggests these toxins may carry out multiple activities within the cell. Until recently, this possibility was a biological curiosity, without support from any experimental evidence. In a series of reports Lamont et al. has shown that TcdA can perturb mitochondria, trigger IL-8 release, cause IkappaB degradation and generate reactive oxygen intermediates prior to detectable modification of substrate (9, 23). Arguably, other targets for LCTs exist within cells and these targets/activities account for the differential death pathways in TcsL intoxicated cells. There are several observations

that must be explained if this is true. Giry et al. reported that transient expression of Rho protects cells from TcdB intoxication (7). Since this is a multiple substrate targeting enzyme it is possible that the over expressed Rho titrates the toxin away from relevant targets. Also Rho promotes cell survival, and over expression of Rho may counter the apoptotic effects of the toxin. In other work, Chaves-Olarte et al. found that a UDP-Glc deficient cell line is resistant to LCTs dependent on this cosubstrate (5). The UDP-Glc deficient cells eventually die when treated with the toxins but at a considerably slower rate compared cells with normal cosubstrate levels. It is possible that the delayed cell death is due to the second, nonsubstrate related toxicity of the toxins.

The difference in the results between the wild-type toxin and the fusion protein might also be explained by varying substrate affinities between these two proteins. In our hands the enzymatic domain is comparable to wild-type toxin in *in vitro* assays and other groups have reported similar observations (11). It is also possible that the fusion protein cannot localize to substrate at cellular locations, which can be accessed by TcsL. The results using caspase inhibitor to block TcsL cell death argue against this possibility. Treatment of cells with TcsL in the presence of the pancaspase inhibitor results in an intoxication profile almost identical to PA, LFnTcsL$^{1-556}$. With the exception of one time point the lines are statistically identical. This result suggests that inhibition of caspase-dependent cell death reveals a death pathway completely dependent on the enzymatic domain.

Caspase-dependent apoptosis can be triggered by interaction with cell surface receptors, such as Fas or TNFα receptor, or by perturbation of the mitochondria and cytochrome c release(15). Cytochrome c activates caspase-9, which subsequently triggers caspase-3 activation. In this study, caspase-dependent apopotosis may occur by TcsL interacting with Fas or TNFα receptor. However, perturbation of the mitochondria is the more likely explanation, since inhibitors of endocytosis protect cells from TcsL (20). Such inhibitors would not prevent TcsL binding to Fas or TNFα, but are capable of preventing TcsL from gaining access to the cytosol. Studies are currently underway to define the impact TcsL has on mitochondria integrity. Caspase-independent apopotosis appears to be directly linked to inactivation of TcsL's target substrates. The mechanisms by which inactivation of Ras, Ral, Rap or Rac could lead to annexin-V staining and nucleosomal fragmentation are not clear, and are the subject of continued investigations.

The isolation of a second toxicity domain outside of the enzymatic region, has not been forthcoming. Since LCT associated genes and gene fragments are notoriously difficult to express in *E. coli*, it is possible that we have not found the appropriate contiguous region or preserved a confirmation needed for activity. It is also feasible that the second domain is ineffective in the absence of the enzymatic region. Thus, Ras signaling pathways may need to be decreased for successful intoxication by the second, yet undefined toxicity domain.

REFERENCES

1. **Amimoto, K., E. Oishi, H. Yasuhar, O. Sasak, S. Katayama, T. Kitajima, A. Izumida, and T. Hirahara** 2001. Protective effects of clostridium sordellii LT and HT toxoids against challenge with spores in guinea pigs J Vet Med Sci. **63:**879-83.

2. **Bangsberg, D. R., J. I. Rosen, T. Aragon, A. Campbell, L. Weir, and F. Perdreau-Remington** 2002. Clostridial myonecrosis cluster among injection drug users: a molecular epidemiology investigation Arch Intern Med. **162:**517-22.

3. **Bitti, A., P. Mastrantonio, P. Spigaglia, G. Urru, A. I. Spano, G. Moretti, and G. B. Cherchi** 1997. A fatal postpartum Clostridium sordellii associated toxic shock syndrome J Clin Pathol. **50:**259-60.

4. **Boquet, P.** 1999. Bacterial toxins inhibiting or activating small GTP-binding proteins Ann N Y Acad Sci. **886:**83-90.

5. **Chaves-Olarte, E., I. Florin, P. Boquet, M. Popoff, C. von Eichel-Streiber, and M. Thelestam** 1996. UDP-glucose deficiency in a mutant cell line protects against glucosyltransferase toxins from Clostridium difficile and Clostridium sordellii J Biol Chem. **271:**6925-32.

6. **Chaves-Olarte, E., M. Weidmann, C. Eichel-Streiber, and M. Thelestam** 1997. Toxins A and B from Clostridium difficile differ with respect to enzymatic potencies, cellular substrate specificities, and surface binding to cultured cells J Clin Invest. **100:**1734-41.

7. **Giry, M., M. R. Popoff, C. von Eichel-Streiber, and P. Boquet** 1995. Transient expression of RhoA, -B, and -C GTPases in HeLa cells potentiates resistance to Clostridium difficile toxins A and B but not to Clostridium sordellii lethal toxin Infect Immun. **63:**4063-71.

8. **Gnad, R., B. Kaina, and G. Fritz** 2001. Rho GTPases are involved in the regulation of NF-kappaB by genotoxic stress Exp Cell Res. **264:**244-9.

9. **He, D., S. J. Hagen, C. Pothoulakis, M. Chen, N. D. Medina, M. Warny, and J. T. LaMont** 2000. Clostridium difficile toxin A causes early damage to mitochondria in cultured cells Gastroenterology. **119:**139-50.

10. **Herrmann, C., M. R. Ahmadian, F. Hofmann, and I. Just** 1998. Functional consequences of monoglucosylation of Ha-Ras at effector domain amino acid threonine 35 J Biol Chem. **273:**16134-9.

11. **Hofmann, F., C. Busch, and K. Aktories** 1998. Chimeric clostridial cytotoxins: identification of the N-terminal region involved in protein substrate recognition Infect Immun. **66:**1076-81.

12. **Hofmann, F., G. Rex, K. Aktories, and I. Just** 1996. The ras-related protein Ral is monoglucosylated by Clostridium sordellii lethal toxin Biochem Biophys Res Commun. **227:**77-81.

13. **Klussmann, E., G. Tamma, D. Lorenz, B. Wiesner, K. Maric, F. Hofmann, K. Aktories, G. Valenti, and W. Rosenthal** 2001. An inhibitory role of Rho in the vasopressin-mediated translocation of aquaporin-2 into cell membranes of renal principal cells J Biol Chem. **276:**20451-7.

14. **LeDell, K. H., R. Lynfield, R. N. Danila, and H. F. Hull** 2001. Unexplained Deaths following Knee Surgery Morb Mortal Wkly Rep. **50:**1080.

15. **Leist, M., and M. Jaattela** 2001. Four deaths and a funeral: from caspases to alternative mechanisms Nat Rev Mol Cell Biol. **2:**589-98.

16. **Leverrier, Y., and A. J. Ridley** 2001. Requirement for Rho GTPases and PI 3-kinases during apoptotic cell phagocytosis by macrophages Curr Biol. **11:**195-9.

17. **Lewis, C. J., and R. D. Naylor** 1998. Sudden death in sheep associated with Clostridium sordellii Vet Rec. **142:**417-21.

18. **Linseman, D. A., T. Laessig, M. K. Meintzer, M. McClure, H. Barth, K. Aktories, and K. A. Heidenreich** 2001. An essential role for rac/cdc42 gtpases in cerebellar granule neuron survival J Biol Chem. **276:**39123-31.

19. **Popoff, M. R., E. Chaves-Olarte, E. Lemichez, C. von Eichel-Streiber, M. Thelestam, P. Chardin, D. Cussac, B. Antonny, P. Chavrier, G. Flatau, M. Giry, J. de Gunzburg, and P. Boquet** 1996. Ras, Rap, and Rac small GTP-binding proteins are targets for Clostridium sordellii lethal toxin glucosylation J Biol Chem. **271:**10217-24.

20. **Qa'Dan, M., L. M. Spyres, and J. D. Ballard** 2001. pH-Enhanced Cytopathic Effects of Clostridium sordellii Lethal Toxin Infect Immun. **69:**5487-93.

21. **Spyres, L. M., M. Qa'Dan, A. Meader, J. J. Tomasek, E. W. Howard, and J. D. Ballard** 2001. Cytosolic delivery and characterization of the TcdB glucosylating domain by using a heterologous protein fusion Infect Immun. **69:**599-601.

22. **Vatn, S., M. A. Tranulis, and M. Hofshagen** 2000. Sarcina -like bacteria, Clostridium fallax and Clostridium sordellii in lambs with abomasal bloat, haemorrhage and ulcers J Comp Pathol. **122:**193-200.

23. **Warny, M., A. C. Keates, S. Keates, I. Castagliuolo, J. K. Zacks, S. Aboudola, A. Qamar, C. Pothoulakis, J. T. LaMont, and C. P. Kelly** 2000. p38 MAP kinase activation by Clostridium difficile toxin A mediates monocyte necrosis, IL-8 production, and enteritis J Clin Invest. **105:**1147-56.

Summary

I was very intrigued with LCTs because of their exceptionally large size, and due to the fact that they are intracellular toxins. In the first two chapters I focused on the mechanism of entry of TcdB and TcsL, while in the last two chapters I studied the role these toxins play in inducing cell death.

In chapter I, bafilomycin was able to protect target cells from the effect of TcdB, which indicated that endosomal acidification is important for toxin entry. An acid pulse allowed the toxin molecules on the cell surface to enter the cell and show CPE. This indicated that TcdB could bypass lipid biological membranes when exposed to low pH. Bafilomycin was also used to estimate the time required by TcdB for cytosol entry. After 40 min, TcdB was capable of intoxicating its target cells which suggests that the actual cytosol entry took less than 40 min. I also studied whether or not the acidic pH induced a conformational change in the toxin molecule. TNS, a molecule that when exposed to hydrophobic domains and upon excitation at certain wavelengths fluoresces, was used to determine the conformational changes. My findings show that TcdB exposes its hydrophobic domains when exposed to low pH, a signal to the toxin to escape before being degraded by lysosomal enzymes, which allows it to insert in the lipid bi-layer to escape the vesicle. My studies with TNS also show that once exposed to neutral pH again in the cytosol, TcdB buries its hydrophobic domains again. Using V8,a proteases that has the same specificity at neutral and acidic pH, the previous results were confirmed, and furthermore, the different profile of proteolytic activity at neutral and acidic pH indicated that there is a considerable conformational change in TcdB.

In chapter II, I showed that bafilomycin also protects cells from the effect of TcsL. This again indicated the importance of acidic pH for TcsL cytosolic entry. It was very clear to me though that TcsL is slower in cell entry as shown in the bafilomycin experiments , and due to the fact that I was able to neutralize TcsL by simple washing or using a specific antibody up to hours after the addition of toxin. An acid pulse again showed that bafilomycin effect can be bypassed, but was more important to me is the fact the minimal intoxicating dose lowered by more than a thousand fold, and the rate was higher and comparable to TcdB. That seemed very logical because C. sordellii causes gas gangerene, which is accompanied by acidification of the site of infection. The acidification clearly activates TcsL and allows it to work under conditions that indicate an onset of infection. TNS was used in the same manner to show that a dramatic conformational change occurs and allows the toxin to escape the vesicle or even insert from the cell surface in an infected site. It became clear to us that the reason behind the delay of intoxication by TcsL was due to the mechanism of entry. To confirm these finding I cloned the enzymatic domain of TcsL in a modified version of anthrax toxin that allows protein delivery to the cytosol, and compared that to a fusion of the same delivery system with the enzymatic domain of TcdB, cloned by another graduate student in my lab. My data shows that if mechanism of entry is normalized for both enzymatic domains, the rate of intoxication is similar.

In chapter III, I studied what happens after the toxin enters the cytosol. Previous reports indicated that LCTs cause cell death due to target inactivation. The targets are members of the Ras superfamily, also called small GTPases, that function as molecular switches

that control various functions in the cell. I did not disagree with these findings, but I believed that there are other pathways involved in the cell death. The proteomic analysis of cell treated with TcdB showed the presence of a cleaved form of a structural protein called vimentin. The mass spectrometry analysis also indicated that vimentin was cleaved by caspase-3. Clearly cells were dying due to the activation of apoptotic pathways. Using a pan caspase inhibitor, I showed that cells were dying slower, but they were still dying eventually. The enzymatic domain of TcdB delivered by the PA/LFn system also caused cell death, but it was slower than the full length toxin, and at a rate equal to cells dying in the presence of the caspase inhibitor after intoxication with TcdB. A cell line that does not express caspase-3 died at the same rate of cells intoxicated with enzymatic domain. I tested for the activation of caspase-3, and found that only the full length toxin activates caspase-3. To address the issue of whether or not the PA/LFn delivery system interfered with caspase-3 activation, I used a cell line transfected with the enzymatic domain of TcdB. Transfected cells died at the same rate of cells intoxicated by the enzymatic domain of TcdB delivered by PA/LFn, and were not capable of activating caspase-3. The enzymatic domain of TcdB, although showed complete target inactivation and caused cell death eventually, was not capable of activating caspase-3. All the previous data lead us to believe that TcdB activates at least two pathways that lead to cell death. After confirming that cell death occurred through apoptosis by the full length toxin or by the enzymatic domain alone, we came to the conclusion that TcdB activates at least two apoptotic pathways, a caspase-3 dependent pathway most probably activated after the membrane translocation domain inserts into the mitochondria, and a caspase-3 independent pathway after target inactivation.

In chapter IV, my data indicated that TcsL also activates a caspase-3 dependent, and a caspase-3 independent pathway. Why does TcdB or TcsL need to activate at least two pathways to cause cell death although one of them is enough?

The theory that seems acceptable to me at this point is that TcdB or TcsL induce apoptosis in the target cells, while inactivating the targets that prevent the cells from going through apoptosis. However it did not seem logical that *C. difficile* is inducing apoptosis, when necrosis is an easier alternative to cause cell death. Although, if *C. difficile* wanted to co-exist with the host, necrosis could not be the choice. Necrosis causes cells to secrete inflammatory substances that will recruit the immune system and make it a harder task on *C. difficile* to co-exist with the host. If cells are induced to go through apoptosis instead, macrophages will engulf the apoptotic body, and secrete IL-10, a cytokine that works as an immunosuppressent (anti-inflammatory in this case to be more specific). By producing TcdB, *C. difficile* guarantees a safer environment with fewer encounters with the immune system.